Next-Generation Energy-Efficient Broadband Access Networks

Maluge Pubuduni Imali Dias

Submitted in total fulfilment of the requirements of the degree of
Doctor of Philosophy

March, 2016

Department of Electrical and Electronic Engineering
THE UNIVERSITY OF MELBOURNE

Produced on archival quality paper

Dedicated to my husband, son, parents, and parents-in-law

Abstract

The popularity of bandwidth-intensive applications and the deployment of virtual private networks (VPNs) have resulted in a rapid growth of the Internet during recent years. The demand for high bandwidths and the necessity to serve customers over an extended reach cannot be met with conventional wired broadband access technologies, such as digital subscriber line (DSL), due to bandwidth limitations of the copper medium. To overcome this bottleneck and deliver high-speed content to customers over various distances, deploying optical fibre in the access network has been proposed as the most appropriate strategy. After considering potential optical fibre configurations for the amount of fibre and the number of transceivers required, the passive optical network (PON) has been selected as the most efficient architecture to provide fibre access to its customers. Today, PONs are not only used as access networks for fixed wire-line customers, but also as backhaul networks for mobile users. PONs are more energy efficient than their copper counterparts as a result of low transmission losses, high bandwidths, and passive components present. Due to their ability to deliver high bandwidths in a cost-effective manner, a large number of PONs have been deployed globally. Wider deployment of PONs increases the number of customers and user equipment in communication networks, thereby increasing the overall energy consumption. The implications of increased energy consumption, such as increased greenhouse gas emissions and operational expenditure, have led to the emergence of energy conserving studies for PON.

The main objective of this thesis is to propose energy-efficient algorithm-based solutions for the PON. For this purpose, we have selected the time division multiplexed (TDM)-PON and the time and wavelength division multiplexed (TWDM)-PON, as they are considered to be the most popular PON choices for current and future high-speed communication networks, respectively. In both TDM-PON and TWDM-PON, each optical network unit (ONU) is allocated a time slot to access the upstream and downstream bandwidths. Beyond this time slot, an ONU re-

mains idle, i.e., does not exchange or process packets. Despite being idle, ONUs continue to operate at their active power level. As a result, the high energy consumption of the PON is attributed to the ONUs, which continuously operate at their active power level and are present in large numbers in current communication networks. As such, minimising ONU energy consumption has been identified as the best approach to reduce overall energy consumption of the PON. For this purpose, transitioning idle ONUs into low-power modes, such as sleep and doze, have been proposed for both TDM-PON and TWDM-PON. In sleep mode, both the ONU transmitter (Tx) and receiver (Rx) are powered down, while in doze mode, only ONU Tx is powered down. Moreover, multiple wavelengths and tunable ONU transceivers (TRXs) present in TWDM-PONs facilitate further energy savings at the OLT through wavelength reallocation. Wavelength reallocation involves switching off idle wavelengths and redistributing the ONUs amongst remaining active wavelengths. In this thesis, we exploit the sleep/doze capabilities and wavelength tunability of the ONUs in designing energy-efficient dynamic bandwidth allocation (DBA) algorithms and dynamic wavelength and bandwidth allocation (DWBA) algorithms to minimise the energy consumption of the TDM-PON and TWDM-PON, respectively.

Proposing sleep/doze-enabled DBA algorithms for the TDM-PON involves addressing key operational and performance challenges that arise in the network due to sleep and doze mode operations. First, sleep/doze mode operations should be incorporated into the underlying DBA algorithm of the network. This thesis investigates how general MAC control messages can be used to exchange sleep/doze control messages between the OLT and ONUs. Another design parameter, sleep or doze duration, is carefully examined in this thesis as it affects both energy savings and quality of service (QoS). Longer sleep/doze duration improves energy-savings at the expense of increased average delay. As a result, energy consumption and average delay cannot be minimised simultaneously. To this end, this thesis explores sleep/doze control functions that adapt to varying traffic loads of the network to reduce energy consumption and also average delay. We also investigate supporting estimation techniques used in these sleep/doze control functions. Fi-

nally, for the TDM-PON, we investigate possible methods of minimising the QoS degradation due to sleep/doze mode operations.

In TWDM-PON, both sleep/doze mode operations and wavelength reallocation can be implemented to minimise energy consumption of the ONUs and OLT, respectively. The DWBA algorithms of this nature address two key challenges, namely, determining the number of active wavelengths and sustaining QoS specifications of the network. In current customer-centric telecommunication networks, network operators are bound to deliver a satisfactory QoS to customers through service level agreements (SLAs). As failure to comply with SLAs results in heavy penalties for network operators, meeting QoS requirements of the network is important to generate positive revenue. However, they also face the challenge of reducing the energy consumption of the network to meet environmental standards as well as to reduce the operational expenditure. To this end, we formulate models that determine the number of active wavelengths to improve energy savings and also to satisfy application-specific delay constraints. The performance of different types of DWBA algorithms is also evaluated under the proposed model. Finally, the performance of our proposed solutions is analysed for various types of network traffic.

Overall, the technical contributions presented in this thesis provide insight into how power saving techniques can be incorporated into the underlying DBA and DWBA algorithms to improve energy savings and sustain delay requirements of the PON. We also discuss how these solutions can be extended to different scenarios and applications in the future.

Declaration

This is to certify that

1. the thesis comprises only my original work towards the PhD,
2. due acknowledgement has been made in the text to all other material used,
3. the thesis is fewer than 100,000 words in length, exclusive of tables, maps, bibliographies and appendices.
4. the chapters 1, 2, and 7 of this thesis have been professionally proofread.

_____

Maluge Pubuduni Imali Dias

_____

Date

Acknowledgements

"The roots of all goodness lie in the soil of appreciation for goodness." -Dalai Lama

First and foremost, I would like to offer my sincere gratitude to my PhD supervisor Assoc. Prof. Elaine Wong. As my primary and only supervisor, the support I got from Elaine throughout my PhD candidature is incomparable. Her depth of knowledge in the area of optical fibre communications and her drive to thrive for the best, make her an exceptional supervisor any PhD candidate would be lucky to have. Her continuous guidance and prompt feedback made my candidature a very efficient one. Most importantly, her support, understanding, and flexibility, when I became a mother during my first year, encouraged me to stay focused at challenging and busy times. In Elaine, I see a passionate and dedicated researcher and most importantly, a compassionate human being who continues to inspire me in many ways. I would like to thank my friend Banie Abeywickrama for introducing me to such a wonderful supervisor to pursue my PhD journey. I would also like to thank the other members of my PhD committee, Prof. Thas Nirmalathas and Assoc. Prof. Brian Krongold for their presence in each milestones of my candidature and for their valuable technical suggestions and feedback.

I would like to thank the University of Melbourne for providing me with the opportunity and resources to pursue my postgraduate studies at such a world-renowned institution. It has been a privilege to work in such a diverse and dynamic research community. I am grateful for the financial assistance provided to me by the University of Melbourne and National ICT Australia (NICTA) in forms of full scholarships and travel funding. In particular, I would like to thank NICTA for funding me for an extra six months and relieving me from the financial burden during my candidature. I would also like to thank the administrative staff at the Electrical and Electronic Engineering department at the University of Melbourne, for their continuous support throughout my candidature.

During my PhD, I had the privilege of working closely with some of the well-

known researchers in my area of research, such as Prof. Luca Valcarenghi, Dr Dung Pam Van, and Dr Michael Muller. Our collaborations had a very positive impact on the technical contributions presented in this thesis and also helped me broaden my knowledge. I would like to offer my appreciation to these individuals and the Technical Institute of Munich, Germany and Scuola Superiore Sant'Anna, Pisa, Italy for making these collaborations possible.

I take this opportunity to thank my teachers and lecturers at the Holy Cross College and the University of Moratuwa, Sri Lanka for laying a solid foundation for my education, which later led me to pursue higher studies. It is with utmost respect that I thank my former principal Rev. Sister Nellie Helen for encouraging me to realise my dreams in the field of engineering.

Although a PhD can be stressful sometimes, my friends from the Photonics Research Lab, from the amazing mothers' group, and friends back in Sri Lanka were always there to cheer me up and make sure I enjoy life outside my studies. Their presence made many hours of simulations bearable. I would also like to thank all the cousins and relatives in my close-knit family for their prayers and blessings throughout this journey.

Most importantly, I would like to thank my parents, Mr Bernard Dias and Mrs Manel Wickramasinghe, who have dedicated their whole life to make my life a better one. Their trust in my abilities, freedom given to me to pursue my dreams, and their unconditional love has made me who I am today. Them flying to Melbourne and staying with us taking care of our son, while I focused on my studies show how they remain to be my strength and support. I am also lucky to have wonderful in-laws, Mrs Vineetha Karunaratne and Mr Bentarage Karunaratne, who have been very understanding and supportive throughout this journey. Their assistance in taking care of our son gave me time to concentrate on my studies.

Finally, my heartfelt love and thank you goes to my husband and my son. In days, when the simulations didn't work and the papers got rejected, the fact that I am going home to my boys was the only hope that kept me going. My husband, Sachintha Karunaratne, has been my pillar of support ever since we met at the University of Moratuwa as undergraduates. His understanding, love, and support

have always helped me sail through many rough waters, both academically and personally. His technical and emotional support throughout this research, while he was following his PhD, is something I am ever grateful for. Our little creation, Methindu, is my little stress reliever. His hugs, giggles, and everyday surprises distracted me from worrying and stressing about my PhD. The fact that his love and affection for me remained unchanged, amidst all the ups and downs of my research journey, always reminded me that there is always life to be enjoyed beyond a PhD.

Contents

List of Figures

List of Tables

Glossary

ALR	Adaptive link rate
BM	Burst mode
DBA	Dynamic bandwidth allocation
CDR	Clock and data recovery
CM	Continuous mode
CO	Central office
DFB	Distributed feedback
DWBA	Dynamic wavelength and bandwidth allocation
EPON	Ethernet passive optical network
EDFA	Erbium doped fibre amplifier
FSAN	Full Service Access Network
FTTH	Fibre to the home
GEM	Gigabit encapsulation method
GPON	Gigabit passive optical network
IEEE	Institute of Electrical and Electronics Engineers
IP	Internet protocol
ITU	International telecommunication union
LAN	Local area network
LLID	Link layer ID
MAC	Medium access control
MPCP	Multi-Point Control Protocol
NG	Next generation
OLT	Optical line terminal
ONU	Optical network unit
PON	Passive optical network
QoE	Quality of Experience
QoS	Quality of service
Rx	Receiver
TDM	Time division multiplexed
TDMA	Time division multiple access
TRX	Transceiver
TWDM	Time and wavelength division multiplexing
Tx	Transmitter
VCSEL	Vertical-cavity surface-emitting laser
WDM	Wavelength division multiplexing

CHAPTER 1

Introduction

1.1 Passive optical networks

During recent decades, the demand for high data rates in fixed and mobile communication networks has increased significantly. This increase in demand is a result of customers using the Internet for more sophisticated services, such as video-on-demand (VoD), IP telephony, and Internet gaming, rather than for basic web access [1]. To cater to this demand, current communication networks are expected to provide reliable and high-speed communication links over an extended reach. Although the core and metro networks have already been upgraded to facilitate high-speed and extended-reach data transfer, conventional copper infrastructure in the access networks is unable to support data rates beyond 16 Mbps [2]. However, optical fibre medium is characterised by high capacity and low transmission losses [3–5]. As a result, fibre to the home/building/curb/cabinet (FTTx) technology has been proposed to overcome the capacity bottleneck in the access segment of communication networks [6]. After considering different fibre deployment strategies, such as point-to-point (P2P), curb-switched networks, and passive optical networks (PONs), PON is selected as the most efficient configuration to deliver FTTx, as it requires low fibre and transceiver deployment. Although PONs cannot satisfy the mobility requirement of mobile users, they serve as high-capacity backhaul in mobile networks [7–9].

A typical PON consists of an optical line terminal (OLT) placed at the central office (CO), optical network units (ONUs) placed at customer premises, and power splitters that connect the ONUs to the OLT via high capacity optical fibre links, placed in between the OLT and the ONUs. The optical components between the

OLT and the ONUs remain passive, meaning they do not consume any power [10]. In the downstream direction, from the OLT to the ONUs, the OLT broadcasts its downstream data to all ONUs served by a given wavelength. In the upstream direction, from the ONUs to the OLT, a group of ONUs follows a multiple access protocol to access upstream bandwidth. Depending on this multiple access criterion, different types of PONs, such as time division multiplexed PON (TDM-PON), wavelength division multiplexed PON (WDM-PON), orthogonal frequency division multiplexed PON (OFDM-PON), and time and wavelength division multiplexed PON (TWDM-PON) have been proposed.

The evolution of next-generation PONs occurred in two main stages, namely, next-generation PON stage 1 (NG-PON1) and NG-PON2 [11]. Under NG-PON1, the TDM-PON was studied extensively, as it is more cost effective and energy efficient [12]. Two TDM-PON variations, Gigabit PON (GPON) and X-GPON, were standardised by Full Service Access Network (FSAN) and Telecommunication Standardisation Sector of the International Telecommunication Union (ITU-T) [13]. Concurrently, Ethernet PON (EPON) and 10 Gbps EPON (10G-EPON) were standardised by Institute of Electrical and Electronics Engineers (IEEE) 802.3 working group [14]. Collectively, these architectures support data rates of up to 10 Gbps, split ratios of 1:256, and a maximum network reach of 20 km.

Meanwhile, forecasts on global IP traffic, Internet traffic, devices and connections, and video traffic indicate a significant growth in these areas [15]. Although current demand for bandwidth, network reach, and number of users are met with technologies proposed under NG-PON1, broadband networks needs to be upgraded to meet future trends in Internet traffic. In order to future-proof the access segment, specifications set by FSAN require future PONs to support a minimum 40 Gbps data rate, 256-1024 ONUs, 20-40 km extended-reach, low energy consumption, low capital expenditure, and coexistence with GPON. The TWDM-PON, which stacks several X-GPONs using multiple wavelengths, has been selected by FSAN as the most appropriate PON architecture that satisfies these specifications [16–18].

1.2 Energy-efficient PONs

One main drawback of this continuously evolving Internet is the increased energy consumption of communication networks. PONs are characterised by a low energy-per-bit due to its high capacity and low transmission losses [3–5]. However, based on estimated growth of the Internet, reported in Cisco Visual Network Index (VNI), global Internet traffic is expected to grow 3.2-fold during the next 5 years [15]. To cater to this future trend, PONs are expected to be deployed in many parts of the world. The wider deployment of PONs will increase the number customers and high-speed components in the network, and eventually increase the overall energy consumption. This increase in energy consumption raises concerns for operational expenditure and particularly for greenhouse gas emissions and carbon footprint [19–21]. As a result, energy-efficient hardware and algorithm design have become an important part of PONs.

As discussed before, in both TDM-PON and TWDM-PON, multiple ONUs share the upstream bandwidth through the TDMA technique. This involves dividing the upstream bandwidth into time slots and assigning them to ONUs. The duration of each time slot depends on the bandwidth allocation criterion followed in the network. For example, a fixed bandwidth allocation algorithm will assign a fixed time slot to an ONU, irrespective of its bandwidth requirement. A dynamic bandwidth allocation (DBA) algorithm, however, will assign time slots based on individual bandwidth requirement of each ONU. The time duration between two consecutive time slots to an ONU is known as the polling cycle time. In a given polling cycle, an ONU transmitter (Tx) remains idle, meaning it does not transmit or process any packets, outside its upstream transmission time slot. Similarly, in the downstream direction, packets destined for a given ONU are sent during its downstream time slot. However, due to the broadcast nature of downstream traffic, they are received by all ONUs in the network. Upon receiving these packets, ONUs process their MAC addresses to identify ones destined to it and discard the ones destined to other ONUs. When an ONU receiver (Rx) is not processing MAC addresses or data packets, it is said to be in an idle state. Due to the slotted nature

of upstream and downstream traffic, an ONU transceiver (TRX) remains idle for a majority of its polling cycle.

Despite being idle, an ONU continuously operates at its active power level. The active power consumption in idle state, coupled with a large number of ONUs present in the PON, make ONUs the main energy consumption contributor of the access segment [22]. As a result, a majority of energy-saving solutions proposed for PON aim to minimise the energy consumption of the ONUs [19–21]. One such technique is to transition an ONU into a low-power mode, such as sleep or doze mode, during its idle time [23]. During sleep mode operation, both the ONU Tx and Rx are powered down, while in doze mode, only ONU Tx is powered down.

In any given polling cycle, an ONU that enters into sleep or doze mode consumes less energy than an ONU that stays active during the idle period. As a result, increasing the time an ONU spends in sleep or doze mode improves the energy efficiency of the network. However, when transitioning from sleep/doze mode to active mode, an ONU incurs a certain overhead time before it can exchange data or control packets with the OLT. For example, an ONU entering sleep mode cannot receive synchronisation bits from the OLT, and spends some time to resynchronise itself after waking up [24]. The time an ONU spends in resynchronising is known as the sleep-to-active overhead time. Similarly in doze mode, the settling time of an ONU Tx corresponds to the doze-to-active overhead time. An ONU will enter into sleep or doze mode, only if the idle time is greater than these overhead times. As the duration an ONU spends in sleep or doze mode is limited by this overhead time, keeping the overhead time to a minimum is considered an appropriate method in maximising ONU energy savings. In addition, reducing the power consumption in each state, i.e., sleep, doze, and active, also reduces the overall energy consumption of PONs. In summary, sleep/doze mode solutions proposed for the TDM-PON involve:

- Hardware-based solutions
  - Improving the sleep/doze capabilities of an ONU
    - Reducing the overhead duration

        * Reducing the power consumption in each state

- Algorithm-based solutions
    - Exploiting the sleep/doze capabilities of the ONUs in DBA algorithms

Meanwhile, a TWDM-PON consists of tunable TRXs at the ONUs and multiple wavelengths at the OLT. At a given network load, the network may not need all wavelength channels to serve the ONUs. As a result, the OLT can switch off certain wavelengths and reallocate ONUs among the remaining active wavelengths. This technique, which will be referred to as wavelength reallocation in the remainder of the thesis, reduces energy consumption of the OLT. In addition to wavelength reallocation, conventional sleep/doze operations can also be implemented at the ONUs to improve the overall energy efficiency of the network [25]. The energy-efficient solutions for TWDM-PON involve:

- Hardware-based solutions
    - Improving the wavelength tunability of the ONU
        * Reducing the wavelength tuning time
- Algorithm-based solutions
    - Exploiting the wavelength tunability and sleep/doze capabilities of the ONUs in dynamic wavelength and bandwidth allocation (DWBA) algorithms

In the following section, we discuss our approach to improving the energy efficiency of TDM-PON and TWDM-PON using sleep/doze mode operations and wavelength reallocation.

1.3 Thesis objectives

As explained in the previous section, sleep/doze mode operations and wavelength reallocation are two methods used to reduce the energy consumption of

the ONUs and the OLT, respectively. These techniques can be incorporated either as hardware-based solutions or as algorithm-based solutions for the PON. In this thesis, we take an algorithm-based approach, in the form of DBA and DWBA algorithms, to minimise the energy consumption of TDM-PON and TWDM-PON, respectively.

An effective sleep/doze-enabled DBA algorithm is a one which addresses performance and operational challenges associated with sleep/doze mode operations. First and foremost, the DBA algorithm should integrate possible energy saving techniques with bandwidth allocation process of the algorithm. Existing work on energy-efficient PONs mostly incorporates only sleep mode operation to improve the energy efficiency of the network. As discussed before, during sleep mode, both Tx and Rx of the ONU are powered down, resulting in significant energy savings compared to doze mode, where only Tx is powered down [24, 26–28]. As a result, sleep mode operation is a favourable technique to consider, especially as it highlights the energy savings achieved through low-power mode operations. However, if the idle time of an ONU is less than its sleep-to-active overhead time, sleep mode operation alone does not yield any energy savings. The first objective of this thesis is to improve the energy savings of the network, even when the ONUs cannot afford to go into sleep mode. For this purpose, we consider using both sleep and doze mode operations at the ONUs.

After identifying the sleep and doze mode operations as efficient means of saving energy, the next objective is to incorporate these operations into DBA algorithms. This involves informing ONUs about their sleep/doze start times and duration. Rather than introducing a new mechanism to transition the ONUs between different modes, the possibility of using existing MAC protocols is to be examined in this thesis.

For any given sleep/doze mode DBA algorithm, determining the sleep/doze duration is as important as incorporating the sleep/doze mode operations into the DBA algorithm. The importance of this parameter is emphasised by its strong correlation with the energy consumption and quality of service (QoS) of the network. Determining the sleep/doze duration based on network load is the preferred ap-

proach, as lightly-loaded ONUs can afford to sleep or doze for longer without affecting QoS parameters, such as average delay. Selecting a statistical parameter that reflects the traffic load of the network and determining the sleep or doze duration based on this parameter will be investigated next in this thesis. Further, an effective technique that successfully estimates the value of this statistical parameter is also to be selected from various estimation techniques, such as arithmetic averaging, exponential smoothing, and Bayesian framework.

Another equally important aspect of a sleep/doze mode DBA algorithm is its effect on QoS parameters, such as average delay. When an ONU enters into sleep or doze mode, the increase in average delay is inevitable. Meanwhile, customers are more sensitive to performance parameters that affect QoS of the network than they are to potential energy savings. As a result, possible measures should be taken to minimise this increased delay, especially when delivering delay-sensitive services over the network. For this purpose, methods of minimising average delay arising from sleep/doze mode operations are to be investigated in this thesis. The thesis will evaluate the improvement in average delay and also the increase in energy consumption, when these techniques are implemented in the network.

As mentioned in the preceding section, in a TWDM-PON, sleep/doze mode operation can be implemented to improve the energy efficiency of ONUs. In addition, wavelength reallocation, supported by tunable ONU TRXs and multiple wavelengths, facilitates energy savings at the OLT as well. Under wavelength reallocation, the OLT determines the number of active wavelength channels required to operate at a given network load. The OLT then switches off the idle wavelengths after reallocating the ONUs among remaining active wavelengths. The most critical part of this process is determining the number of active wavelengths. With Internet being used for many interactive applications today, QoS has become an important consideration. As such, in the energy-efficient DWBA algorithm proposed in this thesis, we aim to analyse the network from a QoS point of view. For this purpose, we wish to consider a delay-constrained TWDM-PON and propose a framework that determines the number of active wavelengths, irrespective of the ONU type, the nature of the DWBA, i.e., offline or online, or the delay constraint.

In this thesis, the performance of the proposed framework is also to be investigated under offline and online DWBA algorithms.

Finally, we wish to verify our proposed solutions for different types of incoming traffic at the ONUs. For this purpose, the performance of our proposed solutions will be analysed under Poisson and bursty traffic.

It is important to note that in analysing the performance of our novel algorithms proposed for TDM-PON and TWDM-PON, we have considered a 10G-EPON for illustrative purposes. However, our proposed solutions can be implemented in any TDM-PON or TWDM-PON with minor changes to the control message formats. Moreover, in both DBA and DWBA algorithms proposed in this thesis, we have considered a 10 Gbps vertical-cavity surface-emitting laser (10G-VCSEL) ONU. The experimental evaluation of this 10G-VCSEL has shown that it can transition from sleep and doze mode into active mode within 2 ms and 330 ns, respectively [29]. Compared to a conventional distributed feedback (DFB) laser ONU, the 10G-VCSEL also consumes 1.068 W less power in active state. As importantly, the 10G-VCSEL is tunable across the wavelength range supported by the TWDM-PON. Due to these physical characteristics, the 10G-VCSEL is a favourable choice for energy-efficient PONs. As such, we have used this 10G-VCSEL as the Tx of our ONU. The Rx and the back-end digital circuitry of the ONU remain the same as that of a DFB ONU. In the remainder of this thesis, this ONU architecture will be referred to as the 10G-VCSEL ONU.

1.4 Thesis outline

This section presents a detailed account of our research undertaken to achieve the objectives mentioned in the preceding section. The rest of the thesis is structured as follows:

Chapter 2: Introduction to energy-efficient passive optical networks

Chapter 2 presents an analytical study of sleep/doze and wavelength reallocation solutions proposed for the TDM-PON and TWDM-PON in existing literature. To

gain a better understanding of the motivation behind our novel sleep/doze and wavelength reallocation solutions proposed for these architectures, we first discuss the operational and protocol details of the PON, TDM-PON, and TWDM-PON. We identify the main causes and complications of the increased energy consumption and possible energy-saving techniques, in particular, the sleep/doze mode operations and wavelength reallocation, for the TDM-PON and TWDM-PON, respectively. We then present an outline of different hardware and algorithm-based solutions that exploit these techniques to improve the energy efficiency of TDM-PONs and TWDM-PONs. In particular, we discuss the suitability of the 10G-VCSEL as an ONU Tx in the configuration considered in our analysis.

Chapter 3: Energy-efficient dynamic bandwidth allocation algorithms for 10 Gbps EPON

This chapter presents our first two energy-efficient DBA algorithms, Just-In-Time DBA (JIT DBA) with varying polling cycle times and the JIT DBA with fixed polling cycle times (J-FIT DBA), proposed for the TDM-PON. As discussed in the previous section, the initial step in any sleep/doze mode DBA algorithm is incorporating the possible energy saving methods into the DBA algorithm. Identifying that sleep mode alone will not result in maximum energy savings, the JIT and J-FIT DBA algorithms incorporate both sleep and doze mode operations to improve energy savings across a wider range of network loads. The two novel DBA algorithms, proposed for an illustrative 10G-EPON, are designed such that the ONUs wake up just-in-time to receive downstream packets from the OLT. To effectively transition the ONUs between different modes, the JIT and J-FIT DBA algorithms utilise existing MAC protocol Multi-Point Control Protocol (MPCP) messages, such as GATE and REPORT. The drawback of the JIT DBA is the reported low energy savings at low network loads. To overcome this shortfall, our novel J-FIT DBA algorithm utilises fixed polling cycle times to increase the idle time and the sleep/doze duration of the ONUs. The J-FIT DBA also uses MPCP control messages. The chapter presents a detailed account of traffic flow, bandwidth and sleep/doze allocation,

and the process of transitioning the ONUs between different modes. Under a comparative study, we evaluate the performance of the JIT and J-FIT DBA algorithms for polling cycle time, the percentage of energy savings, and average delay. Although it is evident that the 10G-VCSEL ONU outperforms a typical 10G-DFB ONU most of the time, we quantify this improvement by comparing the performance of the JIT and J-FIT DBA algorithms using 10G-VCSEL ONU and 10G-DFB ONU.

Chapter 4: Bayesian estimation and prediction-based dynamic bandwidth allocation algorithm for 10 Gbps EPON

In this chapter, we address two critical aspects of a sleep/doze DBA algorithm, i.e., determining the sleep/doze duration of an ONU and reducing the average delay resulting from the sleep/doze mode operations. As discussed in the preceding chapter, JIT DBA yields low energy savings at low network loads. The J-FIT, which is proposed to achieve improved energy savings at low network loads, results in increased average delay due to fixed polling cycle times. As such, the sleep/doze durations reported under the JIT and the J-FIT DBA algorithms are not optimum. Meanwhile, allocating longer sleep/doze durations for lightly loaded network loads and vice versa, is considered as an effective method of balancing energy savings and average delay of an ONU. Under this approach, using a statistical parameter that reflects the network load of an ONU is considered more effective in literature. Moreover, using an effective technique to estimate this statistical parameter is equally important.

Taking all these design requirements into consideration, in this chapter, we propose the JIT DBA with Bayesian estimation and prediction (BEP DBA). BEP DBA uses the average inter-arrival time of packets as the statistical parameter and follows the Bayesian framework to estimate its value. The superiority of the Bayesian estimation method is verified by comparing its performance against the estimation techniques frequently used in literature, such as arithmetic averaging and exponential smoothing. Further, to minimise the average delay resulting from

sleep/doze mode operations, we propose to use traffic prediction at the OLT. We evaluate the percentage of predicted traffic that should be taken into account when allocating bandwidth to each ONU. To quantify the improvement in average delay and the increase in energy consumption associated with traffic prediction, the performance of our BEP DBA is evaluated with and without the prediction mechanism.

Chapter 5: Energy-efficient framework for time and wavelength division multiplexed passive optical networks

The novel sleep/doze mode DBA algorithms discussed in the previous chapters are proposed for TDM-PON. However, based on expected growth of the Internet, FSAN requires future broadband networks to support a minimum 40 Gbps data rate, 256-1024 ONUs, 20-40 km extended-reach, low energy consumption, low capital expenditure, and coexistence with GPON. After considering potential network architectures, TWDM-PON is foreseen as the most favourable configuration that supports these demands. As explained before, a TWDM-PON facilitates wavelength reallocation due to tunability of ONU TRXs and multiple wavelengths at the OLT. In wavelength reallocation, the criterion followed in determining the number of active wavelengths is of great importance. For this purpose, in this chapter, we propose a novel framework that determines the number of active wavelengths at a given network load, for a delay-constrained TWDM-PON. The framework determines the maximum polling cycle time of a given ONU that satisfies the specified maximum delay of the network. The maximum bandwidth corresponding to this polling cycle time is used as a threshold and a new wavelength is introduced to the network when the average requested bandwidth of an ONU exceeds this bandwidth threshold. Using offline and online DWBA algorithms, the performance of our novel framework is analysed for the number of active wavelengths, percentage of energy savings at the OLT, percentage of energy savings at the ONUs, and average delay.

Chapter 6: Energy-efficient dynamic wavelength and bandwidth allocation algorithms under bursty traffic

The DBA and DWBA algorithms proposed in Chapters 3-5 are simulated using Poisson-distributed upstream traffic at the ONUs. However, with the Internet traffic becoming bursty in nature, it is important to validate the performance of our proposed solutions using bursty traffic. For this purpose, we consider the OFF-DWBA algorithm proposed in Chapter 5, as it includes both wavelength reallocation and sleep/doze mode operations. In this chapter, we discuss two main principles of bursty traffic, self-similarity and long-range dependence, in detail and select the long-tail Pareto distribution to generate incoming traffic at the ONUs. Using Pareto-distributed bursty traffic, we evaluate the performance of our OFF-DWBA algorithm for energy efficiency and average delay.

1.5 Original contributions

The original contributions of this thesis are presented here. It is important to note that the simulations of the novel DBA and DWBA algorithms proposed in this thesis are performed using C++. The algorithms comply to the MPCP control messages GATE and REPORT to transition the ONUs between different modes, to allocate bandwidth to each ONU, and also to allocate ONUs among different wavelengths. The original contributions are:

- Development of a new DBA algorithm, JIT DBA, that incorporates both sleep and doze capabilities of a 10G-VCSEL ONU to improve the energy efficiency of a 10G-EPON. The proposed JIT DBA algorithm transitions an ONU into sleep or doze mode depending on its idle time. The use of doze mode operation increases the energy saving capability of an ONU, even when its idle time is less than sleep-to-active transition time. The proposed JIT DBA yields tangible energy savings across a wide range of network loads. Further, the average delay experienced by the packets, in particular for practical network loads 0.6, remains below 100 ms to support delay-sensitive services, such as

VoD (Chapter 3).

- Development of a novel DBA algorithm, J-FIT DBA, to increase the energy savings at low network loads of a 10G-EPON. The J-FIT DBA algorithm also incorporates both sleep and doze mode operations but uses fixed polling cycle times to increase the sleep/doze duration of an ONU. For the fixed polling cycle times considered in this analysis, the proposed algorithm achieves energy savings of 65% at low network loads. Further, the average delay remains below 100 ms and can deliver delay-sensitive services over the 10G-EPON (Chapter 3).

- The design of a new criterion that assigns longer sleep/doze durations to the lightly loaded ONUs and shorter sleep/doze durations to heavily loaded ONUs thereby, balancing the average delay and the energy savings of the network. Under the proposed method, traffic load of an ONU is realised through the average inter-arrival time of packets, which is estimated using the Bayesian estimation. Compared to the existing techniques, the Bayesian framework accurately estimates the average inter-arrival time of packets with a lower number of packets (Chapter 4).

- Development of a new DBA algorithm, BEP DBA, which incorporates a sleep and doze control function and traffic prediction. Using traffic prediction and the estimated average inter-arrival time of packets, the OLT can estimate the number of packets accumulated during the sleep/doze duration of an ONU. Simulation results indicate that for the proposed sleep/control function, BEP DBA achieves significant energy savings of 65% and the average delay remains below the specified 10 ms. Further, our findings indicate that the proposed prediction mechanism can reduce the reported average delay by 13% with an increase of only 0.01% of energy consumption (Chapter 5)..

- First development of a general framework that determines the number of active wavelengths of a delay-constrained TWDM-PON. The framework determines the maximum polling cycle time that achieves improved energy

savings while satisfying the delay constraints of the network. The maximum polling cycle time is then used to determine the number of active wavelengths.

- The first development of offline and online DWBA algorithms, OFF-DWBA and ON-DWBA, derived from the previously proposed general framework. The simulation results indicate that the ON-DWBA algorithm achieves more energy savings both at the OLT and the ONUs while both ON-DWBA and OFF-DWBA satisfy the delay constraint of the network.

- Simulation analysis of the OFF-DWBA algorithm for bursty traffic. Based on our findings, the OFF-DWBA behaves very similarly, under both Poisson and bursty traffic.

1.6 Publications

This section presents the journal and conference publications related to each technical contribution chapter.

Chapter 3

Journal

- M. P. I. Dias and E. Wong, “Sleep/doze controlled dynamic bandwidth allocation algorithms for energy-efficient access networks," Optics Express, vol. 21, no. 8, pp. 9931-9946, 2013.

Conference

- M. P. I. Dias and E. Wong, “Energy-efficient dynamic bandwidth allocation algorithm for sleep/doze mode VCSEL ONU," Proc. of Asia Communications and Photonics Conference (ACP), ATh1D.4 (2012).

- M. P. I. Dias and E.Wong, “Performance evaluation of VCSEL ONU using energy-efficient just-in-time dynamic bandwidth allocation algorithm," Proc. of Photonics Global Conference (PGC), (2012).

- M. P. I. Dias and E. Wong, “Energy-efficient dynamic bandwidth allocation algorithm with fixed polling cycle times," Proc. of Opto Electronics and Communications Conference (OECC) 2013

Chapter 4

Journal

- M. P. I. Dias, B. S. Karunaratne, and E. Wong, “Bayesian estimation and prediction based dynamic bandwidth allocation algorithm for sleep/doze mode passive optical networks,” Journal of Lightwave Technology, vol. 32, no. 14, pp. 2560 - 2568, 2014

Conference

- M. P. I. Dias and E. Wong, “Sleep/Doze controlled dynamic bandwidth allocation algorithm with Bayesian estimation,” Proc. of Asia Communications and Photonics Conference (ACP), 2013.

Chapter 4

Journal

- M. P. I. Dias, D. P. Van, L. Valcarenghi, and E. Wong, “An energy-efficient framework for wavelength and bandwidth allocation in TWDM PON,” Journal of Optical Communication and Networks (JOCN), Vol. 7, no. 6, pp. 496-504, 2015.

Conference

- M. P. I. Dias, D. P. Van, L. Valcarenghi, and E. Wong, "Energy-efficient dynamic bandwidth allocation algorithm for TWDM PON with tunable VCSEL ONUs," Proc. of Opto Electronics and Communications Conference (OECC), 2014.
- M. P. I. Dias, D. P. Van, L. Valcarenghi, and E. Wong, "Energy-efficient TWDM PON with VCSEL ONUs", Proc. of Asia Communications and Photonics Conference (ACP), 2014.
- M. P. I. Dias, D. P. Van, L. Valcarenghi, and E. Wong, "Offline energy-efficient dynamic wavelength and bandwidth allocation algorithm for TWDM-PONs", Proc. of International Conference on Communications (ICC), 2015

Other related publications

- E. Wong, M. Muller, C. A. Chan, and M. P. I. Dias, "Vertical-cavity surface-emitting laser transmitters for energy efficient broadband access networks," Proc. of International Conference on Communications (ICC), Networks and Systems Symposium, 2012.
- E. Wong, M. Muller, M. P. I. Dias, C. A. Chan, and M.C. Amann, "Energy saving strategies for VCSEL ONUs," Proc. of Optical Fiber Communication Conference and Exhibition/National Fiber Optic Engineers Conference (OFC/NFOEC), paper OTu1H5, 2012.
- E. Wong, M. Muller, M. P. I. Dias, C. A. Chan, and M. C. Amann, "Energy-efficiency of optical network units with vertical-cavity surface-emitting lasers," Optics Express, vol. 20, no. 14, pp. 14960-14970, 2012
- M. Mueller, P. Wolf, C. Grasse, M. P. I. Dias, M. Ortsiefer, G. Boehm, E. Wong, W. Hofmann, D. Bimberg, M. C. Amann, "1.3 μm short-cavity VCSELs enabling error-free transmission at 25 gbit/s over 25 km fibre link," Electronics Letters, Vol. 48, No. 23, pp. 1487-1489, 2012.

- D. P. Van, M. P. I. Dias, E. Wong, and L. Valcarenghi, "Energy-efficient dynamic bandwidth allocation in long reach passive optical networks," Proc. of Opto Electronics and Communications Conference (OECC), 2014.

- D. P. Van, M. P. I. Dias, E. Wong, and L. Valcarenghi, "Advanced sleep-sware dynamic bandwidth allocation for 10G-EPONs", Globecom 2014.

- D. P. Van, L. Valcarenghi, M. P. I. Dias, K. Kondepu, P. Castoldi, and E. Wong, "Energy-saving framework for passive optical networks with ONU sleep/doze mode," Optics Express, vol. 23, no. 3, pp. A1-A14, 2015.

CHAPTER 2

Introduction to energy-efficient passive optical networks

2.1 Passive optical networks

In recent years, the exponential growth of the Internet has been fuelled by the increasing user demand for bandwidth-intensive applications [29] and the deployment of cooperate virtual private networks (VPNs). In particular, bandwidth-intensive applications such as video-on-demand (VoD) and video gaming have increased the demand for data rates both in fixed and mobile networks. To meet this demand from a communication network perspective, network operators are encouraged to future-proof both core [30, 31] and access networks [32] in terms of the link capacity and network reach. Despite core networks experiencing rapid changes to meet this demand, access networks are advancing at a much slower pace.

During the initial stages of broadband technologies, digital subscriber line (DSL) and community antenna television (CATV) networks were used to deliver Internet access to customers. The maximum bandwidth offered by the DSL technology is limited to 16 Mbps, which is further reduced by poor wire-line conditions and distance. Similarly, the bandwidth provided by CATV networks is shared by a large number of users, resulting in unsatisfactory user experience. To alleviate the capacity limitations in existing copper-wired access networks, optical fibre is selected as the preferred medium. Compared to the conventional copper wires, optical fibre experiences significantly lower transmission losses and supports higher link capacities, making it the key technology in high-speed Internet access [33].

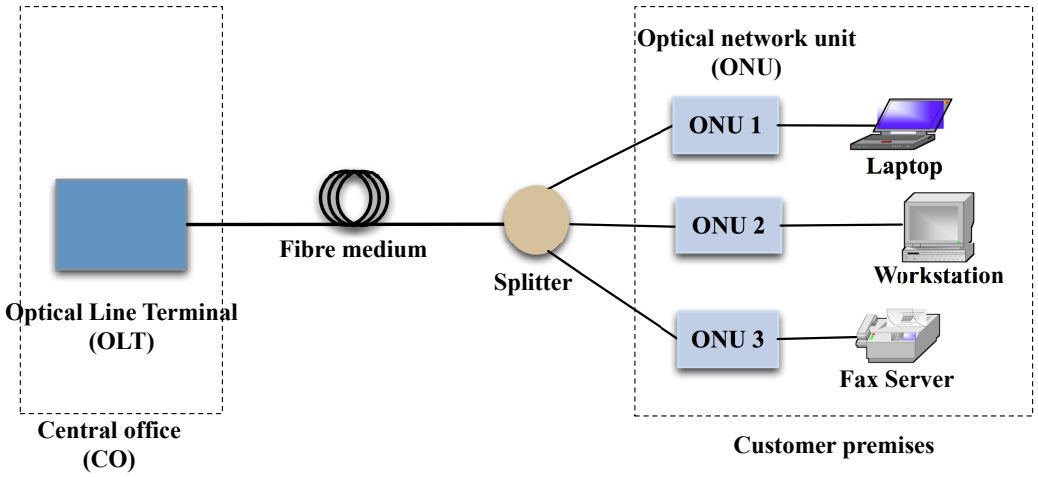

Figure 2.1: General architecture of a PON.

Today, optical fibre is used to deliver high-speed Internet access to different points in the access segment of communication network through fibre-to-the x (FTTx) technology, where x stands for curb, office, cabinet, or building [6]. In order to deliver FTTx technology in the access network, different network configurations such as point-to-point (P2P), curb-switched networks, and passive optical networks (PONs) have been evaluated for the required number of transceivers (TRXs) and optical fibre [34]. Consider a network with N number of users at an average distance of L km from the central office (CO). A P2P network requires $2N$ number of TRXs and NxL fibre length, whereas a curbed-switched network requires $2N + 2$ number of TRXs but only L fibre length. PON, on the other hand, requires only N number of TRXs and L fibre length. As a result, PON is selected as the most-efficient architecture to deliver FTTx services in the access segment of communication network [35–37].

Figure 2.1 illustrates the basic architecture of a PON. A typical PON is a point-to-multi-point network that hosts an optical line terminal (OLT) at the CO and optical network units (ONUs) at the customer premises [38]. Optical splitters placed in-between, connect the OLT and the ONUs via high-capacity optical fibre links. The network between the OLT and ONU is known as the optical distribution network (ODN). Apart from the OLT and the ONUs, the intermediate components

such as optical fibre, optical splitters, and splicers, are all passive, meaning they do not consume any power [2, 10].

In the downstream direction, from the OLT to the ONUs, the OLT broadcasts its data and control packets to all ONUs served by a wavelength. Upon receiving these packets, ONUs process their medium access control (MAC) addresses to identify the ones destined for itself and to discard the ones intended for the other ONUs. In the upstream direction, from the ONUs to the OLT, bandwidth is shared among multiple ONUs, with the directionality of the optical splitters preventing an ONU from broadcasting its data to other ONUs in the network. If more than one ONU attempts to access the upstream bandwidth simultaneously, packet collisions may occur. To avoid collisions in the upstream direction, a multiple access technique needs to be deployed in the medium access level to control (1) start time and (2) duration of upstream bandwidth access of each ONU. Depending on the multiple access scheme, different types of PONs exist, namely,

- Time division multiplexed PON (TDM-PON) - ONUs access the upstream bandwidth via different time slots
- Wavelength division multiplexed PON (WDM-PON) - ONUs access the upstream bandwidth via different wavelengths
- Orthogonal frequency division multiplexed PON (OFDM-PON) - ONUs access the upstream bandwidth via different frequencies
- Time and wavelength division multiplexed PON (TWDM-PON) - ONUs access the upstream bandwidth via different time slots and wavelengths

In the next section, a brief discussion on the evolution of the PON architectures, mentioned above, is presented.

2.1.1 Evolution of next-generation PONs

PONs were initially proposed by the Full Service Access Network (FSAN) and later standardised by the Institute of Electrical and Electronics Engineers (IEEE)

and the Telecommunication Standardisation Sector of the International Telecommunication Union (ITU-T). As explained in Chapter 1, next-generation PONs (NG-PONs) are evolving in two main stages, namely, NG-PON stage 1 (NG-PON1) and NG-PON2. The following sections present the main network architectures proposed under these two phases.

2.1.1.1 Next-generation PON stage 1

The NG-PON project groups were established to propose and standardise network architectures that would future-proof FTTx. Under NG-PON1, the TDM-PON and the WDM-PON are considered as the most suitable candidates for future deployments [12]. In the WDM-PON however, individual wavelength channels are allocated to each customer. Due to significant outside fibre plant deployment required to support this configuration, WDM-PON is cost-prohibitive when used to cater to a large number of users. The TDM-PON, on the other hand, is both cost-efficient and bandwidth-enriched. As a result, TDM-PONs have become very popular, particularly among service providers [39]. In this discussion, we will focus on the evolution of TDM-PONs under NG-PON1.

Gigabit PON (GPON) was first standardised by the FSAN/ITU-T under ITU-T G.984 listing different aspects of the GPON such as general characteristics, physical medium, and management and control [13, 40–42]. The proposed GPON supports data rates of 2.5 Gbps and 1.25 Gbps in the downstream and upstream directions, respectively. Fuelled by its rapid deployment, FSAN/ITU-T standardised the XG-PON to cater for higher data rates in 2010 [43]. XG-PON supports 10 Gbps and 1 Gbps data rates in the downstream and upstream directions through 1575 nm - 1580 nm and 1260 nm - 1280 nm wavelength bands, respectively. Today, GPON has become the most popular technology of choice in some areas of Europe and North America.

Meanwhile, the IEEE standardised the Ethernet PON (EPON) under IEEE 802.3 ah [14,44]. Integrated with conventional Ethernet technology, EPON enables seamless integration with IP and Ethernet technologies. The EPON supports 1.25 Gbps

link rate in both upstream and downstream directions and a 20 km network span. Later in 2006, the IEEE 802.3av Task Force standardised the 10 Gbps EPON (10G-EPON) to cater to a growing customer demand for higher bandwidths. The 10G-EPON supports two network configurations, namely, symmetric and asymmetric EPON. Symmetric 10G-EPON supports 10 Gbps data rates in both upstream and downstream directions while asymmetric 10G-EPON supports 10 Gbps downlink and 1 Gbps uplink. The 802.3av standards emphasise on two architectures co-existing in the outside plant, a feature possible through wavelength separation [45]. In the downstream direction, the 10 Gbps and 1 Gbps use 1575-1580 nm and 1480-1500 nm wavelength bands, respectively. In the upstream direction, the 10 Gbps and 1 Gbps use wavelength bands 1260-1280 nm and 1260-1360 nm, respectively. In current context, EPON is prevalent in the Asian region, especially in countries such as Japan and Korea.

2.1.1.2 Next-generation PON stage 2

While EPON and GPON technologies are currently meeting the demand for high data rates, forecasts on Internet-based applications imply the potential capacity and reach limitations these technologies may face in the future [46, 47]. Further, introducing services such as VoD to mobile users have significantly increased the required data rates in mobile networks. Although PON cannot meet the mobility requirement of these networks, PON is an excellent choice in providing mobile-backhaul [7–9]. To future-proof access networks to cater to both fixed and mobile subscribers, FSAN and ITU-T specified baseline requirements of next-generation access networks under ITU-T G.989 [16–18]. These requirements include a minimum 40 Gbps data rate, 256 - 1024 ONUs, 20 - 40 km extended-reach, low energy consumption, low capital expenditure, and coexistence with GPON [48]. After analysing prospective network architectures such as 40 Gbps TDM-PON (XLG-PON) [49–51], WDM-PON [52, 53], OFDM-PON, TWDM-PON, and opportunistic and dynamic spectrum management (ODSM)-PON, TWDM-PON was selected as the most appropriate network configuration to provide high-speed broadband ac-

cess in the future, by FSAN/ITU-T [54, 55].

As explained in Chapter 1, the main objective of this thesis is to propose algorithm-based solutions to improve the energy efficiency of the TDM-PONs and TWDM-PONs. In following our proposed solutions, an understanding of the characteristics and protocol details of these two network configurations is of great importance. As such, in the next section, we present a detailed account of the TDM-PONs and TWDM-PONs.

2.1.2 Time division multiplexed PON

Figure 2.2 illustrates the general architecture of a TDM-PON. Similar to the general PON configuration discussed in Section 2.1, a TDM-PON hosts an OLT at the CO and ONUs at customer premises. The number of ONUs allocated to a wavelength channel depends on the allowable power budget. The splitting ratio of a passive splitter placed at the remote node, is typically 1:8, 1:16, 1:32, and 1:64. Most importantly, a TDM-PON uses two distinct wavelengths, λ and λ', for downstream and upstream data transmission, respectively. In the downstream direction, the OLT broadcast its packets through λ to all ONUs in the network. Upon receiving these packets, each ONU processes their MAC addresses and discards the packets meant for other ONUs in the network.

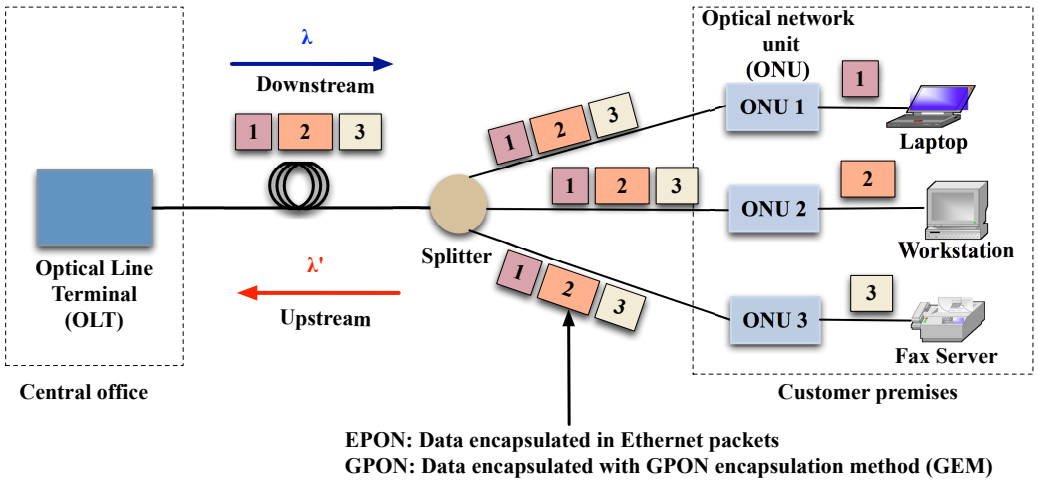

Figure 2.2: General architecture of a time division multiplexed passive optical network (TDM-PON).

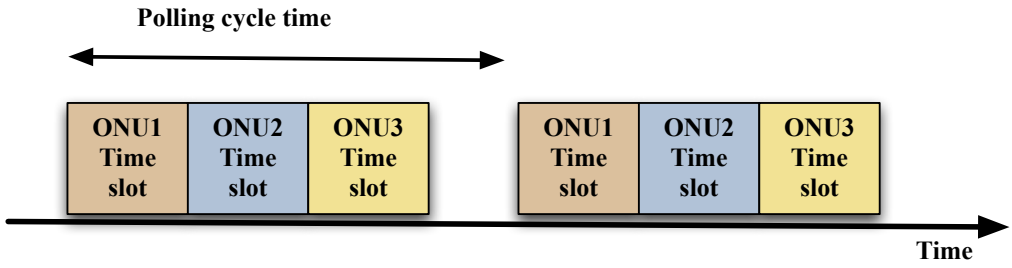

Figure 2.3: Upstream bandwidth allocation of the TDM-PON.

In the upstream direction, multiple ONUs share the upstream bandwidth using time division multiple access (TDMA). Figure 2.3 illustrates the upstream bandwidth (time slot) allocation of a TDM-PON with three ONUs. The upstream wavelength, λ', is divided into separate time slots which are assigned to each ONU to access the OLT. The duration between two consecutive time slots allocated to an ONU is defined as the polling cycle time. Within this time slot, the full upstream bandwidth is available to a given ONU. In order to allocate time slots or bandwidth among ONUs, the OLT needs to be aware of the bandwidth requirement of each ONU. Further, the ONUs need also be made aware of the designated time slots for transmission. For these purposes, MAC protocols are implemented to allocate bandwidth by the OLT and to request bandwidth.

Two popular TDM-PON architectures frequently discussed in literature, are the GPON and EPON. Although these two networks share the same general concepts such as PON operation, ODN, and wavelength plan, they exhibit distinct features concerning protocols, operation, and features. The next sections present a detailed account of these architectures.

2.1.2.1 Ethernet PON

The EPON leverages the features, compatibility, and performance of the Ethernet protocol with a cost-effective PON architecture to serve customers with high-bandwidth requirements [14]. As shown in Fig. 2.4, Ethernet packets are transmitted natively across the PON. As Ethernet technology is widely deployed in current local area networks (LANs), incorporating Ethernet into PON requires minimum

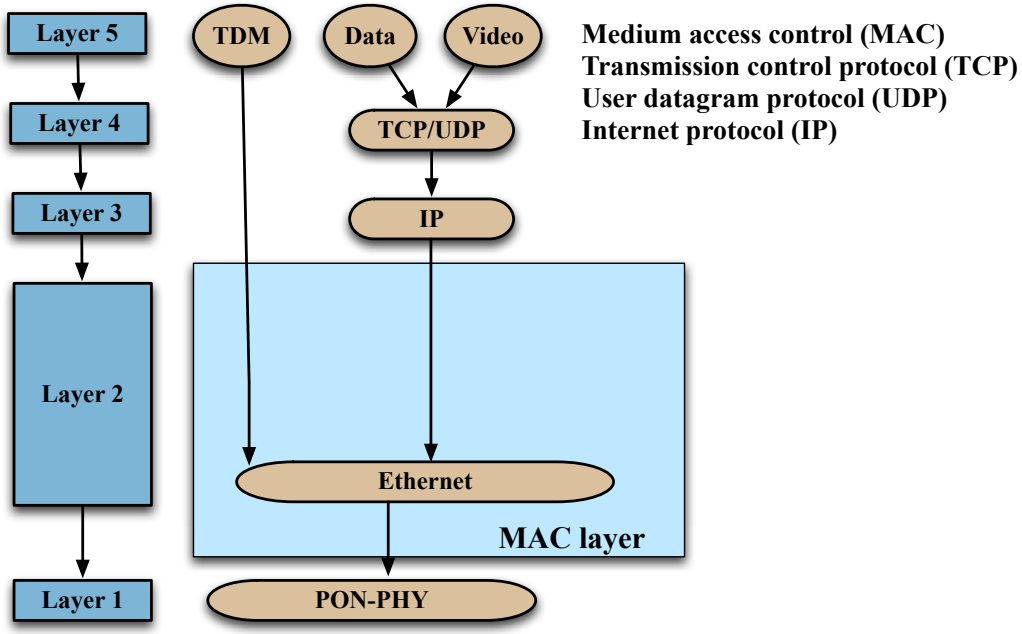

Figure 2.4: EPON framing structure (adapted from [56]).

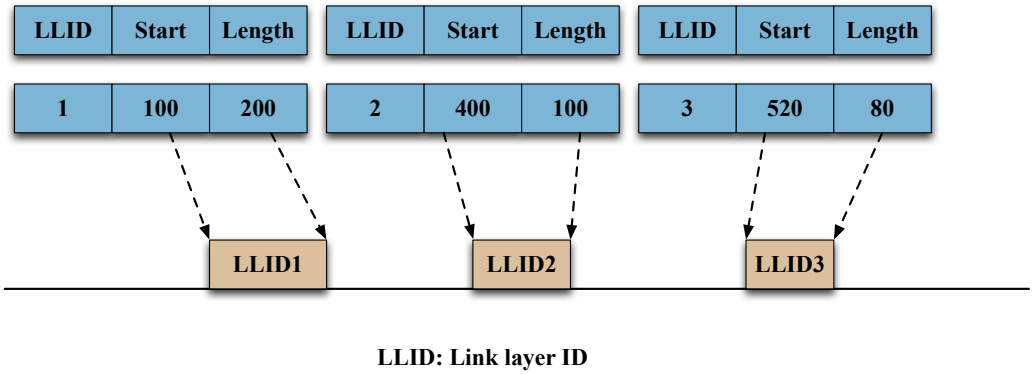

Figure 2.5: Downstream Ethernet packet structure (adapted from [56]).

transition as far as hardware and technical know-how are concerned [57].

As a TDM-PON, the ONUs in an EPON follow a time division multiple access technique, where the upstream bandwidth is divided into distinct time slots. In order to gather information on the bandwidth requirement of each ONU and to inform an ONU of its allocated time slot, an EPON employs Multi-Point Control Protocol (MPCP) control messages [38]. There are two modes of operation for MPCP: auto-discovery and normal operation. The auto-discovery is an initialisa-

tion process where the OLT identifies the ONUs initiated recently in the PON. On the other hand, the normal operation allocates transmission time slots to ONUs discovered during the initialisation process. The primary MPCP control messages used for each purpose are as follows [14]:

- Auto-discovery: REGISTER REQ, REGISTER, and REGISTER ACK.
- Normal operation: GATE and REPORT.

In our proposed algorithms, we focus on MPCP control messages used during normal operation, GATE and REPORT. The GATE message, sent from the OLT to the ONUs, is used to grant bandwidth (transmission time slots) to the ONUs. The GATE specifies the start time and the length of a transmission window as shown in Fig. 2.5 and is sent per link layer ID (LLID). A LLID is attached to the preamble of the downstream packets and uniquely identifies an ONU in the network. The REPORT message, sent from each ONU to the OLT, contains the bandwidth requirements of the ONUs. The MPCP is not unique to a particular bandwidth allocation algorithm, rather, it is a supporting protocol that encourages the execution of different bandwidth allocation schemes in the EPON.

2.1.2.2 Gigabit PON

As previously mentioned, the EPON and GPON share similar PON operation. However, the GPON distinctively differs from EPON in its frame structure. While data is transmitted as native Ethernet packets in the EPON, in the GPON, data is encapsulated further, before entering the physical medium. As shown in Fig. 2.6, the GPON Transmission Convergence (GTC) layer is responsible for aggregating traffic generated from different services, e.g., voice and video, into a common service-independent framework. Before entering the physical medium, Ethernet packets are encapsulated into the GTC Encapsulation Method (GEM) frames and then into GTC frames [56].

Figure 2.7 illustrates a downstream GTC frame in detail. The GTC header carries an upstream bandwidth map, which includes information on transmission

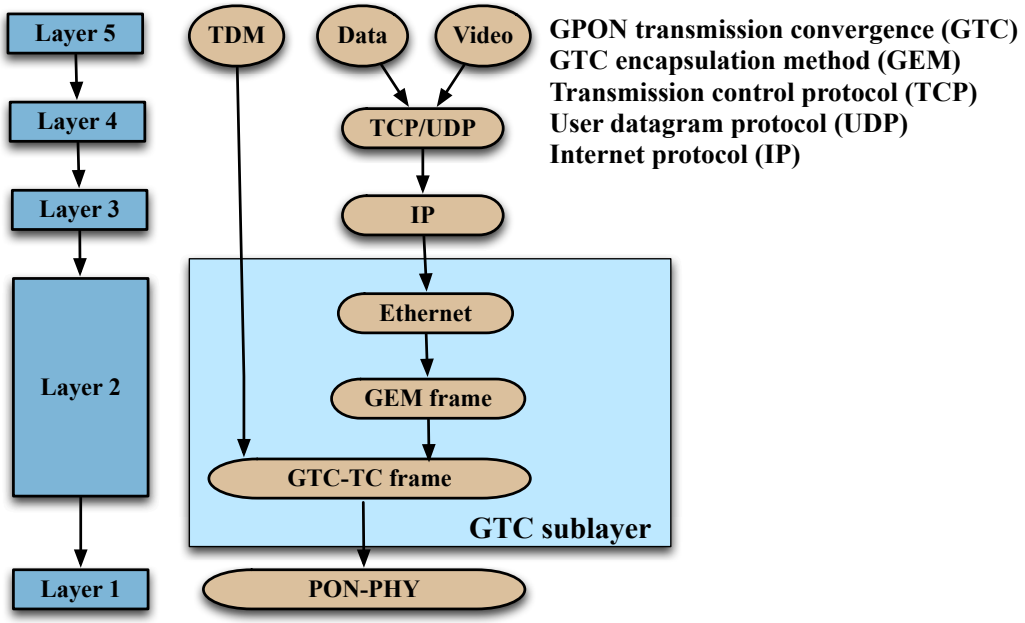

Figure 2.6: GPON framing structure (adapted from [56]).

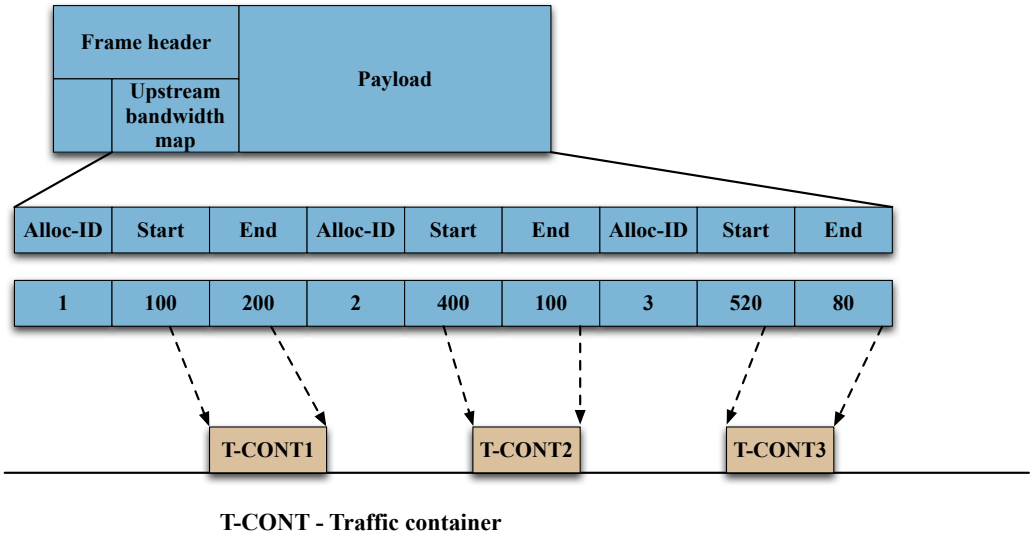

Figure 2.7: Downstream GPON packet structure (adapted from [56]).

time slots allocated to each ONU. It is important to note that although in EPON, the bandwidth grant is for an LLID, in the GPON, the bandwidth grant is per traffic container (T-CONT). A T-CONT is an ONU object representing a group of logical connections that appear as a single entity for the purpose of upstream bandwidth

assignment on the PON. For example, a GPON may have multiple T-CONTs per ONU, each dedicated for a different traffic class, e.g. best-effort and high priority. The allocation ID (Alloc-ID) is used to identify uniquely a T-CONT. The ONUs utilise the dynamic bandwidth report (DBRu) field, located in the header of the upstream GTC frame, to inform the queue length of each T-CONT to the OLT.

2.1.3 Time and wavelength division multiplexed PON

In this section, we will explain the physical and protocol particulars of the TWDM-PON in detail. Figure 2.8 outlines the general architecture of a TWDM-PON. The network comprises multiple wavelengths, fixed-tuned or tunable TRXs at the OLT, and tunable TRXs at the ONUs. A TWDM-PON stacks multiple XG-PONs [58] using these multiple wavelengths to facilitate higher upstream and downstream data rates. A TWDM-PON, therefore, exploits both the increased network capacity of a WDM-PON and resource-sharing of a TDM-PON [59]. In addition to stacking multiple XG-PONs, TWDM-PONs support 10G/10G upstream/downstream transmission, a feature not available in XG-GPON under NG-PON1. Unlike ex-

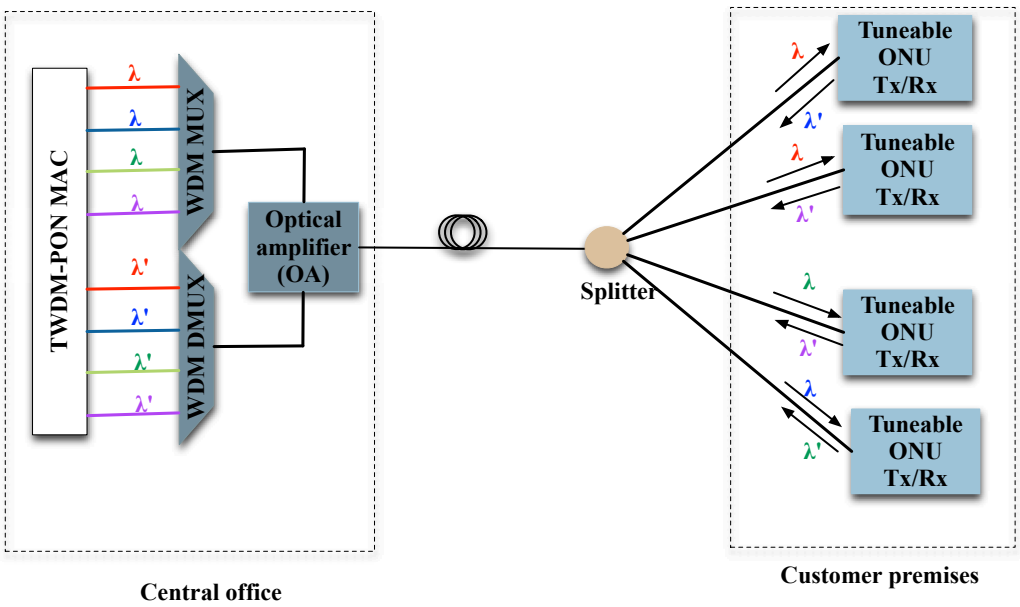

Figure 2.8: General architecture of a time and wavelength division multiplexed passive optical network (TWDM-PON).

isting seeded/reflective WDM-PONs, a TWDM-PON does not have a centralised colourless light source deployed at the OLT and as a result, the TRXs at the ONUs are tunable, allowing access to multiple wavelengths supported by the TWDM-PON. These tunable TRXs at ONUs transmit on wavelengths λ'_1.....λ'_N and receive on wavelengths λ_1.....λ_N as shown in Fig. 2.8. Although deploying tunable TRXs increases the cost of an access network, it also promotes wavelength reconfiguration and energy-savings at the OLT.

One variation of the TWDM-PON frequently discussed in the literature, is the flexible TWDM-PON [60]. Figure 2.9 depicts the main functional blocks of a flexible TWDM-PON. In addition to the ONUs in an ODN sharing multiple wavelengths, in a flexible TWDM-PON, the wavelengths are shared amongst different ODNs as well. The wavelength-sharing across different ODNs yields enhanced capacity and also energy-savings [61]. Although neither TWDM-PON or the flexible TWDM-PON are commercially deployed, they have been numerically analysed [62, 63], simulated [59, 64, 65], and experimentally evaluated [60, 66–71] in recent studies.

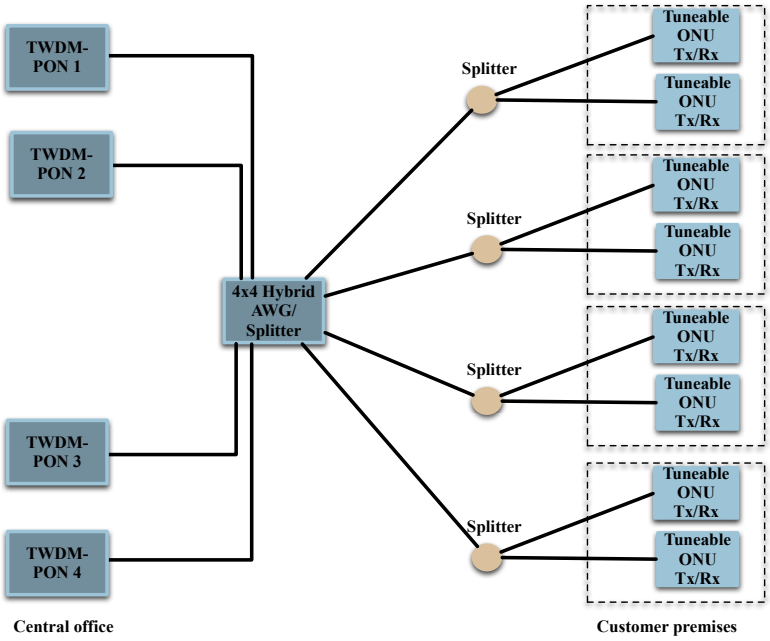

Figure 2.9: General architecture of a flexible TWDM-PON (adapted from [72]).

2.2 Energy-efficient PONs: Challenges and Opportunities

As the popularity of PONs continues to grow, the energy consumption of PONs has become a frequently discussed topic in literature [73–76]. Existing studies have shown that PONs are more energy-efficient, i.e., have lower energy per bit, compared to other wire-line access networks. The low energy consumption is attributed to the lower transmission losses and high data rates of the optical fibre medium [3–5]. Based on current statistics, the ICT contribution towards global energy consumption is 8%, with 30% of it originating from communication networks [77]. Figure 2.10 presents a view of the historical benchmarks for total Internet traffic, which has increased exponentially over the last twenty years [46]. Further, Fig. 2.11 presents the expected growth of the Internet in the next few years. Considering the past and future statistics, the ICT contribution towards carbon footprint is expected to rise from 2%, reported in 2010, to 3% in 2020 [75, 78]. Further, if no energy-conserving technique is applied, the total power consumption is expected to increase from 175.2 TWh/year in 2010 to 13140 TWh/year in 2025 [79]. The potential increase in energy consumption will see network operators investing heavily on operational expenditure (OPEX) and on methodologies to minimise carbon emissions [19–21]. In the long term, the most effective way of addressing these challenges would be to reduce the overall energy consumption of the communication networks. For this purpose, numerous energy-efficient schemes for the PON have been explored by the research community in recent years.

As explained in the previous sections, in both TDM-PON and TWDM-PON, each ONU is assigned a time slot to access upstream bandwidth. Outside this time slot, ONU transmitter (Tx) remains idle, i.e., does not transmit any packets to the OLT. In the downstream direction also, each ONU is assigned a time slot, during which the downstream packets destined for that ONU is sent by the OLT. However, as explained before, due to the broadcast nature of downstream traffic, each ONU receives downstream packets intended for all ONUs in the PON. An ONU processes the MAC addresses of these packets to identify the ones destined for

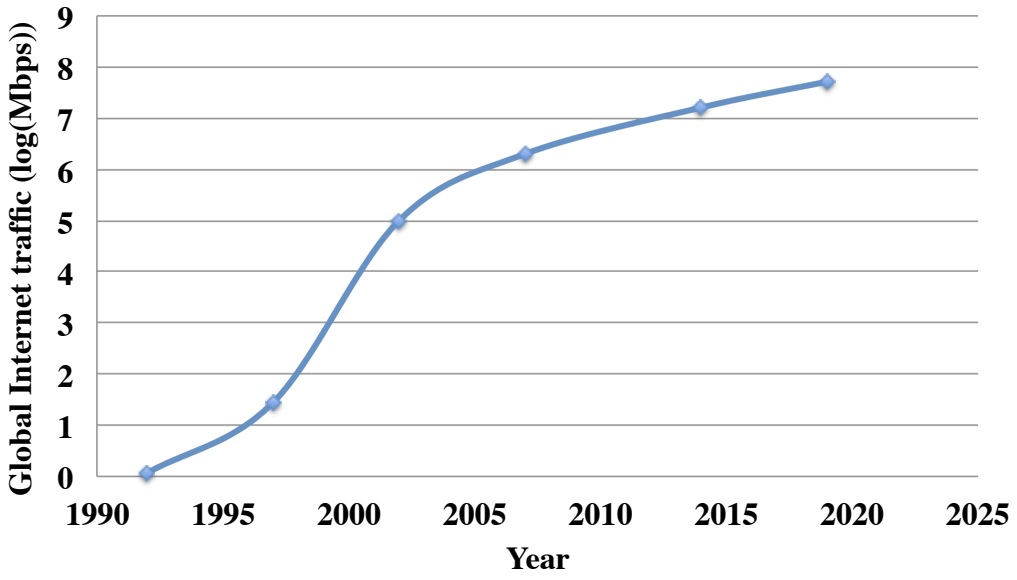

Figure 2.10: Historical benchmarks for total Internet traffic (adapted from [72]).

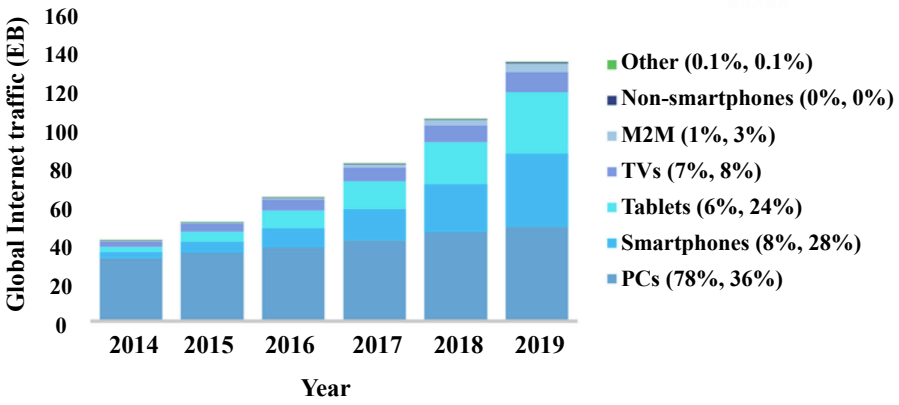

Figure 2.11: Global IP traffic forecast [72].

itself and to discard the rest. As a result, an ONU receiver (Rx) is idle when it is not processing its own packets or the MAC addresses. Due to these upstream and downstream bandwidth access criteria, an ONU TRX is in idle state, i.e., does not transmit/receive or process packets, for a majority of its polling cycle. Despite being in idle state, an ONU continues to operate at its maximum power level, known as the power consumption in active mode. This active power consumption, coupled with the large number of ONUs present in the network, make the ONUs, the

major contributor in energy consumption of the access segment [1, 22, 80]. Instead of remaining active, if an idle ONU can transition into a low-power mode during its idle time, the energy consumption of the access network can be significantly reduced.

After analysing user traffic patterns and ONU architectures, sleep, doze, and power shedding operations were identified by ITU-T as appropriate methods of minimising the energy consumption of a TDM-PON [23]. These operations involve powering down individual components of the ONUs based on the network traffic and the idle time. In a TWDM-PON, supported by the tunability of the ONUs, idle wavelengths could also be switched off to improve the energy-savings at the OLT. Before we present our technical contribution that exploits the sleep/doze operations and wavelength reallocation, this chapter presents a comprehensive analysis of existing studies carried out to improve the energy-efficiency of the TDM-PON and TWDM-PON, using these techniques. As an introduction to this analysis, the next sections explain the sleep/doze operations and wavelength reallocation method in detail.

2.2.1 Power shedding, sleep, and doze operations

Before being implemented in PONs, sleep, doze, and power shedding operations were first proposed to improve the energy-efficiency of wireless sensor networks [81–83] and local area networks (LANs) [20, 84–86]. As wireless sensor nodes are battery operated, reducing the energy consumption and thus prolonging the operating lifetime outweighed meeting quality of service (QoS) requirements in wireless sensor networks. In an attempt to get the wireless networks more customer-focused, the IEEE 802.16 working group standardised the wireless metropolitan area networks (WMANs) and next generation broadband wireless access systems [87–89]. With the high mobility of mobile stations (MSs) added as an essential requirement of these future wireless networks [90], prolonging the battery life of MSs became a critical issue [91]. As a solution, sleep mode operation was first introduced in the IEEE 802.16e standard. Since then, sleep-capable energy-efficient

wireless networks have been studied extensively by various research groups in literature [92–97].

Meanwhile, the comparable behaviour between wireless networks and PONs pointed at the possibility of incorporating sleep mode in the PONs as well. As a result, the sleep, doze, and power shedding operations were standardised by the ITU-T G.45 for PON [23]. The sleep mode operation is further divided into cyclic sleep and deep sleep, where the cyclic sleep involves an ONU periodically waking up to see if there are any incoming packets from the OLT. Under deep sleep, an ONU sleeps for the duration of its idle time, without waking up intermittently.

To understand these operations, we will first explain the building blocks of a typical ONU. An ONU consists of a TRX, a continuous mode clock and data recovery (CM-CDR) unit, and a back-end digital data circuit [24]. The TRX sends and receives packets to and from the OLT while the CM-CDR keeps the ONU in sync with the OLT. The back-end circuitry carries out digital signal processing activities, such as buffering upstream data received on the customer network interface (CNI), analysing downstream packets, and error correction and equalisation. During power shedding operation, certain parts of an ONU is powered down based on the network load. However, when in power shedding mode, the TRX block is always kept "on". During sleep mode, both Tx and Rx are powered down, while, in doze mode, only the ONU Tx is powered down [98]. It is important to note that in both sleep and doze mode operations, the digital back-end circuitry is always kept active to receive incoming packets at the CNI.

Sleep mode saves more energy than doze mode, as more components are powered down during sleep mode operation. However, during its normal operation, an ONU receives a continuous clock and data recovery bit stream from the OLT, which is used by an ONU to stay in-sync with the OLT. When an ONU enters into sleep mode, as the Rx is powered down, the ONU cannot receive this bit stream. As a result, an ONU has to incur some overhead time, sleep-to-active transition time, $T_{sleep-to-active}$, before resuming its packet exchange with the OLT. During doze mode operation, however, an ONU can still receive synchronisation bits from the OLT. Consequently, the $T_{sleep-to-active}$, of an ONU is generally higher

than its doze-to-active transition time, $T_{doze-to-active}$. The $T_{doze-to-active}$ accounts for the settling time of an ONU when transitioning from doze to active mode.

2.2.2 Wavelength reallocation

In a network with a single wavelength allocated in each direction, only sleep or doze mode will result in energy-savings. However, as discussed in Section 2.1.3, a TWDM-PON deploys multiple wavelengths in both upstream and downstream directions and the TRXs at the ONUs are tunable across these multiple wavelengths. Due to the tunability, depending on the network load, certain wavelengths may be switched off, and the ONUs can be reallocated amongst remaining active wavelengths [99]. This technique, referred to as wavelength reallocation for the rest of the thesis, results in substantial energy-savings at the OLT.

Wavelength assignment can be done either separately or jointly with the bandwidth assignment. These two techniques are known as separate time and wavelength scheduling (STWS) and joint time and wavelength scheduling (JTWS) [100]. In STWS, the wavelength assignment can be either static or may adapt to varying network loads. In JTWS, the OLT follows the first wavelength available (FWA) criterion and assigns a given ONU to the first available wavelength. If no wavelength is available, the wavelength with the earliest finish time (EFT) is selected as the potential wavelength. When following this approach, however, voids may appear in the time domain. To overcome the inefficiencies caused by voids, the criterion known as void-filling EFT (VF-EFT) [101] is followed by the OLT. Under the VF-EFT criterion, the OLT keeps track of unused time slots in the upstream wavelengths and assigns an ONU to the first available void that is greater than the ONU's bandwidth requirement.

As a TWDM-PON combines multiple XG-PONs, the sleep/doze mode operations previously proposed for the TDM-PON can also be incorporated into the TWDM-PON as well. While the wavelength reallocation minimises the energy consumption at the OLT, conventional sleep and doze mode operations minimise the energy consumption at the ONUs, thereby minimising the overall energy con-

sumption of the TWDM-PON the energy consumption of the TWDM-PONs. Next, a detailed account of how these energy-saving techniques are used in minimising the energy consumption of the TDM-PON and the TWDM-PON, is presented.

2.3 Energy-efficient TDM-PONs using sleep and doze mode operations

When improving the energy-efficiency of PONs using sleep and doze mode operations, two main approaches are taken; (1) hardware improvements to the ONU architecture and (2) algorithm-based improvements incorporating sleep and doze operations. As hardware improvements enable the use of sleep/doze mode operations in the algorithms, we will first discuss the hardware improvements carried out on the ONU structure. This will be followed by a discussion on sleep/doze mode bandwidth allocation algorithms.

2.3.1 Hardware improvements to support sleep/doze mode operations

In a given ONU polling cycle, the energy consumption of a sleep/doze-capable ONU can be expressed as follows:

$$E = P_{active} * T_{active} + P_{sleep/doze} * T_{sleep/doze} \tag{2.1}$$

where parameters E, P_{active}, T_{active}, $P_{sleep/doze}$, and $T_{sleep/doze}$ represent the energy consumption of an ONU per cycle, the ONU power consumption in active mode, the time an ONU spends in active mode, the ONU power consumption in sleep/doze mode, and the time an ONU spends in sleep/doze mode, respectively. Based on Eq. 2.1, reducing the power consumption values of each state, i.e., sleep, doze, and active, reduces the energy consumption of an ONU.

Moreover, an ONU in sleep or doze mode consumes comparatively less power than an active one. Therefore, in a given cycle, increasing the time an ONU spends in sleep or doze mode also reduces the energy consumption of an ONU. As an ONU waking up from sleep/doze mode incurs a certain overhead time before

resuming its operation, $T_{sleep-to-active}$ and $T_{doze-to-active}$, the actual time an ONU spends in sleep or doze mode, $T_{sleep/doze}$, is expressed as follows:

$$T_{sleep/doze} = T_{idle} - T_{sleep/doze-to-active} \tag{2.2}$$

where parameter T_{idle} represents the idle time of an ONU. Based on Eq. 2.2, reducing the transition times, $T_{sleep-to-active}$ or $T_{doze-to-active}$, reduces the energy consumption of an ONU. The hardware improvements to the ONU architecture, therefore, involve reducing the power consumption in each state and reducing the transition overhead times of the ONUs. The distributed feedback ONUs (DFB ONUs) and the vertical-cavity surface-emitting laser ONUs (VCSEL ONUs) are the two main types of ONUs considered in existing literature. In the following sections, we discuss the hardware improvements made to these two architectures in detail.

2.3.1.1 Hardware improvements to distributed feedback laser ONU

In [24], Wong *et al.* proposed two ONU architectures to minimise the sleep-to-active overhead time. Instead of the conventional CM-CDR circuit, the proposed design uses a burst mode CDR (BM-CDR) for clock recovery and employs a local oscillator (LO) to keep relative clock synchronisation with the OLT. The new architecture is capable of reducing the $T_{sleep-to-active}$ to as low as 1 ns. Compared to the typical sleep overhead time of 2-5 ms, a value in the scale of ns will result in significant energy-savings. The purpose of the second ONU architecture is not to reduce the energy consumption, but in fact, to lower the cost of the ONU. Even though the cost of the LO is not significant, in the proposed second architecture, the LO is replaced with a new sleep control unit to minimise the cost of the ONU further. The authors experimentally evaluate the first architecture in [28] and show that the ONU can transition between sleep and active modes in 74 ns. Under their proposed just-in-time (JIT) DBA algorithm, this fast-clock-recovery ONU achieves 60% of energy-savings at low network loads.

Igwa *et al.* propose an ONU with a burst mode TRX employing dynamic power saving control [102]. Identifying the doze mode as a favourable power-saving

mechanism at high network loads, the proposed ONU reports a short settling time of 736 ns when transitioning between doze and active states. The fast transition is made possible by the LD driver block that activates the burst mode operation. The performance of the proposed ONU is evaluated and compared against an ONU with a $T_{doze-to-active}$ of 2 ms and an ONU with no power-saving control. Compared to a conventional doze mode ONU, the proposed burst mode ONU yields percentage energy-savings of 37 % and 67 % at the packet inter-arrival times of 1 ms and 100 ms, respectively.

As explained in Section 2.2.1, during cyclic sleep mode, an ONU wakes up periodically to check for arriving downstream traffic from the OLT. Even though cyclic-sleep results in substantial energy-savings, frequent waking up prevents an ONU from achieving maximum possible energy-savings. In [103], Newaz *et al.* propose a sleep mechanism where the ONUs wake up only if there is downstream data from the OLT. The proposed solution is realised using a hybrid ONU (H-ONU) architecture, which is a conventional ONU equipped with a low-cost low-energy consuming IEEE 802.15.4 module. This module powers on the ONU when it needs to receive downstream traffic, thereby eliminating periodical waking-up. The proposed solution, however, requires all the H-ONUs to be part of a wireless sensor network, thus increasing the complexity of the system.

2.3.1.2 Hardware improvements to vertical-cavity surface emitting laser ONU

In laser technology, much consideration is given to decreasing the length of the gain medium as it reduces the number of modes supported by the laser, thereby mitigating modal dispersion. From a practical perspective, it is easier to change the vertical distance of such gain material than changing its horizontal distance. As a result, vertical-cavity surface-emitting lasers (VCSEL) have become popular in the area of optical Txs. Figure 2.12 illustrates a basic block diagram of a VCSEL ONU considered in our work. A VCSEL consists of a short active region sandwiched between layers of dielectric mirrors. The light travels vertically and leaves through the mirrors. In the studies reported in [104–108], a new 10 Gbps VCSEL

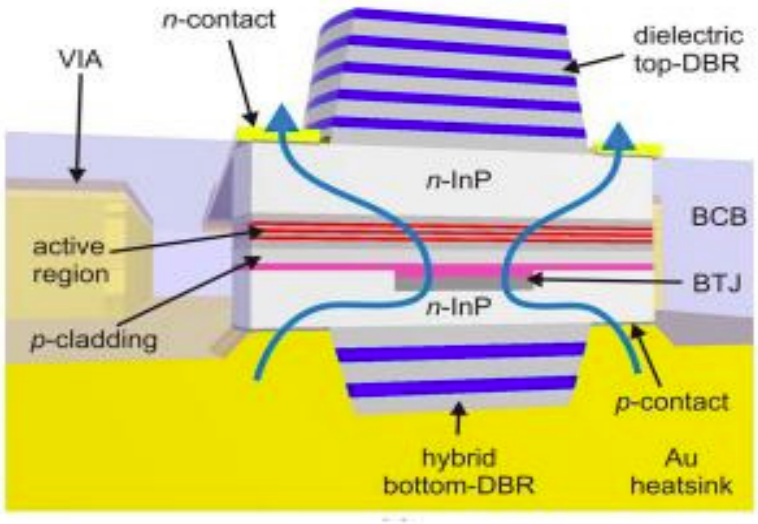

Figure 2.12: General architecture of a 10 Gbps VCSEL [72].

(10G-VCSEL) Tx is proposed and experimentally evaluated for bit rate and supported wavelengths. Studies reported in [105, 106], present a detailed description of the device structure and its DC and thermal characteristics. In [29, 109], the authors used this VCSEL as the ONU Tx and experimentally evaluated the settling times of the 10G-VCSEL ONU. Based on this study, the 10G-VCSEL ONU is able to transition into sleep and doze modes and have $T_{sleep-to-active}$ and $T_{doze-to-active}$ of 2 ms and 330 ns, respectively. The 10G-VCSEL ONU therefore, has a comparative advantage over the DFB ONU, which has a slower $T_{doze-to-active}$ of 736 ns [102]. Further, compared to DFB ONUs, which consume 5.05 W of power when active, the 10G-VCSEL ONU consumes only 3.94 W power in the active state [29]. The short $T_{doze-to-active}$ and low power consumption in the active state make the 10G-VCSEL ONU a good contender for energy-efficient PONs. It is important to note that in our proposed solutions presented in Chapters 3-6, we have used this 10G-VCSEL as the Tx of our ONU. Table 2.1 lists the power consumption and switching values of the 10G-VCSEL ONU.

Table 2.1: Power consumption and switching values of 10G-VCSEL ONU [29]

Parameter	Value
Doze-to-active transition time	330 ns
Sleep-to-active transition time	2 ms
Power consumption (active)	3.984 W
Power consumption (doze)	3.85 W
Power consumption (sleep)	0.75 W

2.3.2 Algorithm-based solutions with sleep/doze mode operations

In one of the early studies reported on energy-efficient bandwidth allocation algorithms for EPON, Zhang *et al.* discussed the importance of having a proper medium access control (MAC) mechanism for the EPON [110]. As we discussed in the previous section, the physical modifications to the ONU architecture enable the ONUs to enter into sleep and doze. Implementing sleep and doze mode operations also has other implications such as a sleeping ONU not receiving synchronisation bits from the OLT and multiple ONUs waking up from sleep/doze trying to access upstream bandwidth simultaneously. To minimise such adverse effects, the communication between the ONUs and OLT should be properly scheduled. For this purpose MAC messages are used for this purpose in the GPON and EPON. As explained in Section 2.1.2, the MAC control protocols such as MPCP are not unique to any bandwidth allocation algorithm. As a result, different types of bandwidth allocation algorithms, that cater to different network requirements, are proposed for the TDM-PON.

In a broad sense, there are two main types of bandwidth allocation algorithms currently investigated in literature, namely, fixed bandwidth allocation (FBA) algorithms and dynamic bandwidth allocation (DBA) algorithms. Under FBA algorithms, the OLT allocates a fixed amount of upstream/downstream bandwidth to an ONU, irrespective of its bandwidth requirement. Although this approach is less complicated, considering the varying bandwidth requirements of different networks at different times of the day, FBA does not make the best use of network resources. Contrary to the FBA, DBA algorithms take the individual bandwidth requirement of ONUs into account when allocating upstream/downstream

bandwidth, resulting in efficient use of network resources and ensuring fairness amongst ONUs. As a result, much attention is paid to DBA algorithms in literature. In this section, we discuss some of the existing sleep/doze mode DBA algorithms proposed for the TDM-PONs.

One of the earliest DBA algorithms proposed for the EPON was interleaved polling with adaptive cycle time (IPACT). If the OLT allocates bandwidth to an ONU and waits until it receives the corresponding REPORT message from the ONU, before it transmits the GATE message to the succeeding ONU, a complete messaging round-trip is wasted during which the upstream channel may remain idle. In the IPACT algorithm, the OLT sends downstream grant messages to succeeding ONUs while receiving transmissions from previously granted ONUs. Later on, many DBA algorithms, incorporating this concept, were proposed to cater to different requirements of the network such as energy-efficiency, latency [111–116], jitter [117–119], and throughput [120–122]. As energy-efficiency is the primary focus of this thesis, in this section, we will look into the energy-efficient DBA algorithms proposed for TDM-PON. These solutions address different aspects of sleep mode operation, such as: (1) maximising energy-savings with sleep/doze operations; (2) determining sleep/doze duration; (3) achieving a balance between energy-efficiency and QoS; and (4) integrating sleep mode with existing energy-saving techniques.

2.3.2.1 Maximising energy-savings with sleep/doze operations

As discussed in Section 2.2.1, compared to the other energy-saving strategies, sleep mode saves more energy in general. Consequently, earlier studies on energy-efficient TDM-PONs incorporated only sleep operation into their DBA algorithms. However, due to the emerging ONU architectures with shorter $T_{doze-to-active}$, and the necessity to achieve energy-saving across a larger range of network loads, doze mode is then incorporated into the DBA algorithms. Irrespective of the energy-saving mode implemented, to maximise the energy-savings through the DBA, the sleep/doze duration should be increased. In this section, we discuss different ap-

proaches taken to increase the sleep/doze length of an ONU.

One of the first DBA algorithms that incorporate sleep mode has been proposed for GPON by Smith *et al.* in [26]. According to the sleep mode operation defined in [23], when the OLT wakes up an ONU in the sleep state, the OLT suspends its services to all othere active ONUs. Given the suspension period of an ONU located 20 km away from the OLT is approximately 250 μs, it adds a relative delay to a network operating in gigabit/s data rate. To overcome this re-activation overhead, within each cycle, a minimum upstream bandwidth is assigned to an ONU in sleep mode. When upstream traffic is present at its customer network interface (CNI), the ONUs can use this bandwidth to send its request to exit from sleep mode. Simulation results reported on this study indicate the proposed solution results in much quicker re-activation process and thereby, allows the ONUs to go into sleep mode frequently. In a similar attempt, Mandin *et al.* presented a detailed analysis of sleep mode and discuss OLT-initiated and the ONU-initiated sleep modes [27]. The study explains the components that are switched off during sleep mode and also presents the energy consumption of electrical and optical components in sleep mode.

To further reduce the energy consumption of a sleep mode ONU, Wong *et al.* proposed a Just-In-Time (JIT) DBA algorithm, where an ONU in sleep mode wakes up JIT to receive its GATE message and the downstream data from the OLT [28]. The significant energy-savings reported in this study is attributed to the ONU with fast clock recovery used this work. In addition to the JIT nature of the proposed DBA, the authors have also synchronised the upstream and downstream transmission time slots. The synchronisation enables the ONUs to switch off both Tx and Rx after sending the REPORT messages, thus increasing sleep duration and the overall energy-savings. In [123], Dung *et al.* followed a similar criterion, where the upstream and downstream communication are scheduled in the same transmission slot and allowing the ONU to sleep during its idle time outside the slot.

In a majority of the DBA algorithms designed for TDM-PON, the OLT uses either upstream or downstream network traffic to allocate upstream and downstream bandwidth. This approach is justified based on the fact that current Inter-

net users upload and download similar amounts of data over the network. However, in [124], Wang *et al.* proposed a double-way polling DBA algorithm, which considers both upstream and downstream bandwidth requirements when allocating bandwidths to respective ONUS. Further, the proposed algorithm follows the standard procedure recommended in IEEE for sleep mode operation and assigns a fixed sleep duration irrespective of the network load. The study reports significant energy-savings, particularly at the low network loads, and acceptable average delay values to support voice and video-on-demand (VoD) services.

In a similar attempt, Van *et al.* proposed cooperative sleep-triggering mechanisms to initiate sleep mode at the ONUs [123, 125]. Under the proposed solution, an ONU enters into sleep mode only if both upstream and downstream is low. The OLT estimate the average inter-arrival time of downstream packets and decides to send an ONU into sleep mode if the estimated value is less than the threshold. Meanwhile, the ONUs estimate the average inter-arrival time of upstream packets, and when an ONU receives a sleep request from the OLT, it enters into sleep mode, only if this estimated value is less than the threshold. As such, both upstream and downstream traffic load is considered before an ONU enters into sleep mode.

In the DBA algorithms discussed so far, the sleep or doze mode operations are implemented only at the ONUs. Due to the broadcast nature of downstream traffic and multiple subscribers (ONUs) sharing its client-side port, the OLT needs to be active most of the time. As a result, the idle time of an OLT is usually less than the $T_{sleep-to-active}$. Several studies, however, have proposed energy-efficient solutions to minimise the energy consumption both at the OLT and the ONUs using both sleep and doze mode operations. In [126], Li *et al.* proposed a DBA algorithm that incorporates both sleep and doze mode operations to improve energy-savings of the entire network. Taking the inter-arrival time of packets, packet size, and sleep duration into consideration, the authors investigate which power saving mechanism, fixed cyclic-sleep mode or dynamic sleep/doze mode, results in maximum energy-savings at the ONUs and the OLT. Simulation results reported in this study indicate that the fixed cyclic-sleep achieves maximum energy-savings at the ONUs

while doze mode is more appropriate for busy OLTs.

In a further analysis, Li *et al.* evaluated different power-saving mechanisms for the entire PON, i.e., OLT, ONUs, and aggregation switches [127]. The findings of this study further support their previous claim that fixed polling cycles yield maximum energy-savings at the ONUs and doze mode is more appropriate for OLTs. The results, however, indicate that when using fixed polling cycle times, there is a trade-off between high energy-savings and packet delay. To meet stringent delay requirements of the network, the authors propose a hybrid sleep mechanism, where the ONUs follow fixed cycle times in the absence of traffic and dynamic cycle times in the presence of traffic.

Another area of interest, usually considered in maximising the sleep/doze duration is altering the control message scheduling. In the energy-efficient DBA (EDBA) proposed in [128], Dung *et al.* exploits the conventional traffic flow between the OLT and the ONUs to increase energy-savings at the ONUs. Under normal operation, after sending its REPORT message, the ONU is idle until it receives the corresponding GATE message from the OLT. In a long-reach PON (LR-PON), due to the long propagation delay, this idle period is significantly high. Using this idle period to improve the energy-savings further, the EDBA transitions an ONU into doze mode during this time. Simulation results show that the EDBA can save a noticeable amount of energy, especially as the round trip time (RTT) increases. Their subsequent work, ASDBA, on energy-efficient LR-PONs enhances the previously reported energy-savings further by changing the scheduling order of the control messages, GATE and REPORT. Instead of sending the REPORT message first and waiting for the corresponding GATE message, the OLT sends the GATE message first, followed by the REPORT from the ONU. After sending the REPORT message, the ONUs enter into sleep mode as specified by the GATE message. As a result, instead of transitioning into doze mode and then sleep mode, the ONUs enter into sleep mode straight after the REPORT message.

In addition to the DBA algorithms we discussed so far, other areas of interest in energy-efficient TDM-PONs involve, sleep mode operation for redundant PON networks [129] and the effect of sleep mode on Transmission Control Proto-

col performance in the PON [130,131]. Under the normal operation of a redundant PON, the OLT monitors the data exchange between the OLT and the ONUs. If an ONU does not respond to a GATE message within a specified time, the OLT assumes it to be a link failure and initiates link switching. When an ONU enters into sleep mode, some ONUs may not wake up in time to respond to the GATE before the fault detection time. As a result, unnecessary link switching may occur in a network. However, if the OLT receives the corresponding REPORT message, no erroneous fault would be detected. For this purpose, the proposed solution in [129] uses "watchdog" ONUs to inspect the GATE message. In sleep/doze DBA algorithms, the data link layer is modified to improve the energy-efficiency of the network. Introducing sleep mode operation also increases the RTT of the message flow, thereby reducing the TCP throughput of the network [130,131].

2.3.2.2 Determining sleep and doze duration

Due to its high correlation with energy-savings and QoS, determining the sleep or doze duration of an ONU is one of the most important aspects of any sleep/doze DBA algorithm. As such, a separate research area of sleep/doze operation is dedicated to investigating various criteria for determining this important parameter. One such method would be to determine the polling cycle time, T_{poll} first and then, derive the sleep/doze duration from it. In studies reported in [24,132], the polling cycle time, T_{poll}, is the sum of transmission time slots, T_{slot}. Under the proposed solution, the sleep duration, T_{sleep}, is calculated as the difference between the T_{poll} and T_{slot}. A low network load results in low T_{slot}, T_{poll}, and eventually low T_{sleep}. Similarly, in [133], low network loads are associated with shorter T_{poll} and T_{sleep}. In both cases, the percentage of energy-savings achieved at low network loads are lower than that of high network loads. The superior energy-savings reported at low network loads in [133] is credited to the minimum sleep time (MST) allotted to each ONU at low network loads and the fast $T_{sleep-to-active}$ of the ONU considered in this work [24]. As per the upstream user profile simulated on [134], practical PONs operate at network loads less than 0.6. Consequently, it is important to en-

sure that energy-savings are maximised at low network loads, irrespective of the type of ONU used. Allocating sleep/doze time based on the traffic load of a given ONU has been identified as an effective way of addressing this problem.

The basis for using traffic load in determining the sleep time is that when the traffic load is low, the ONUs can afford to go into sleep/doze mode for a longer duration without influencing the QoS of the network. For this approach to be successful, the OLT should be made aware of the traffic condition at each ONU. For this purpose, the average inter-arrival time of packets at the ONUs is used as a useful parameter that reflects the network load of the ONUs. Along with its bandwidth requirement, an ONU sends the average inter-arrival time of incoming packets through the REPORT message.

In initial studies utilising average inter-arrival time to determine the sleep/doze time, a fixed sleep duration is allocated to an ONU, when its inter-arrival time exceeds a given threshold. In their proposed hybrid method, Wong *et al.* assigned a fixed T_{sleep}, if the average inter-arrival time is $\leq$ a given threshold. Despite the fact that the proposed solution is less complicated, it adversely affects QoS parameters such as average delay. When the network load increases, a fixed T_{sleep} will increase the polling cycle time, resulting in an increase in the average delay. Although a fixed but shorter T_{sleep} will solve this problem, it will prevent the network from achieving maximum energy-savings at low network loads. As such, allocating a fixed T_{sleep} is not an attractive solution.

To address this shortcoming, allocating a variable T_{sleep} that adapts to varying network loads is proposed in recent literature. One such approach is exponentially increasing the T_{sleep} based on the network load. In studies reported in [135–138], the OLT allocates a minimum T_{sleep} to an idle ONU and exponentially increases the T_{sleep} until it reaches a maximum. The maximum and minimum sleep values are determined based on the QoS restrictions on the network.

A similar approach widely used in determining the sleep or doze duration is using a pre-determined sleep/doze control function. This technique involves allocating a particular sleep or doze period for a given network load. When the OLT determines the network load through the average inter-arrival time, it refers to the

sleep/doze control function to determine the sleep/doze duration. In [139], Kubo *et al.* proposed a sleep-control function with two threshold values. Based on the average inter-arrival time, the OLT will allocate one of the two sleep durations associated with these thresholds. To make the solution more adaptive towards network load, Kubo *et al.* and Fiammango *et al.* also proposed linear sleep control functions in [140,141]. Under the proposed solutions, the sleep duration is linearly increased with the increase in average inter-arrival time.

In the solutions that associate sleep/doze time to the network load, determining the average inter-arrival time of upstream/downstream packets is a critical aspect. The average inter-arrival time, used by the OLT, is usually evaluated at the ONUs using different estimation techniques, such as arithmetic averaging [141] and exponential smoothing [140]. Like in any other estimation method, the accuracy of these estimation techniques improve with the sample size of inter-arrival times considered.

2.3.2.3 Sleep mode and other energy-saving techniques

The popularity of sleep operation also motivated work that combined sleep mode with existing power-saving methods, such as adaptive link rate (ALR) control. Compared to a high-rate data link, a low-rate consumes less power. Exploiting this general concept, the ALR function involves changing the bit rate of a communication link based on the amount of network traffic. In [84], Gunaratne *et al.* showed that due to the high probability of a LAN link operating at a low link rate, significant energy-savings can be achieved by downgrading the link rate. In [142, 143], Kubo *et al.* proposed an energy-saving mechanism that uses sleep mode operation in conjunction with ALR. Using illustrative two link rates, 1 Gbps and 10 Gbps, the authors show that the proposed solution results in significant energy-savings both in the presence and absence of network traffic.

In [142, 143], the DBA algorithms uses fixed threshold values to determine the line rate and to decide whether to enter sleep mode or otherwise. Also, as the sleep duration of an ONU is fixed at 10 ms, the ALR control function proposed

in [142, 143] does not achieve maximum energy-savings across the entire range of network loads. To overcome this problem Zhang *et al.* proposed a DBA algorithm that exploits no only both sleep mode and ALR, but also uses variable threshold values and sleep durations for optimum energy-savings [144].

So far in this discussion, we have highlighted the positive outcomes the sleep and doze mode operations. However, incorporating sleep/doze mode operations present few challenges that should be carefully addressed. In the next section, we discuss these key challenges and steps taken to address them.

2.3.2.4 QoS and sleep/doze mode operations

One of the disadvantages of implementing sleep mode is the penalty it imposes on QoS parameters such as delay and throughput. In their impact study on energy-savings and QoS, Newaz *et al.* evaluated the effect of different sleep durations on energy-savings and average delay experienced by the ONUs. Based on their findings, a longer sleep duration increases energy-savings, but also increases the average delay. As illustrated in [22, 144], when using sleep mode, the QoS and energy-savings cannot be improved simultaneously, resulting in numerous efforts made to achieve a balance between the energy-savings and QoS.

In [145], Sarigiannidis *et al.* proposed an energy-efficient DBA algorithm that also improves the throughput of the network. At low network loads, when there is no packets at its incoming queue, an ONU may send null REPORT messages to the OLT during multiple cycles. However, in such a scenario, the ONU is able to sleep for multiple cycles, rather than waking up to send the control message to the OLT. In this study, each ONU maintains a sleep window, which represents the number of cycles the ONU is able to sleep. When no traffic is present in its queue, rather than sending a null REPORT message, the ONU increases its sleep window by one. Moreover, the OLT will not poll a sleeping ONU, unless it receives a REPORT message from the ONU. As this scheme reduces the number of control messages exchanged between the OLT and the ONUs, it improves the network throughput as the OLT can assign more bandwidth for actual data delivery rather than for

control messages [145].

In similar attempts, Ren *et al.* [135] and Bang *et al.* [146] mathematically analysed the effect of sleep mode on average delay. In general, a longer sleep duration increases the potential energy-savings at the expense of average delay. As such, the sleep duration cannot be increased arbitrarily. In the probabilistic model proposed in [135], Ren *et al.* considered two sleep durations, T_{min} and T_{max}. In the beginning, the OLT allocates a minimum sleep duration of T_{min} to an idle ONU and, based on the traffic load at the ONU, exponentially increases the sleep duration until it reaches T_{max}. The study investigates the effect, different T_{min} and T_{max} have on energy-savings and average delay. In [146], using state probabilities of sleep and active states, Bang *et al.* mathematically derived the optimum sleep duration that will ensure a balance between average delay and energy-savings. These analytical models are crucial aspects of the sleep/doze mode energy studies, as they allow us to formulate mathematically different aspects of the network, namely power consumption, delay, and throughput, using network parameters such as the number of ONUs, propagation delay, and RTT. When designing DBA algorithms for TDM-PONs, these analytical models are frequently used to determine the energy-savings and expected average delay of the network.

One of the important factors usually overlooked when incorporating sleep mode operation is the ONU buffer size. When an ONU enters into sleep mode, packets are accumulated at the UNI. To avoid excessive packet losses, the ONU buffer size should be increased accordingly. To address this issue, Bang *et al.* implemented an analytical model to find the ONU buffer sizes required to achieve optimum energy-savings [147]. Using the state probabilities associated with buffer sizes, sleep periods, and inter-arrival time of packets, the authors formulated the average buffer levels, power consumption, and delay. These values are then used to estimate buffer size and the variable sleep period required for optimum energy-savings.

In addition to QoS degradations, frequent switching of network equipment may also adversely affect the performance of network equipment. As pointed out in [148], frequent switching between active and sleep states can increase the risk of

equipment failure, which in turn results in higher operational expenditure. When an ONU changes its state between sleep and active, it undergoes a temperature variation. According to the Coffin-Mason model when a device is put into sleep mode more frequently, it reduces the lifetime of the device [149, 150]. Concluding our discussion of sleep/doze mode operations in the TDM-PON, we can deduct that the energy-savings due to sleep mode operation is beneficial to a certain extent compared to its QoS degradation and the cost associated with equipment failure.

2.4 Energy-efficient TWDM-PON with wavelength optimisation and sleep/doze operations

Although the TWDM-PON has only being proposed recently, its energy-efficiency has already drawn noticeable attention [3, 151, 152]. In their analytical study of prospective NG-PON2 architectures, Lambart *et al.* evaluated the energy consumption of NG-PON2 technologies, such as XLG-PON, TWDM-PON, OFDM-PON, and Coherent ultra-dense WDM (Co-UDWDM)-PON [151, 152]. In view of their numerical results shown in Fig. 2.13, the TWDM-PON is an attractive solution from an energy perspective. While the power consumption of the OLT is com-

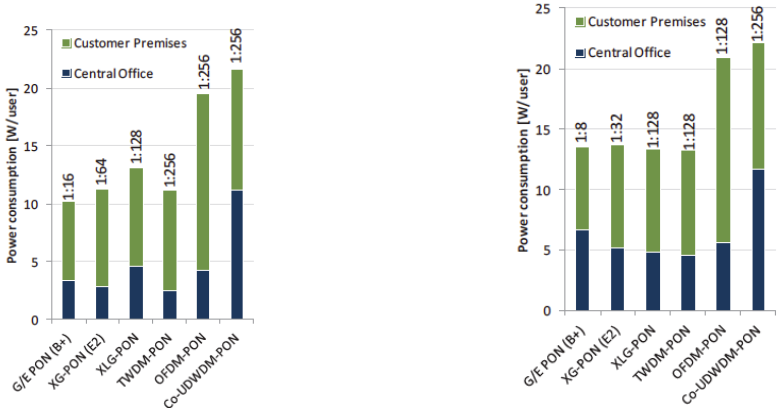

(a) 600 Mb/s (b) 1 Gb/s

Figure 2.13: Power consumption at the customer premises equipment (CPE) and CO of the considered PON solutions for a target bandwidth of (a) 600 Mb/s and (b) 1 Gb/s using an ODN with a flexible split ratio

paratively higher in TWDM-PON due to multiple line cards and wavelengths, the large number of subscribers serviced by the TWDM-PON results in lower energy per user. Although the TWDM-PONs are energy-efficient by nature, considering its expected growth, future-proofing the TWDM-PON regarding energy-efficiency has become an important issue. As a result, the energy-saving potential of the TWDM-PON has been investigated from different perspectives in recent literature.

As discussed in Section 2.1.3, a TWDM-PON consists of multiple wavelengths and most importantly, tunable ONU TRXs that can tune to any of the wavelengths present in the network. The tunability of the ONUs offers a certain degree of freedom to dynamically reconfigure the network. For example, at low network loads, the network may not need all the wavelengths in the network to operate, and some wavelengths may be switched off, after transitioning the ONUs supported by these wavelengths to other wavelengths. The tunability of the wavelengths, therefore, leads to potential energy-savings at the TWDM-PON [25, 153], specifically at the OLT, while conventional power-saving methods, sleep, and doze, are can be implemented at the ONUs to achieve overall energy-efficiency [22]. As a result, recent energy-efficient solutions for TWDM-PON include dynamic wavelength and bandwidth allocation (DWBA) algorithms incorporating wavelength reconfiguration and sleep/doze mode operations. The DWBA algorithms, therefore, rely on the physical characteristics, tunability, and the sleep/doze capabilities, of the ONUs for this purpose. As we have already discussed the hardware-based solutions proposed for sleep/doze mode operations, we will only evaluate the tunability of the ONUs in this section. We will then explain the DWBA algorithms proposed using these physical characteristics.

2.4.1 Hardware improvements to support wavelength reallocation in TWDM-PON

As we explained in the previous section, to switch off idle wavelengths, the ONUs must be able to tune into different wavelengths deployed in the network. As such, numerous studies have examined methods of improving the tunability of different

types of ONUs.

In [154], Suzuki *et al.* proposed a DWDM-SFP TRX for the WDM-PON that is λ-tunable across the L-band. The proposed TRX supported four channels with 100 GHz spacing or eight channels with 50 GHz spacing. The tunable TRX proposed by Taguchi *et al.* is also able to switch between wavelengths within 100 ns [155]. The given architecture, which supports C-band and L-band wavelengths in upstream and downstream directions, consists of an electro-absorption (EA) modulator integrated DFB laser as the Tx. The fast λ-switching time of 100 ns, achieved in this study, is attributed to the optical MUX/DEMUX, the 4-channel laser diodes (LD)/photo diodes (PD), and the electric switches. In [156], Miller *et al.* proposed a fast wavelength-switching TRX using a fast-tuning digital super-mode distributed Bragg reflector (DS-DBR) laser. This TRX module can rapidly tune (within 130ns) over 89, 50 GHz spaced channels within the C-band. The proposed work investigated the common issues found in fast-switching optical circuits such as mode hops and channel interference arising from spurious modes generated during the laser tuning time. In [157], Scholtz *et al.* discussed potential wavelength bands for the NG-PON2 and proposed to realise these wavelengths using wavelength blocking filters (WBFs), designed as thin film optical filters (TFF).

In addition to the DFB lasers discussed so far, VCSEL-based TRXs have been successfully tested for tunability in recent years. In one of the earlier studies on tunable VCSELs, Hasnain considered the possibility of using VCSELs in WDM applications and tuning it across the wavelength range supported by the WDM-PON [158]. This study provided insight into the physical architecture of the VCSEL and its inherent attributes that support tunability. The author also discusses achieving tunability in VCSEL ONUs using injection locking (IL) in [159]. The short-cavity (SC) VCSEL, evaluated in [48], is proposed specifically for the TWDM-PON. The experimental evaluation of this architecture shows that the SC-VCSEL supports a tuning range of 800 GHz in the C-minus band. The 800 GHz range accounts for 8, 100 GHz spaced 10 Gbps channels, resulting in an 80 Gbps aggregate transmission capacity. The SC-VCSEL also supports 40 km distance and a 1:128 split ratio per wavelength channel, without any dispersion compensation

or equalization. The proposed SC-VCSEL also have some compelling advantages such as having a fast $T_{doze-to-active}$ of 205 ns and comparatively low power consumption in active and doze mode. Similarly in [160], a tunable VCSEL array that supports 16 channels with a 50 GHz channel separation, is proposed for the next generation TWDM-PON.

The tunability or the sleep/doze capabilities of the ONUs will not result in any energy-savings, unless they are incorporated into the DWBA algorithms deployed in the network. So, in the next section, we discuss the DWBA algorithms proposed to exploit the tunability and the sleep/doze capabilities of the ONUs in achieving energy-savings.

2.4.2 Dynamic wavelength and bandwidth allocation algorithms for TWDM-PON

If no energy-efficiency is expected, a TWDM-PON will have all its wavelengths and ONUs active during the entire polling cycle time. As we have discussed in the previous section, the tunability and the sleep/doze capabilities of the network components present more opportunities to minimise the energy-consumption of the TWDM-PON. In literature, there exists three main categories of energy-efficient DWBA solutions proposed for the TWDM-PON, namely: (1) DWBA algorithms that switch off idle wavelengths for improved energy-efficiency at the OLT; (2) DWBA algorithms that use sleep/doze mode operations in conjunction with option 1; and (3) the DWBA algorithms that minimise the effect of wavelength tuning time on average delay [161]. In this section, we will discuss the existing work done in each category in detail.

2.4.2.1 Wavelength reallocation

Due to the nature of the Internet traffic, ONUs in any PON may frequently change its status between active and idle. If all wavelengths are kept active, there is high probability of them being idle, especially at less busy time of the day. Unless switched off, an idle wavelength still operates at its full power consumption

level. In such an instance, it is reasonable to migrate the ONUs supported by this wavelength to other operating wavelengths in the network and switch off the idle one. One of the most important aspects of this process is determining how many wavelengths to be switched off without affecting the system performance. Optimising the number of active wavelengths, subjected to different parameters of the network such as wavelength tuning time or distance from the OLT, has become the preferred technique in making this decision.

In [55], Luo *et al.* proposed two ONU migration schemes; one with more emphasis on tuning time (algorithm A) and the other with load balancing based on the ONU tuning time (algorithm B). Under A, when a new ONU emerges, the OLT assigns it to the wavelength with the least tuning cost, while, in B, the ONU is assigned to the wavelength with the least load. Even though the proposed schemes form a foundation for wavelength reconfiguration, this may still result in a majority of the wavelengths being active for most of the day.

Following this initial work, Yang *et al.* proposed a more energy-focused wavelength allocation scheme in [162]. The authors analyse the network profile and determine the minimum number of active ONUs required to operate the network, subjected to a maximum number of ONUs a wavelength can support. The study also analyses the effect the migration interval has on their ONU migration scheme and the service level agreement (SLA). This study was later extended to multi-PON systems where the proposed wavelength optimisation is applied to a group of TWDM-PONs for resource sharing [163,164]. Although the proposed solution is simple and straightforward, in a practical set up, the ONUs are distributed at different distances from the OLT. Consequently, lightly-loaded ONUs further away from the OLT may need more wavelengths to meet the optical power budget requirements. The wavelength optimisation criteria by Dixit *et al.*, therefore, takes the distance to each ONU from the OLT, when determining the number of active wavelengths [165].

As a variant of the conventional TWDM-PON, wavelength reallocation has been proposed for the flexible TWDM-PON as well. In the configuration considered in [72], the network consists of four ODNs, each comprising of four wave-

lengths. Taken individually, the four ODNs will each require at least one active wavelengths, even under minimum network load. However, due to the extra flexibility added by the hybrid AWG/power splitter, the four ODNs can operate using just one wavelength pair, resulting in significant energy-savings at the OLT.

By the time wavelength reallocation is introduced for the TWDM-PON, sleep and doze mode operations were already extensively studied for pure TDM-PONs such as EPON and GPON. Because the TWDM-PON stacks multiple TDM-PONs and the ONUs in these PONs are sleep/doze capable, it is natural to implement sleep/doze mode operations at the TWDM-PONs as well. In such a hybrid mechanism proposed by Dixit *et al.* in [100, 166], the DWBA algorithm utilised wavelength optimisation in conjunction with sleep/doze mode operations. Under the proposed DWBA algorithms, wavelength reconfiguration achieves energy-savings at the OLT, while sleep/doze operations result in energy-savings at the ONUs.

2.4.2.2 Wavelength reallocation and QoS

Similar to the delay penalty imposed by sleep/doze operations in the TDM-PONs, wavelength reallocation also degrades QoS parameters such as delay and availability of service of the TWDM-PON. As explained in [110], after receiving a migration command from the OLT, an ONU will take some time to tune to the new wavelength as specified by the OLT. If the tuning time is assumed to be negligible, unlimited wavelength switching could be practised in a network. Although unlimited wavelength switching may theoretically result in significant energy-savings, in reality, the tuning time of an ONU is significant. In fact, the tuning time of an ONU Tx can range from nanosecond to sub-second order while the ONU Rx tuning time can range from nanosecond to second order based on implementation [167]. In a standard QoS-aware network, this non-zero tuning time can limit the frequency of wavelength reconfiguration.

In [168], Kondepu *et al.* investigated the trade-off between the energy-savings and frame delay under different network parameters and wavelength allocation schemes. The study examines the energy-savings and frame delay under different

ONU tuning times, the number of reconfigurations, and round-trip times using static and dynamic wavelength allocation criteria. The results indicate that an increase in ONU tuning time increases the energy-savings and also the average frame delay. In separate but similar studies, it has also been shown that the ratio between the tuning time and the polling cycle time [169] and the OLT's awareness of the wavelength tuning time [170] are strongly correlated to performance matrices. As such, when considering a TWDM-PON with non-zero wavelength tuning time, the wavelength reconfiguration scheme we select results in a trade-off between energy-savings and network performances such as average delay and throughput. In this section, we discuss different efforts proposed to minimise the adverse effects of wavelength tuning time of the ONUs.

One straightforward way of tackling this problem would be to incorporate the wavelength tuning time into the optimisation criterion itself. In the delay-aware DWBA algorithm proposed in [64], the decision to migrate from the existing wavelength is taken based on wavelength tuning time. The authors follows the conventional EFT process in assigning an ONU to a wavelength. However, to mitigate the effects of wavelength tuning time, the OLT migrates an ONU from its current wavelength to the one satisfying EFT, only if the advantage of changing the wavelength outperforms the disadvantage of wavelength tuning time.

In the delay-mitigating solutions, we have discussed so far, the reported average delay values and energy-savings are heavily dependent on the physical characteristics of the ONUs used in the simulations/experiments. Meanwhile, different networks may use different network equipment with varying physical parameters. However, the delay requirements of a network are service dependent, meaning each service has specific delay requirements that should be met to provide a satisfactory quality of experience (QoE) to the customers. Under such scenarios, the average delay is usually used as a constraint in the optimisation criteria [171]. In their proposed optimisation scheme, Xu *et al.* attempted to decrease the energy consumption while keeping the average delay under a specified maximum. The number of wavelengths resulting from this wavelength optimisation criterion is taken as the optimum number of active wavelengths.

In addition to the optimisation criterion, the polling sequence is another approach taken to minimise the possible increase in average delay. In [172], Wang *et al.* proposed to change the polling sequence of the EFT algorithm such that the minimum number of ONUs will require tuning into a new wavelength. Assuming two wavelengths λ_1 and λ_1 and two cycles i and $i+1$, then the last ONU to use λ_1 will be assigned again to λ_1 in the $i+1^{th}$ cycle. Simulation results on packet delay and channel utilisation of this study shows significant performance improvement over the conventional EFT approach.

In the algorithms that we discussed so far, a constant tuning time is assumed for all ONUs in the TWDM-PON. One essential requirement for the evolution of the PONs is the smooth transition from existing PON technologies to the TWDM-PON. For example, when implementing the TWDM-PON, it is imperative that a complete change of equipment is not necessary. As a result, in a given TWDM-PON, there may exist optical and electrical components with different physical characteristics. Considering such a diverse TWDM-PON, Buttaboni *et al.* proposed a DWBA algorithm that handles ONUs with different tuning times [170]. The proposed solution changed the conventional VF-EFT algorithm to incorporate different tuning times and examined the importance of the OLT being aware of the tuning times of the ONUs. Based on the simulation values, this awareness at the OLT significantly reduces the average delay.

In addition to the algorithm-based solutions proposed to mitigate the QoS degradation, recent studies have also discussed hardware modifications to overcome this problem. Recently, Taheri et al. proposed an energy-saving solution where the number of line cards necessary at the OLT is determined based on the network traffic [173]. The authors formulated the upstream and downstream traffic on each segment of the network using the capacity of each uplink and downlink fiber as the constraint. The maximum of the upstream and downstream traffic is considered in determining the number of active line cards. The authors proposed to use optical, optomechanical, and cascaded switches at the OLT chassis to minimise the switching time when transitioning between different line cards [173].

Apart from the solutions proposed specifically for the TWDM-PON, the algo-

rithms designed for its predecessors such as hybrid WDM/TDM-PONs can also be seamlessly implemented in the TWDM-PONs. Some of these solutions include heuristic scheduling problems for arbitrary wavelength tuning times [174], automatic load-balancing DWBA algorithm that is capable of handling ONUs with tuning times 10 ms longer than the DBA cycle [175], load-balancing DWBA algorithm that minimises the number of wavelength reallocations [176].

2.5 Conclusions

Based on the studies reported in this chapter, energy-efficiency is one of the most important aspect of next-generation PONs. Due to slotted nature of upstream and downstream bandwidth access, ONU TRX remains idle for a majority of the polling cycle time. However, these idle ONUs operate at their full power level even during idle state. The effect of this energy consumption is further increased by the large number of of ONUs present in the access segment. As a result, reducing idle energy consumption of the ONUs is identified as an appropriate approach to improve the overall energy-efficiency of the access network.For this purpose, sleep and doze mode operations are proposed and standardised for the PON.

The sleep/doze mode solutions discussed in this chapter include hardware and algorithm-based solutions proposed for TDM-PON. The hardware improvements involve reducing the power consumption in each state and reducing the sleep-to-active or doze-to-active overhead times. The algorithm-based solutions exploit these sleep and doze mode capabilities of the ONUs to minimise the energy consumption at the OLT.

Meanwhile, in the TWDM-PON, wavelength tunability of the ONUs allows idle wavelengths to be switched off at low network loads, prompting energy-savings at the OTL. Considering existing work as our foundation, we propose DBA and DWBA algorithms for the TDM-PON and TWDM-PON to address the shortcomings of these existing solutions. A detailed description of our technical contribution towards energy-efficient TDM-PON and TWDM-PON will be presented in Chapters 3 to 6.

CHAPTER 3

Energy-Efficient Dynamic Bandwidth Allocation Algorithms for 10 Gbps Ethernet Passive Optical Networks

3.1 Introduction

Passive optical networks (PONs) are being deployed in the access segment to cater to the growing customer demand for higher bandwidths and longer reach. As discussed in Chapter 2, under next-generation PON stage 1 (NG-PON1), time division multiplexed PON (TDM-PON) is considered to be the most favourable architecture due to cost, capacity, and energy considerations. Two popular TDM-PONs, Ethernet PON (EPON) [14] and Gigabit PON (GPON) [23], are currently being deployed in many parts of the world to facilitate high-speed Internet access.

The EPON specifically, gained its popularity due to the seamless integration with ubiquitous Ethernet end user equipment [14, 44]. As explained in Chapters 1 and 2, PONs are more energy-efficient, i.e., consume low energy-per-bit, than copper-based access networks due to high bandwidths and low transmission losses. However, with wider and rapid deployment of EPONs, large number of additional end user equipment are added to the access segment. This in turn, has increased the overall energy consumption of the access segment and prompted concerns over greenhouse gas emissions and operational expenditure. To over-

come these challenges, network operators and research community have proposed various energy-saving solutions for the EPON [19, 20, 99, 177]. Although an illustrative 10 Gbps EPON (10G-EPON) is used in designing and simulating our novel dynamic bandwidth allocation (DBA) algorithms proposed in this chapter, the underlying concepts of these algorithms are applicable to any TDM-PON. Before presenting our technical contributions on energy-efficient EPON, a brief introduction to the EPON architecture is provided in the following section.

3.1.1 EPON: An overview

Figure 3.1 illustrates the basic architecture of an EPON. An EPON hosts an optical line terminal (OLT) at the central office (CO) and optical network units (ONUs) at customer premises. The network assigns two separate wavelengths, λ and λ', for downstream and upstream transmissions, respectively. In the downstream direction, from the OLT to the ONUs, the OLT uses wavelength λ to broadcast its downstream data to all ONUs in the network. In the upstream direction, from the ONUs to the OLT, multiple ONUs share the upstream wavelength channel λ' using time division multiple access (TDMA) technique.

As multiple ONUs share the upstream bandwidth, collisions may occur if more than one ONU attempts to communicate with the OLT simultaneously. As such,

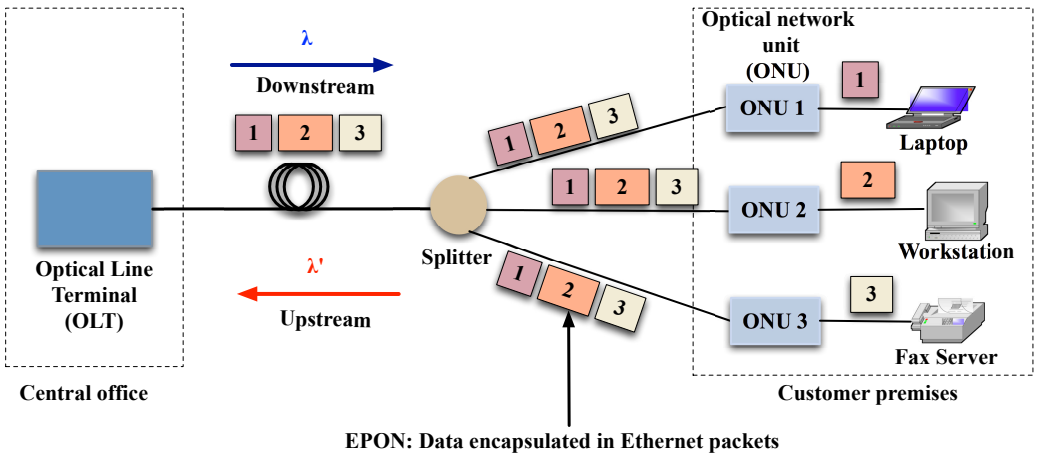

Figure 3.1: General architecture of a Ethernet passive optical network (EPON).

in the upstream direction, TDM-PON requires an arbitration mechanism to avoid collisions and to share the upstream capacity fairly. For this purpose, the EPON utilises Multi-Point Control Protocol (MPCP) messages, such as GATE and REPORT, to assign upstream time slots to each ONU and to facilitate collision-free data transmission between the OLT and the ONUs. The GATE message, sent from the OLT to the ONUs, contains the bandwidth allocated to an ONU, while the REPORT, sent from the ONUs to the OLT, informs an ONU's bandwidth requirement to the OLT.

3.1.2 Energy-efficiency through dynamic bandwidth allocation algorithms

In general, the bandwidth allocation process in a TDM-PON involves assigning an ONU with upstream and downstream time slots to exchange packets with the OLT. Allocating a time slot is usually referred to as a transmission grant and the time duration between two consecutive transmission grants to a given ONU is defined as its polling cycle time. The upstream and downstream time slots to an ONU can be synchronised or not, depending on the algorithm design. As discussed in Chapter 2, the bandwidth allocation process can be either fixed or dynamic. A fixed bandwidth allocation (FBA) algorithm allocates a fixed transmission time slot, irrespective of the bandwidth requirement of an ONU. A DBA algorithm on the other hand, takes upstream and/or downstream traffic load of an ONU into account, when allocating upstream/downstream time slots. Although a FBA is simple to implement, it does not ensure fairness among ONUs. As such, in this thesis, we focus on the DBA criterion.

As explained in the previous section, ONUs in EPON follow the TDMA technique in accessing the upstream bandwidth. Under TDMA, each ONU is allocated an unique time slot, during which it has full access to the upstream bandwidth. Outside this time slot, an ONU transmitter (Tx) remains idle, i.e., does not transmit any packets to the OLT. Similarly in downstream direction, packets destined to an ONU are sent during a certain time slot. In contrary to upstream traffic, downstream data is broadcast to all ONUs in the network. As a result, an ONU processes

MAC headers of all downstream packets and discard the ones destined for other ONUs. When an ONU receiver (Rx) is not processing its own packets or MAC headers of other ONUs, it is said to be idle. Due to slotted nature of downstream and upstream traffic, an ONU spends a majority of its polling cycle time in idle state. An idle ONU, however, operates at its active power level. This behaviour, coupled with a large number of ONUs present in current networks, makes ONUs the main energy consumption contributor of access network [1]. Instead of operating at its active power level, if an ONU can transition into a low-power mode during its idle time, substantial energy savings can be achieved in the access segment.

To implement this concept, Telecommunication Standardisation Sector of the International Telecommunication Union (ITU-T) proposed sleep and doze mode operations for idle ONUs in the PON [23, 27]. During sleep mode, both Tx and Rx of an ONU are powered down, preventing an ONU from receiving data packets and synchronisation bits from the OLT and also from transmitting packets to the OLT. During doze mode, only the ONU Tx is powered down, allowing the ONUs to receive synchronisation bits from the OLT, but preventing it from transmitting packets to the OLT. Because the ONUs cannot receive their synchronisation bits from the OLT during sleep mode, an ONU transitioning from sleep to active mode incurs more overhead (for re-synchronisation) time than a one transitioning from doze to active mode. As a result, sleep-to-active transition time, $T_{sleep-to-active}$, of an ONU is longer than its doze-to-active transition time, $T_{doze-to-active}$.

The sleep and doze mode capabilities of an ONU can be exploited in different ways to improve the energy savings of the network. Referring to the energy equation presented in Chapter 2, the overall energy consumption of a sleep/doze-capable ONU can be written as follows:

$$E = P_{active} * T_{active} + P_{sleep/doze} * T_{sleep/doze} \tag{3.1}$$

where parameters E, P_{active}, T_{active}, $P_{sleep/doze}$, and $T_{sleep/doze}$ represent the energy consumption of an ONU per cycle, the ONU power consumption in active mode,

the time an ONU spends in active mode, the ONU power consumption in sleep/doze mode, and the time an ONU spends in sleep/doze mode, respectively. Based on eqn. (3.1), reducing power consumption in each mode, P_{active} and $P_{sleep/doze}$, reduces the overall energy consumption of an ONU.

Meanwhile, within a given polling cycle, increasing the time an ONU spends in sleep or doze mode also improves the energy efficiency of the ONUs. The respective sleep and doze durations of an ONU, T_{sleep} and T_{doze}, are calculated as follows:

$$\begin{aligned} T_{sleep} &= T_{idle} - T_{sleep-to-active} \\ T_{doze} &= T_{idle} - T_{doze-to-active} \end{aligned} \tag{3.2}$$

The idle time of an ONU, T_{idle}, can be written as a function of its polling cycle time, $T_{poll\ cycle}$, and transmission time slot, $T_{tx\ slot}$, as follows:

$$T_{idle} = T_{poll\ cycle} - T_{tx\ slot} \tag{3.3}$$

Based on eqn. (3.2), for a given network load, an ONU with a shorter $T_{doze-to-active}$, $T_{sleep-to-active}$ or longer T_{idle} experiences a longer T_{doze} or T_{sleep}, and in turn, achieves improved energy savings. Summarising these equations, the main criteria for improving energy efficiency through sleep/doze mode are as follows:

- Minimising the ONU power consumption in each state, i.e., sleep, doze, and active.
- Reducing the overhead times $T_{sleep-to-active}$ and $T_{doze-to-active}$ for longer T_{sleep} and T_{doze}.
- Incorporating the sleep and doze mode operations into the underlying bandwidth allocation algorithm.

The first two methods are classified as hardware improvements to the ONU architecture whilst the last method is an algorithm-based solution. As explained

in Chapters 1 and 2, in this thesis, we focus on the latter approach, where the bandwidth allocation algorithm performs both bandwidth allocation and sleep or doze control. The key challenges associated with this process are; (1) maximising the sleep or doze duration; (2) determining the sleep or doze duration; and (3) transitioning the ONUs between different modes without affecting the communication between the OLT and the ONUs. These challenges have been addressed using different techniques in studies reported on energy-efficient EPON [19, 24, 26–29, 99, 135, 141, 142, 178].

For the existing sleep/doze-capable ONUs, the difference in energy consumption, between active and doze modes, is low, compared to the difference between sleep and active modes. Consequently, an ONU in sleep mode achieves more energy savings than a one in doze mode [24, 29]. Existing studies on energy-efficient EPONs have therefore, incorporated only sleep mode into their proposed solutions. However, if $T_{idle} < T_{sleep-to-active}$, using sleep mode *only* will prevent any energy savings at particular network loads [24, 26, 27, 135, 141, 142, 178, 179]. Further, owing to the recent developments in ONU architectures that consume low power in doze mode [180] and that have low $T_{doze-to-active}$ [102, 106, 180], incorporating doze mode operation will have a noticeable impact on the ONU energy consumption. As such, it is important to design DBA algorithms that incorporate *both* sleep and doze operations for improved energy-efficiency of the EPON.

For this purpose, in this chapter, we propose two DBA algorithms that exploit *both* sleep and doze capabilities of an ONU. Compared to existing DBA algorithms that use only sleep mode, our DBA algorithms minimise the ONU energy consumption across a wider range of network loads. To this end, we consider for illustrative purposes, a 10 Gbps EPON (10G-EPON) whereby the ONUs can transition into sleep and doze modes (i.e. sleep/doze ONUs). The two DBA algorithms, namely Just-In-Time (JIT) DBA with varying polling cycle times [181, 182] and JIT DBA with fixed polling cycle time (J-FIT) are designed to exploit the 10 Gbps vertical-cavity surface-emitting laser (10G-VCSEL) ONU that can transition from doze-to-active mode in 330 ns and from sleep-to-active mode in 2 ms [29, 180]. Based on the switching and power consumption values of the 10G-VCSEL ONU

Table 3.1: Power consumption and switching values of the 10G-VCSEL ONU and the 10G-DFB ONU

Parameter	Value
Doze-to-active transition time - VCSEL ($T_{doze-to-active}$) [29]	330 ns
Doze-to-active transition time - DFB ($T_{doze-to-active}$) [102]	760 ns
Sleep-to-active transition time - VCSEL ($T_{sleep-to-active}$) [29]	2 ms
Sleep-to-active transition time - DFB ($T_{sleep-to-active}$ [29]	2 ms
Power consumption - VCSEL, active ($P_{vcsel,act}$) [29]	3.984 W
Power consumption - DFB, active ($P_{DFB,act}$) [29]	5.052 W
Power consumption - VCSEL, doze ($P_{vcsel,doze/sleep}$) [29]	3.85 W
Power consumption - DFB, doze ($P_{DFB,doze/sleep}$) [29]	3.85 W
Power consumption - VCSEL, sleep ($P_{vcsel,doze/sleep}$) [29]	0.75 W
Power consumption - DFB, sleep ($P_{DFB,doze/sleep}$) [29]	0.75 W

and the 10Gbps distributed feedback (10G-DFB) ONU presented in Table 3.1, the 10G-VCSEL is more energy-efficient. As such, we use this energy-efficient and sleep/doze-capable 10G-VCSEL as the Tx of our ONU, but keep rest of the ONU circuit the same as a conventional DFB ONU. Both JIT and J-FIT DBA algorithms comply with the MPCP control messages GATE and REPORT to transition the 10G-VCSEL ONUs between active, doze, and sleep modes. To highlight the motivation and novelty of our proposed algorithms, some of the existing work done in the research area of sleep mode DBA algorithms is discussed in the next section.

3.2 Related work

As explained in Section 3.1.2, T_{idle} is a crucial parameter that determines the energy savings achieved through sleep/doze mode operations. The parameter T_{idle} in turn, depends on the DBA algorithm deployed in the network. As a result, various attempts have been made to maximise T_{idle} in sleep mode DBA algorithms proposed in recent literature. In one of the earlier studies reported in this area, Smith *et al.* [26] proposed a DBA algorithm that frequently transitions the ONUs into sleep mode in the GPON. For the ONUs entering sleep mode, this algorithm assigns a minimum bandwidth in the upstream direction, which allows the ONUs to send their bandwidth requests when upstream traffic is present at the subscriber network interface (SNI). In a similar attempt, Mandin *et al.* proposed a sleep mech-

anism and discussed the OLT and ONU-initiated sleep mode operation and handshake processes in detail [27]. Following a different approach, Gunaratne *et al.* proposed an adaptive link rate (ALR) control mechanism to reduce the energy consumption of EPONs [183]. The authors use the general principle that a low data rate link consumes less power than a high data rate link and changes the upstream link rate between two values, depending on the network load of the ONUs. Using the same principle, Kubo *et al.* discussed how the energy consumption can be further reduced by using a hybrid mechanism that combines sleep mode and ALR control [142]. The sleep mode mechanism switches an ONU between sleep and active modes depending on the presence or absence of traffic while the ALR control switches the link rate between 1 Gbps and 10 Gbps depending on the amount of traffic, saving energy even in the presence of traffic. Ren *et al.* [135] proposed an analytical model to analyse the 10 Gbps PON using Poisson distributed traffic. Under their proposed solution, the OLT first assigns a minimum sleep duration to an ONU and exponentially increases this value depending on the network load. Wong *et al.* proposed a JIT bandwidth allocation algorithm for TDM-PON exploiting the fast wakeup capability of an ONU [28]. The proposed JIT algorithm allows ONUs to go into variable sleep lengths based on a sleep time optimiser and uses the same GATE and REPORT messages as in IEEE 802.3ah standard [14], to transition the ONUs between sleep and active modes. Similarly, Fiammengo *et al.* proposed a criterion for determining the sleep time of an ONU based on the inter-arrival time of incoming packets at the ONU [141]. The proposed study utilises different estimation techniques, arithmetic average and exponential smoothing average, to estimate the inter-arrival time of packets. Using this estimated value and a pre-determined sleep control function, they determine the variable sleep length allocated to an ONU. In [178], Praet *et al.* proposed a bit-interleaving TDM downstream protocol (Bi-PON) to minimise the power consumed in complex processing of packets destined for other ONUs in the PON. The protocol organises bits in an interleaved form thereby reducing the number of functional blocks required to extract packets at the ONU. The Bi-PON protocol also incorporates sleep command in the operation, administration, and maintenance (OAM) header to minimise the

energy consumed during the idle time. In [179], Yan *et al.* proposed an energy management mechanism (EMM) that minimises the energy consumption of the 10G-EPON. The proposed mechanism minimises the awake time of the ONUs to reduce the energy consumption of the ONUs. As reducing the awake time can adversely affect the QoS of the network, the proposed mechanism imposes a latency constraint when determining the sleep duration of an ONU. The authors also proposed upstream and downstream-centric scheduling algorithms that allocates awake time based on the upstream and downstream bandwidth allocation, respectively. In [184], Zhang *et al.* proposed a mechanism to minimise the energy consumption associated with ONUs listening and analysing the headers of all downstream traffic. The proposed method considers only downstream traffic and consists of a bandwidth allocation rules at the OLT and sleep scheduling rules at the ONUs. The bandwidth allocation rules are made known to the ONUs, thereby allowing the ONUs to infer their downstream queue status and enter sleep state effectively. The sleep scheduling rules are also known to the OLT, thereby allowing the OLT to queue the downstream traffic destined for a given ONU. In [185], Taheri *et al.* proposed an energy-saving mechanism that prevents an ONU from frequently changing its states between active and sleep. As frequent changes lead to energy being wasted in ONU trying to resynchronise with the OLT, the authors argues it is more efficient for the ONU to spend some time in the listening mode before putting each component in sleep mode. The study defines six states, Rx Awake, Rx Listen, Rx Sleep, Tx Awake, Tx Listen, and Tx Sleep, based on the nature of traffic. Rather than exchanging overheads, the sleep control mechanism proposed in this work is based on the mutual inference between the OLT and the ONU.

In the existing DBA algorithms discussed above, only sleep mode operation is considered to reduce the energy consumption of the EPON. As we have explained before, when $T_{idle} < T_{sleep-to-active}$, no energy savings will be possible with sleep mode operation. In the next section, we discuss how our proposed algorithms, JIT and J-FIT DBAs, incorporate both sleep and doze mode operations to overcome this problem and improve the energy efficiency of the 10G-EPON.

3.3 Proposed dynamic bandwidth allocation algorithms

An effective sleep/doze controlled DBA algorithm is a one that can successfully cater for varying traffic demands of the network and can transition the ONUs from sleep or doze mode into active mode with minimal effect on the traffic flow between the OLT and the ONUs. In this section, we explain how our proposed JIT and J-FIT DBA algorithms achieve these objectives, in detail.

3.3.1 Just-In-Time DBA with varying polling cycle times

The JIT DBA is our initial attempt at incorporating both sleep and doze mode operations into a DBA algorithm. JIT DBA is an offline DBA, meaning the OLT processes the bandwidth requests from all ONUs, before deciding the sleep/doze duration and the bandwidth allocated to each ONU. The proposed algorithm uses MPCP control messages, GATE and REPORT, to transition the ONUs in sleep/doze mode into active mode just-in-time to receive downstream packets from the OLT.

Initially, the Internet was mainly used to access the world wide web and downstream data dominated the data flow between the ONUs and the OLT. However, with emerging user applications, such as peer-to-peer file sharing, Internet gaming, and video conferencing, the proportion of upstream traffic has increased significantly. Considering the rapid growth of these applications as predicted in [186], we have assumed a symmetric upstream and downstream bandwidth utilisation in the network, in both JIT and J-FIT DBA algorithms [24].

The actual traffic flow in the 10G-EPON under the JIT DBA is shown in Fig. 3.2. The parameter T_{wakeup} accounts for either $T_{sleep-to-active}$ or $T_{doze-to-active}$. The Ethernet frames from the OLT to each ONU consist of data and the GATE message. When an ONU receives this Ethernet frame, it analyses the GATE message and learns the transmission start time, transmission duration, and sleep/doze duration. Under the JIT DBA, immediately after analysing the GATE message, an ONU starts transmitting its upstream data to the OLT. When an ONU completes its upstream data transmission, it generates the REPORT message and sends it to the OLT. The ONU then enters into sleep or doze mode for a period specified in

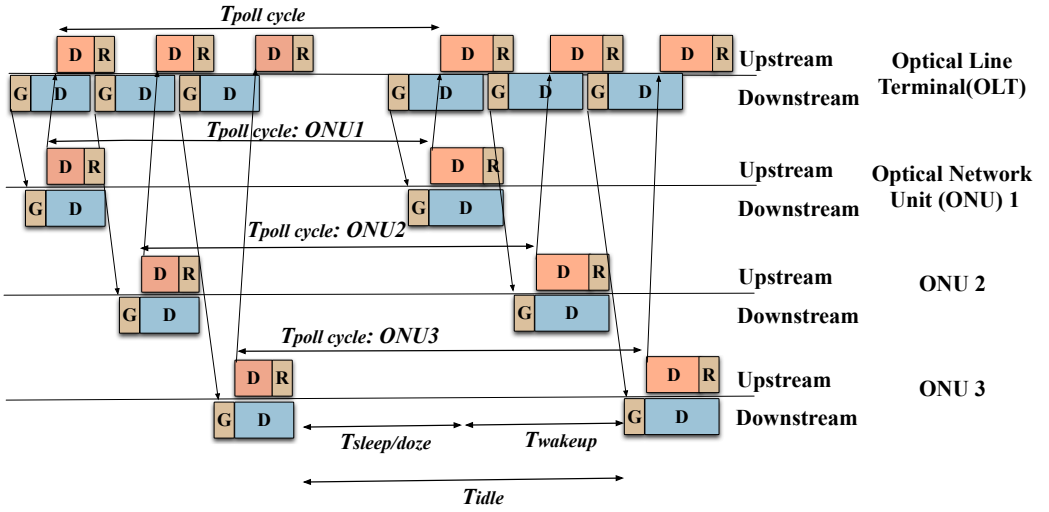

Figure 3.2: Traffic flow of the JIT DBA algorithm. D-Data, R-REPORT and G-GATE.

the GATE and wakes up just-in-time to receive downstream packets from the OLT in the next cycle. In the following sections, we discuss the individual functions executed at the OLT and the ONUs under the JIT DBA.

Figure 3.3 illustrates the flow chart of the JIT DBA executed at the OLT. Initially, each ONU inspects its incoming queue and generates a REPORT message that contains the bandwidth requirement of that ONU. The OLT waits until it receives REPORT messages from all ONUs and processes each bandwidth request to calculate the average bandwidth, BW_{avg}, required by each ONU. The OLT then compares the BW_{avg} with the maximum allowable bandwidth, BW_{max}, that satisfies a given maximum polling cycle time, $T_{max\ poll\ cycle}$. The $T_{max\ poll\ cycle}$ corresponds to the maximum duration between two consecutive transmissions to a given ONU, and is derived by controlling the BW_{max} that satisfies the delay and jitter specifications of the network. Depending on the decision of this comparison, the OLT allocates either BW_{max} or BW_{avg} to each ONU, in the subsequent polling cycle.

In any given cycle, due to the offline nature, the OLT has knowledge of the bandwidth allocated to each ONU in advance. Thus, the OLT can determine the T_{idle} of each ONU during each cycle. Using the switching values of 10G-VCSEL ONU considered in our 10G-EPON (as listed in Table 3.1), the OLT makes the following decisions.

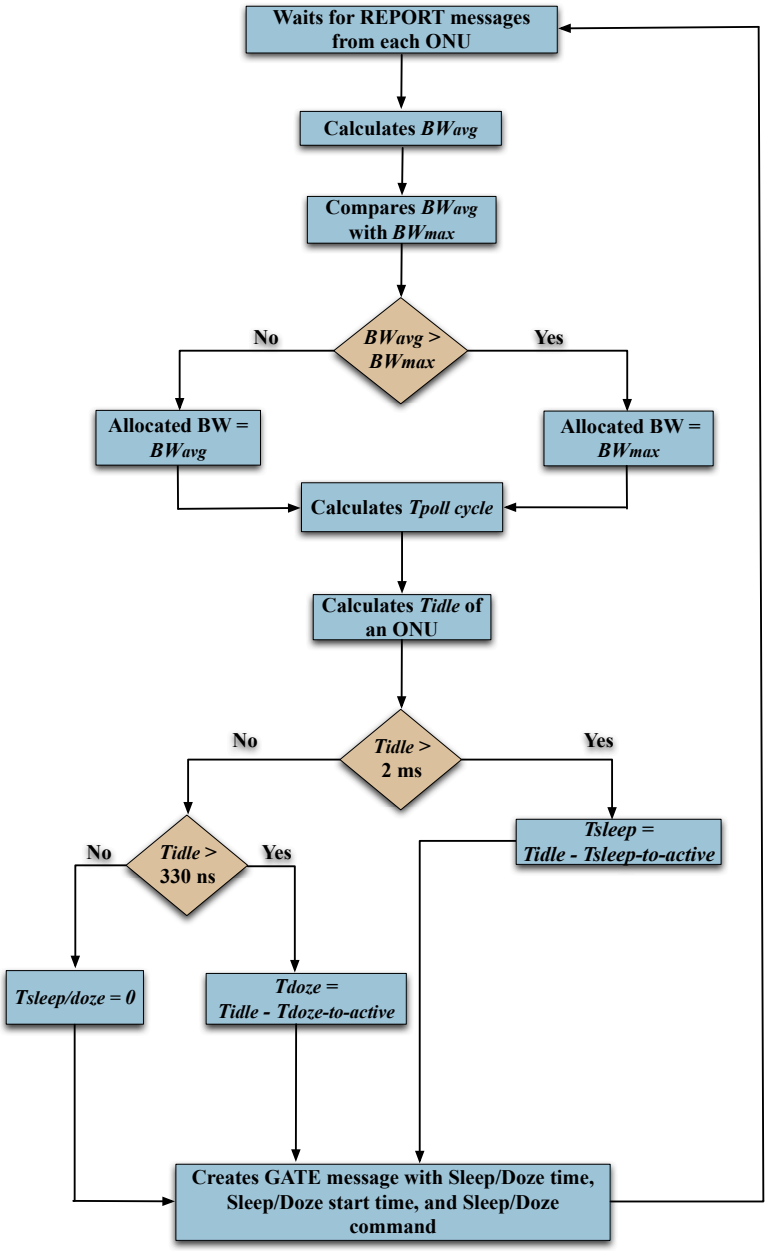

Figure 3.3: Flow chart of the JIT DBA algorithm executed at the OLT.

- $T_{idle} \geq 2$ ms : ONU enters into sleep mode
- 330 $ns \leq T_{idle} < 2$ ms : ONU enters into doze mode
- 330 $ns \geq T_{idle}$: ONU stays active

Figure 3.4 illustrates the flow chart of the JIT DBA algorithm executed at each

ONU. In any given cycle, an ONU wakes up from sleep or doze mode just-in-time to receive the GATE message and data from the OLT. In addition to the conventional bandwidth allocation information, the GATE message under JIT DBA, also contains the sleep start time, the sleep duration, and the sleep/doze/active com-

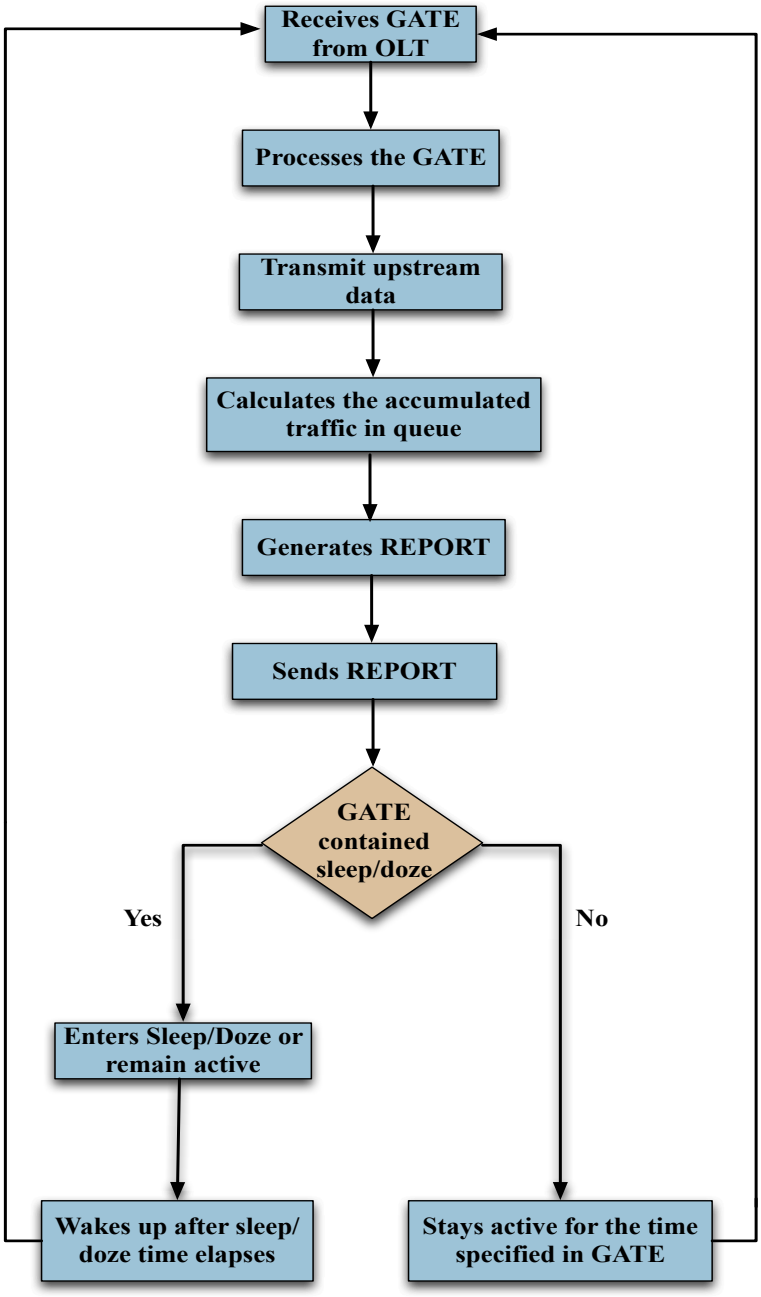

Figure 3.4: Flow chart of the JIT DBA algorithm executed at the ONU.

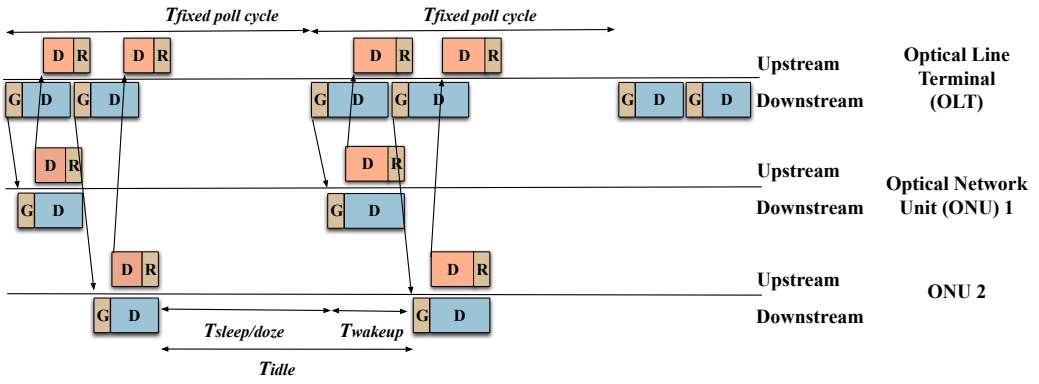

Figure 3.5: Traffic flow of the J-FIT DBA algorithm. D-Data, R-REPORT and G-GATE.

mand. After processing the GATE message, the ONU transmits its upstream data and the REPORT message to the OLT and immediately enters into sleep or doze mode for a duration specified by the GATE message.

3.3.2 Just-In-Time DBA with fixed polling cycle times

In the JIT DBA algorithm, $T_{poll\ cycle}$ is the sum of all $T_{tx\ slot}$ that is allocated to each ONU. In other words, $T_{tx\ slot}$ corresponds to the bandwidth allocated to an ONU. When the network load is low, the BW_{avg} is low, resulting in a short $T_{tx\ slot}$ and eventually, a short $T_{poll\ cycle}$. Within a short $T_{poll\ cycle}$, an ONU may not be able to enter sleep mode, but will enter doze mode or remain active. As we have discussed in Section 3.1.2, the difference in power consumption between doze and active modes of the 10G-VCSEL ONU is only 0.134 W (refer to Table 3.1), which leads to low percentage of energy savings at low network loads. From a more practical point of view, low network loads are quite common in communication networks and at these low network loads, ONUs can afford to sleep or doze for a longer duration without compromising quality of service (QoS) parameters, such as delay. The main objective of our J-FIT DBA, therefore, is to overcome the apparent drawback of the JIT DBA, low energy savings due to shorter $T_{poll\ cycle}$ at low network loads, using fixed polling cycle times. In this section, we discuss the design specifications of the J-FIT DBA in detail.

Figure 3.5 illustrates the overall traffic flow in the 10G-EPON between the OLT and two ONUs under the J-FIT DBA. The J-FIT DBA is designed with a fixed polling cycle time, $T_{fixed\ poll\ cycle}$, that is independent of the BW_{avg} of the 10G-EPON. Similar to the JIT DBA, an ONU initially inspects its incoming queue and determines the bandwidth requirement in the next cycle. The ONU then generates the REPORT message and sends it to the OLT. Algorithm 3.1 presents a summary of our J-FIT algorithm executed at the OLT after receiving REPORT messages from all ONUs. The parameters $T_{tx\ start}$ and T_{mode} represent the ONU transmission start time and ONU sleep/doze/active time, respectively. As J-FIT is also an offline DBA algorithm, after receiving REPORT messages from all ONUs, the OLT calculates BW_{avg} for each ONU. The OLT then compares this value against a threshold, BW_{max}, to ensure that for any given polling cycle, the total allocated bandwidth does not exceed the bandwidth that corresponds to $T_{fixed\ poll\ cycle}$. Based on the outcome of this comparison, the OLT assigns either BW_{avg} or BW_{max} to an ONU in the upcoming fixed polling cycle.

Referring to eqn. (3.1), in the J-FIT DBA, the T_{idle} of an ONU in any given cycle corresponds to $T_{fixed\ poll\ cycle}$ - $T_{tx\ slot}$. As shown in Algorithm 3.1, the OLT follows the same conditions as in JIT DBA to determine the mode and the sleep/doze/active duration. This information is included in the GATE message destined to each ONU in the subsequent cycle.

In any given cycle, an ONU wakes up just-in-time to receive packets that consist of the GATE message and downstream data from the OLT. The ONU processes the GATE message and learns its upstream transmission start time and duration. After completing its upstream data transmission, the ONU generates the REPORT message that contains its future bandwidth requirement and sends it to the OLT. The ONU then enters into sleep, doze, or active mode for a duration specified in the GATE message. Similar to JIT DBA, the J-FIT DBA is also designed to ensure that the upstream and downstream transmissions coincide under the assumption of equal traffic loads in both directions [28].

Figures 3.6 (a) and (b) compare the polling cycle times of the JIT and J-FIT DBAs at a given ONU, corresponding to two network loads $L1$ and $L2$ where $L1 < L2$,

respectively. When the network load is low ($L1$), J-FIT DBA results in a longer T_{idle}, and therefore, facilitates longer sleep/doze durations and increased energy savings. On the other hand, a longer T_{idle} may result in degradation of QoS parameters. In the following section, we critically analyse the effect of varying network loads and polling cycle times on the energy efficiency and the average delay.

3.4 Performance evaluation

In this section, the performance of the JIT and J-FIT DBA algorithms are evaluated with respect to the polling cycle time, energy consumption per cycle, percentage of energy savings per cycle, and average delay. For this purpose, we performed simulations using C++ with Poisson distributed incoming traffic at the ONUs. Table 3.2 lists the network and protocol parameters used in our simulations. The normalised network load (e.g., a normalised network load of 1 = 10 Gbps network load) is varied from 0.1 to 1. As highlighted before, compared to a conventional

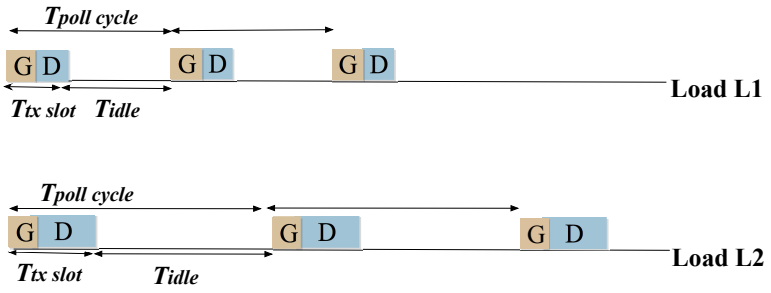

(a) JIT DBA

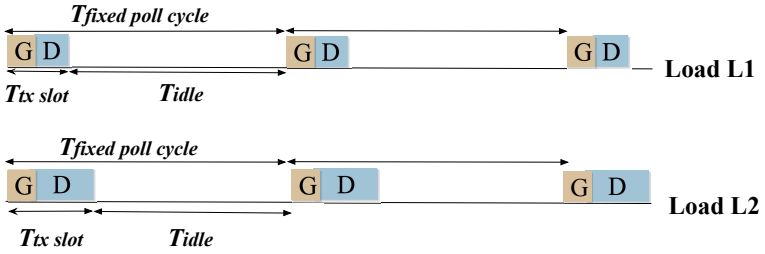

(b) J-FIT DBA

Figure 3.6: Polling cycle times at ONU1 of the JIT and J-FIT DBA algorithms.

Algorithm 3.1: Pseudocode of the J-FIT DBA algorithm executed at the OLT for N number of ONUs

```
After receiving REPORT messages from all the ONUs
Total_BW_Requested = ∑^N ONU(i).BW_Requested BW_avg = Total_BW_Requested/ N
for i = 1 to N do
    ONU(i)_T_tx slot = Calculate_T_tx slot (i) //Compares the Avg_BW_requested to a threshold and
    returns the Tx time slot
    ONU(i)_T_tx start = Calculate_ONU_T_tx start (i)
    ONU(i)_T_idle = T_fixed poll cycle - ONU(i)_T_tx slot
    if ONU(i)_T_idle > 2 ms then
        Mode = SLEEP
        ONU(i)_T_mode = ONU(i)_T_idle - 2 ms
    else
        if 330ns ≤ ONU(i)_T_idle < 2 ms then
            Mode = DOZE
            ONU(i)_T_mode = ONU(i)_T_idle - 330 ns
        else
            Mode = ACTIVE
            ONU(i)_T_mode = ONU(i)_T_idle
    Generate_GATE(i) //generate the GATE message with T_tx slot, T_tx start, Mode, and T_mode
```

Table 3.2: Network and Protocol Parameters

Parameter	**Value**
Downstream and upstream line rate	10 Gbps
Number of ONUs	32
Normalised network load	0.1 - 1
Maximum and fixed cycle time of JIT and J-FIT	2ms-10 ms
Propagation delay	100 μs
Inter-frame gap in upstream	1μs
Average Ethernet packet size	791 bytes

DFB ONU, the 10G-VCSEL ONU considered in our DBA algorithms, consumes less power in active state (5.05 W vs 3.984 W) and has a shorter $T_{doze-to-active}$ (Table 3.1). The 10G-VCSEL ONU is, therefore, more energy-efficient than a conventional DFB ONU. In order to quantify the comparative advantage the 10G-VCSEL ONU has over a 10G-DFB ONU, in this section, we also compare the performance of each ONU architecture under JIT and J-FIT DBA algorithms. Table 3.1 lists the power consumption and switching values of the 10G-DFB and 10G-VCSEL ONU used in this analysis.

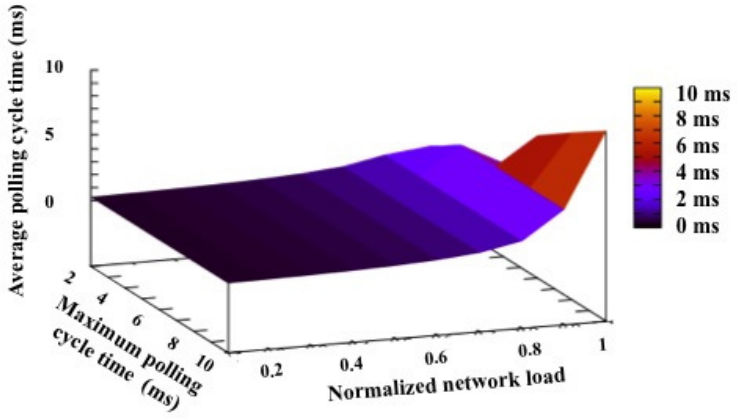

(a) JIT DBA

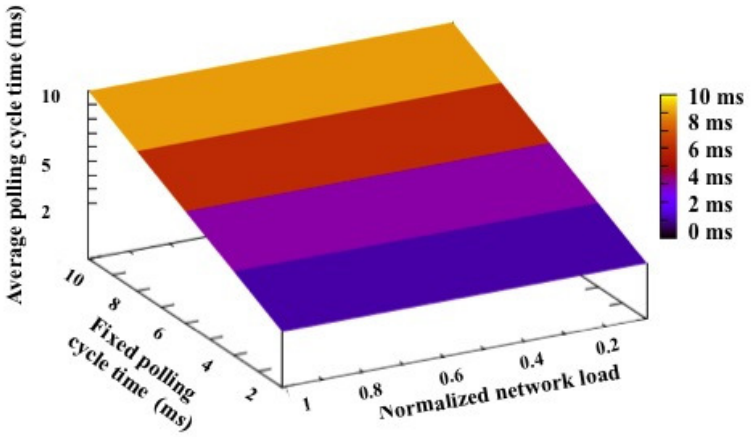

(b) J-FIT DBA

Figure 3.7: Average polling cycle time as a function of normalised network load and polling cycle time.

3.4.1 Performance comparison between JIT and J-FIT DBA algorithms

The $T_{poll\ cycle}$ of the JIT and J-FIT DBA algorithms is strongly correlated to the energy savings and the average delay of the network. As the rest of our findings on energy efficiency and average delay depend on the $T_{poll\ cycle}$, we will first analyse the behaviour of $T_{poll\ cycle}$ under each algorithm. Figures 3.7(a) and 3.7(b) illustrate the average polling cycle time of the sleep/doze 10G-VCSEL ONU as a function

of normalised network load and maximum and fixed polling cycle times of the JIT and J-FIT DBA algorithms, respectively. In the JIT DBA, for a given $T_{max\ poll\ cycle}$, the average polling cycle time gradually increases with the increase in network load. When the network load increases, the number of packets arriving at the ONUs increases, thereby increasing BW_{avg} in the PON. The increase in BW_{avg}, increases the $T_{tx\ slot}$ allocated per ONU. As discussed in Section 3.3.1, $T_{poll\ cycle}$ of the JIT DBA is the sum of $T_{tx\ slot}$ allocated per each ONU. Thus, an increase in the $T_{tx\ slot}$ results in an increase in $T_{poll\ cycle}$. As the J-FIT DBA is designed with fixed polling cycle times, irrespective of the network load, $T_{poll\ cycle}$ remains constant.

Figure 3.8(a) illustrates the average power consumption per 10G-VCSEL ONU per polling cycle time as a function of normalised network load and maximum polling cycle time for the JIT DBA. For the JIT DBA, for any given $T_{max\ poll\ cycle}$, the average power consumption remains constant at 3.85 W up to a network load of 0.8. The average power consumption then decreases with the increase in network load. In the JIT DBA, T_{idle} of the ONUs remains below 2 ms up to a network load of 0.8, because of the low average polling cycle times shown in Fig. 3.7(a). This short $T_{poll\ cycle}$ prevents an ONU from entering into sleep mode. However, because T_{idle} is higher than $T_{doze-to-active}$ of 330 ns, the ONUs transition into doze mode during their idle time. This results in an average power consumption of 3.85 W, which corresponds to the power consumption of a 10G-VCSEL ONU in doze mode, as listed in Table 3.1. For network loads $\geq$ 0.8, T_{idle} satisfies the condition for the ONUs to enter into sleep mode. As the power consumption of a 10G-VCSEL ONU in sleep mode is 0.75 W, average power consumption values as low as 1.5 W is achieved at network loads $\geq$ 0.8, for the JIT DBA.

Figure 3.8(b) illustrates the average power consumption per 10G-VCSEL ONU per polling cycle time as a function of normalised network load and fixed polling cycle time for the J-FIT DBA. For a given network load, the power consumption per ONU per fixed polling cycle time decreases with the increase in $T_{fixed\ poll\ cycle}$. For a particular network load, an increase in $T_{fixed\ poll\ cycle}$ allows an ONU to remain in sleep or doze mode for a longer duration, resulting in reduced power consumption at the ONU. It is important to note that in the J-FIT DBA, ONUs enter into

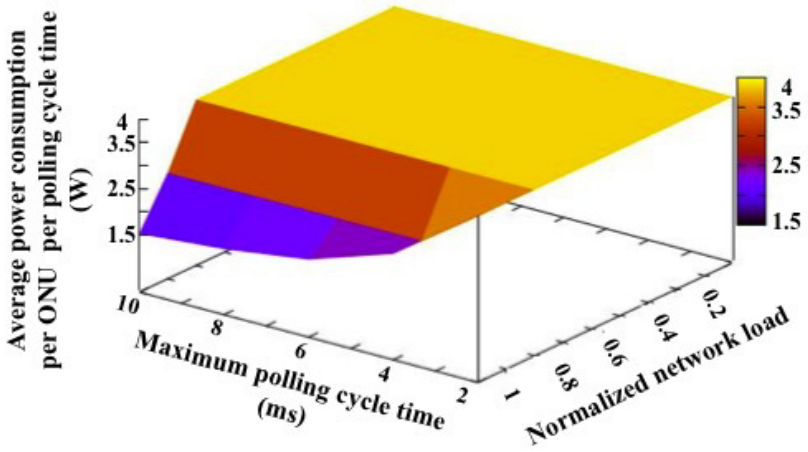

(a) JIT DBA

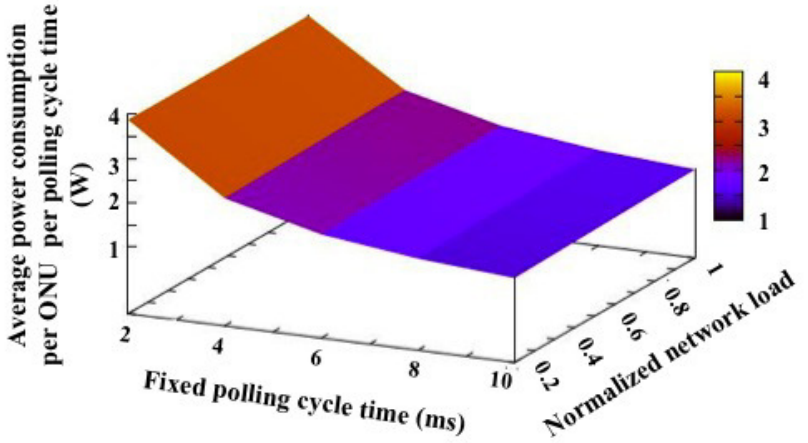

(b) J-FIT DBA

Figure 3.8: Average power consumption per 10G-VCSEL ONU per polling cycle time as a function of normalised network load and polling cycle time.

sleep mode for fixed polling cycle times $\geq$ 2ms for any given network load. As the power consumption in sleep mode is 0.75 W, average power consumption values as low as 1.4 W is observed at low network loads. For $T_{fixed\ poll\ cycle} \leq$ 2ms, however, ONUs enter into doze mode, resulting in an average power consumption of 3.85 W, which corresponds to the doze mode power consumption of a 10G-VCSEL ONU.

As shown in Fig. 3.8(b), for any given $T_{fixed\ poll\ cycle}$, the power consumption

increases with the increase in network load for the J-FIT DBA. When the network load increases, it increases $T_{tx\ slot}$, i.e., the ONUs remains active for a longer duration, thereby increasing the average power consumption at the ONUs. These findings on power consumption indicate that while both JIT and J-FIT DAB algorithms have improved the energy efficiency, J-FIT DBA is more energy-efficient at low network loads.

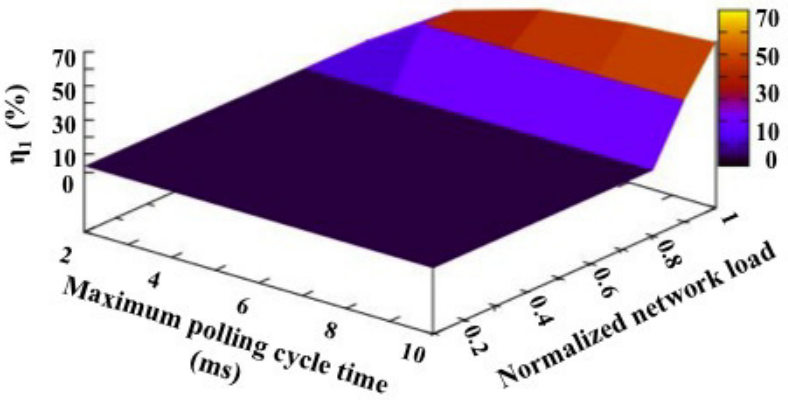

(a) JIT DBA

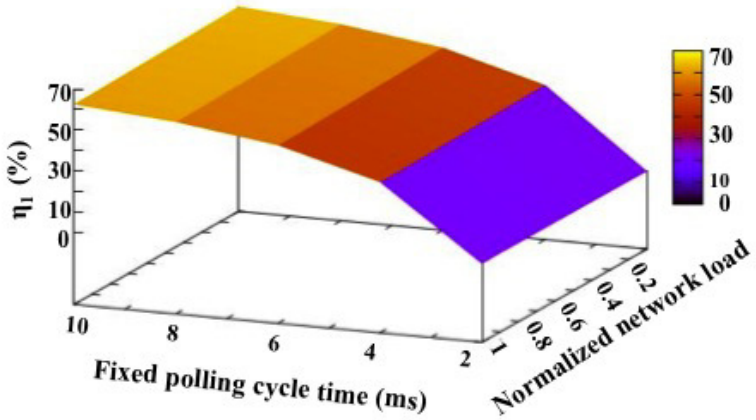

(b) J-FIT DBA

Figure 3.9: Percentage of energy savings (η_1) as a function of normalised network load and polling cycle time.

Figure 3.9(a) illustrates the percentage of energy savings of a sleep/doze-capable 10G-VCSEL ONU compared to an always-ON 10G-VCSEL ONU, as a function of network load and maximum polling cycle time for the JIT DBA. The percentage of energy savings η_1 is calculated as follows:

$$\eta_1 = \left(1 - \frac{P_{vcsel,act}T_{act} + P_{vcsel,doze/sleep}T_{doze/sleep}}{P_{vcsel,act}(T_{act} + T_{sleep/doze})}\right)\% \tag{3.4}$$

where parameters $P_{vcsel,act}$ and $P_{vcsel,doze/sleep}$ represent the power consumption of a 10G-VCSEL ONU in active mode and sleep/doze modes, respectively. As shown in Fig. 3.9(a), for any given $T_{max\ poll\ cycle}$, η_1 is only 3% for network loads up to 0.8. For network loads $\geq$ 0.8, η_1 increases with the increase in network load. As explained earlier, a 10G-VCSEL ONU enters into doze mode for network loads $\leq$ 0.8. As a result of the small difference in power consumption (0.134 W) between active and doze modes of a 10G-VCSEL ONU, η_1 of only 3% is achieved. For network loads $\geq$ 0.8, the ONUs enter into sleep mode, resulting in energy savings as high as 61%, due to the large difference in power consumption (3.234 W) between active and sleep modes of a 10G-VCSEL ONU.

Figure 3.9(b) illustrates η_1, as a function of normalised network load and fixed polling cycle time for the J-FIT DBA. For the J-FIT DBA, η_1 is calculated as follows:

$$\eta_1 = \left(1 - \frac{P_{vcsel,act}T_{act} + P_{vcsel,doze/sleep}T_{doze/sleep}}{P_{vcsel,act}T_{fixed\_cycle}}\right)\% \tag{3.5}$$

In the J-FIT DBA, for a given network load, an increase in $T_{fixed\ poll\ cycle}$ allows an ONU to spend more time in sleep/doze mode, thereby increasing η_1. On the other hand, for a given $T_{fixed\ poll\ cycle}$, when the network load increases, T_{active} increases, resulting in an increase in energy consumption and therefore, a decrease in η_1. As explained before, the J-FIT DBA allows the ONUs to enter into sleep mode for $T_{fixed\ poll\ cycle} \geq$ 2ms. Due to the large difference in power consumption (3.234 W) between sleep and active modes of a 10G-VCSEL ONU, the percentage of energy savings of up to 65% is achieved at low network loads with the J-FIT DBA algorithm. Compared to the JIT DBA, where significant energy savings is only possible at network loads $\geq$ 0.8, the J-FIT DBA results in improved energy

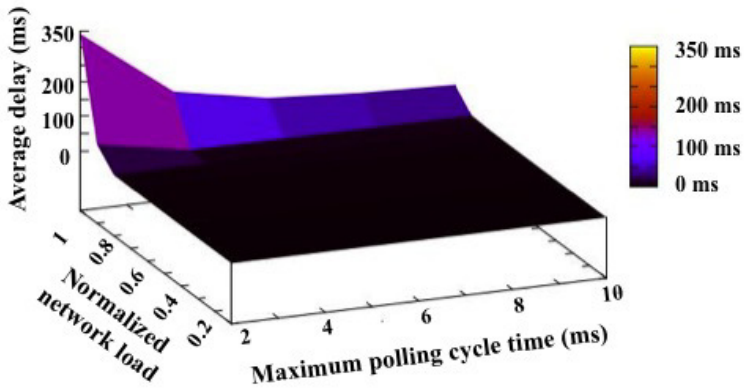

(a) JIT DBA

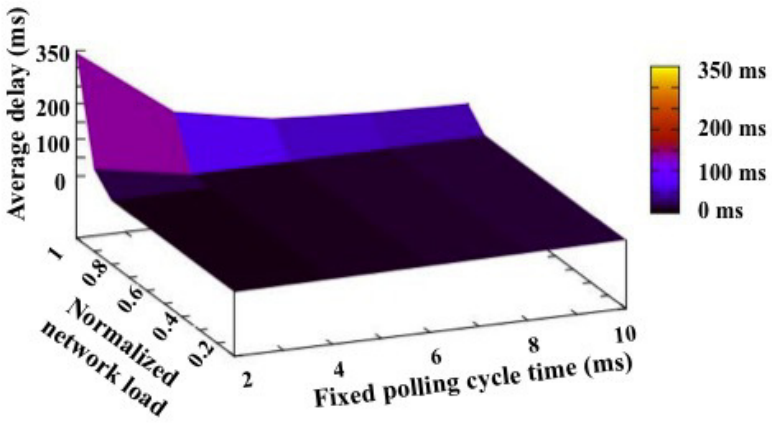

(b) J-FIT DBA

Figure 3.10: Average delay as a function of normalised network load and polling cycle time.

savings at a wider range of network loads.

Figures 3.10(a) and 3.10(b) illustrate the average delay of a sleep/doze 10G-VCSEL ONU as a function of maximum and fixed polling cycle times and normalised network load for the JIT and J-FIT DBA algorithms, respectively. In the JIT DBA, when the network load increases, the corresponding $T_{poll\ cycle}$ increases. With the increase in $T_{poll\ cycle}$, the packets have to wait for a longer duration before

they are scheduled for transmission in the next polling cycle. For normalised network loads ≤ 0.9, irrespective of the $T_{max\ poll\ cycle}$, $T_{poll\ cycle}$ remains the same (3.7). Consequently, for a given network load, the packets experience the same average delay. At the network load of 1, the link is fully utilised and more packets are accumulated at each ONU queue. Due to the unconstrained buffer lengths assumed in our simulations, these accumulated packets experience longer queuing delays at the network load of 1. Similarly in the J-FIT DBA, for a given network load, when the $T_{fixed\ poll\ cycle}$ increases, the average delay increases as well. Also, for a given $T_{fixed\ poll\ cycle}$, when the network load increases, the average delay increases. However, this increase is not quite apparent as the increase in $T_{tx\ slot}$ is comparatively smaller than $T_{fixed\ poll\ cycle}$. Compared to the JIT DBA, there is an increase in average delay at each network load for the J-FIT DBA. Nonetheless, when considering practical network loads of less than 0.6 [29], the average delay, remains below 1.32 ms and 16 ms for the JIT and the J-FIT DBA algorithms, respectively. Thus, the delay values of both algorithms remain within an acceptable range of $\leq$ 100 ms [34] to support delay-sensitive services, such as video over the 10G-EPON.

3.4.2 Performance comparison between 10G-VCSEL ONU and 10G-DFB ONU

This section provides a comparative analysis of the energy saving capabilities of the 10G-VCSEL ONU and 10G-DFB ONU in detail. Figure 3.11(a) illustrates the percentage of energy savings achieved using a sleep/doze 10G-VCSEL ONU compared to an always-ON DFB ONU, as a function of maximum polling cycle time and normalised network load for the JIT DBA. The percentage of savings η_2 is calculated as follows:

$$\eta_2 = \left(1 - \frac{P_{vcsel,act}T_{act} + P_{vcsel,doze/sleep}T_{doze/sleep}}{P_{DFB,act}(T_{act} + T_{sleep/doze})}\right)\% \tag{3.6}$$

where parameter $P_{DFB,act}$ represents the power consumption of an always-ON DFB ONU. As shown in Fig. 3.11, at any given $T_{fixed\ poll\ cycle}$, the sleep/doze mode 10G-VCSEL ONU results in energy savings of 24% up to a network load of 0.8. Beyond

the network load of 0.8, the 10G-VCSEL ONU achieves significant energy savings with the maximum of 70% being reached at the network load of 1 and $T_{fixed\ poll\ cycle}$ of 10 ms. This noticeable increase in η_2 results from the ONUs entering into doze mode up to a network load of 0.8 and into sleep mode beyond the network load of 0.8. As shown in Table 3.1, the difference in power consumption between an active 10G-DFB ONU (5.052 W) and a sleep mode 10G-VCSEL ONU (0.75 W) is higher than that of an active 10G-DFB ONU and a doze mode 10G-VCSEL ONU (3.85 W). This difference has resulted in higher energy savings for network loads ≥ 0.8.

Figure 3.11(b) plots η_2 as a function of $T_{fixed\ poll\ cycle}$ and normalised network load for the J-FIT DBA. As explained in Fig. 3.9(b), when $T_{fixed\ poll\ cycle}$ increases, it allows an ONU to spend more time in sleep or doze mode and, therefore, increases η_2. For a given $T_{fixed\ poll\ cycle}$, when the network load increases, an ONU spends more time in active mode, resulting in a decrease in η_2. However, as previously explained, the J-FIT DBA results in low power consumption compared to the JIT DBA as J-FIT allows an ONU to enter into sleep mode for $T_{fixed\ poll\ cycle} \geq 2$ms. This results in higher η_2 values in J-FIT across all the network loads, as compared to the JIT DBA. The results shown in Fig. 3.11 emphasise on the energy efficiency of the sleep/doze mode 10G-VCSEL ONU compared to an always-ON 10G-DFB ONU.

Figures 3.12(a) and 3.12(b) illustrate the percentage of energy savings achieved using a sleep/doze VCSEL ONU compared to a sleep/doze DFB ONU, as a function of maximum and fixed polling cycle times and normalised network load of the JIT and J-FIT DBA algorithms, respectively. The percentage of savings η_3 is calculated as follows:

$$\eta_3 = \left(1 - \frac{P_{vcsel,act}T_{act} + P_{vcsel,doze/sleep}T_{doze/sleep}}{P_{DFB,act}T_{act} + P_{DFB,doze/sleep}T_{sleep/doze})}\right)\% \tag{3.7}$$

where parameter $P_{DFB,doze/sleep}$ represents the power consumption of a 10G-DFB ONU in sleep or doze mode. As the figures show, the sleep/doze 10G-VCSEL ONU outperforms the sleep/doze 10G-DFB ONU under both algorithms. As listed in Table 3.1, sleep/doze 10G-VCSEL ONU has a shorter $T_{doze-to-active}$ (330 ns) com-

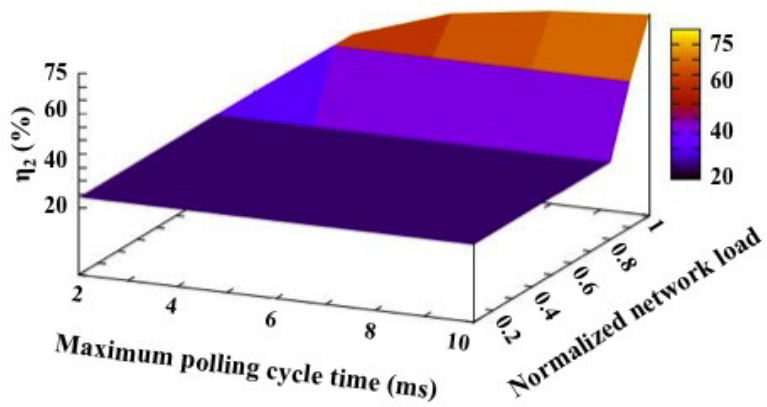

(a) JIT DBA

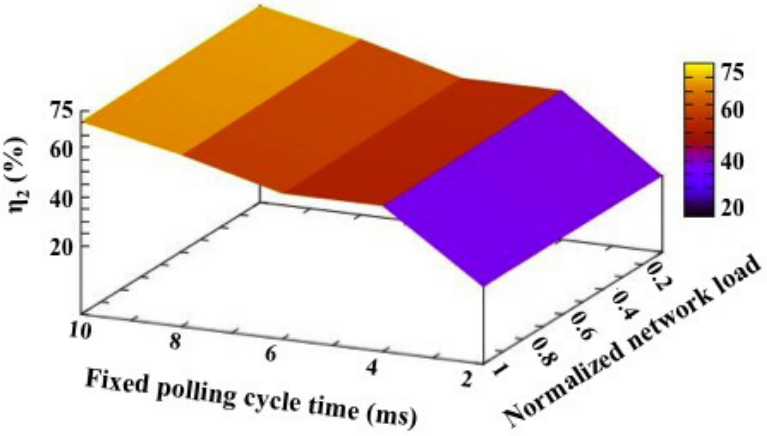

(b) J-FIT DBA

Figure 3.11: Percentage of energy savings (η_2) as a function of normalised network load and polling cycle time.

pared to a sleep/doze 10G-DFB ONU (760 ns). The sleep/doze 10G-VCSEL ONU also consumes less power in active mode, as compared to a sleep/doze 10G-DFB ONU. These inherent characteristics of the sleep/doze 10G-VCSEL ONU have resulted in better energy efficiency performance. It is also important to note that compared to the JIT DBA, the J-FIT DBA algorithm results in better energy savings as J-FIT allows an ONU to enter into sleep mode for $T_{fixed\ poll\ cycle} \geq$ 2ms. These results highlight the energy efficiency of the sleep/doze-capable 10G-VCSEL ONU

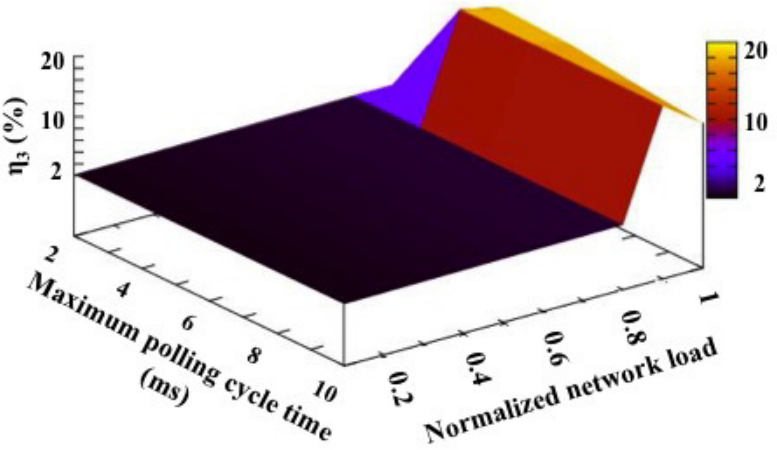

(a) JIT DBA

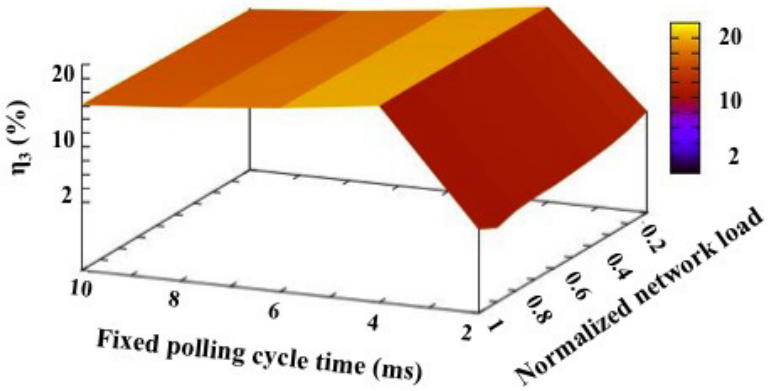

(b) J-FIT DBA

Figure 3.12: Percentage of energy savings (η_3) as a function of normalised network load and polling cycle time.

and also of the J-FIT DBA.

3.5 Conclusions

In this chapter, we proposed two novel DBA algorithms to improve the energy efficiency of the 10G-EPON. The algorithms, JIT DBA and J-FIT DBA, incorpo-

rate both the sleep and doze capabilities of a 10G-VCSEL ONU to reduce the energy consumption of the ONUs. The JIT and J-FIT DBA algorithms are designed with varying and fixed polling cycle times, respectively. The algorithms utilise the MPCP control messages, such as GATE and REPORT, to allocate bandwidth and also to transition the ONUs between sleep/doze and active modes. Both JIT and J-FIT DBA algorithms are designed such that an ONU in sleep/doze mode wakes up just-in-time to receive the next Ethernet packet from the OLT.

The most important outcome of these two algorithms is the improved energy savings across a wider range of network loads. When $T_{idle} \leq 2$ ms, an ONU cannot afford to transition into sleep mode and, therefore, cannot achieve any energy savings. Incorporating doze mode into the underlying DBA algorithm ensures energy savings even at shorter polling cycle times. While both JIT and J-FIT DBA algorithms achieve promising energy savings due to sleep and doze mode operations, the J-FIT DBA is able to outperform the JIT DBA in terms of energy savings, specially at low network loads, due to its fixed polling cycle time. Although the sleep and doze mode operations introduce additional delay in to the network, our results indicate that the average delay values of the JIT and J-FIT DBA algorithms remain below 1.32 ms and 16 ms, respectively, and well within the acceptable range of 100 ms to support the QoS requirements of practical access networks.

Further, simulation results indicate that our 10G-VCSEL ONU outperforms the conventional 10G-DFB-ONU in energy savings. The low power consumption in active mode and the shorter $T_{doze-to-active}$ results in both JIT and J-FIT achieving improved energy savings with the 10G-VCSEL ONU, compared to a 10G-DFB ONU. Based on these findings, our novel JIT and J-FIT DBA algorithms improve the energy efficiency through doze mode operation and increase the idle time to allow an ONU to spend more time in sleep/doze mode, respectively. As discussed in Chapter 2, this is one of the algorithm-based approaches in improving the energy-efficiency of the PON and it is successfully implemented using our JIT and J-FIT DBA algorithms.

The next important aspect of a sleep/doze DBA algorithm is determining the sleep/doze duration of an ONU. Although the OLT determines the sleep/doze

duration in the JIT and J-FIT DBA algorithms, it follows a simple criterion that depends on the instantaneous network load observed at the ONUs. The downside of this method is that resource allocation based on instantaneous bandwidth requests may not represent the overall behaviour of the network and may result in under or over-provisioning of network resources. Further, in the JIT DBA specifically, the sleep/doze duration is short at low network loads and yields low energy savings. Considering the fact that communication networks rarely operate at their maximum capacity, it is important to save more energy at low network loads. As a lightly-loaded ONU can afford to remain in sleep or doze mode for longer, without affecting QoS parameters, an effective sleep/doze allocating mechanism should assign longer sleep/doze duration at low network loads and shorter sleep/doze durations at high network loads. For this purpose, in the next Chapter, we present our Just-In-Time DBA with Bayesian estimation and prediction (BEP DBA) and discuss how it affectively assigns sleep/doze durations at different network loads and addresses both energy and QoS requirements of the TDM-PON.

CHAPTER 4

Bayesian Estimation and Prediction Based Dynamic Bandwidth Allocation Algorithm for 10 Gbps Ethernet Passive Optical Networks

4.1 Introduction

In the preceding chapter, we discussed different methods of incorporating sleep and doze mode operations into dynamic bandwidth allocation (DBA) algorithms to minimise energy consumption of time division multiplexed passive optical networks (TDM-PONs). A TDM-PON hosts an optical line terminal (OLT) at the central office (CO) and optical network units (ONUs) at the customer premises. In the upstream direction, from the ONUs to the OLT, the network facilitates bandwidth sharing through time division multiple access (TDMA). Under TDMA, an ONU is allowed to transmit its upstream packets only during its upstream time slot. Similarly in the downstream direction, packets destined to a given ONU is transmitted during its downstream time slot. However, due to broadcast nature of downstream traffic, these packets are received by all ONUs in the network. As a result, although an ONU receiver (Rx) does not receive its own packets beyond its downstream time slot, it continues to process medium access control (MAC) head-

ers of packets destined to other ONUs, before discarding them. As discussed in Chapter 3, if an ONU transceiver (TRX) does not receive or transmit any packets, it is said to be in idle state. Despite being in idle state for a significant duration of time, an ONU continues to operate at its active power level. As a result of the large number of ONUs present in current PONs, a significant proportion of energy consumption in access segment is attributed to the ONUs [1]. Instead of staying active, an ONU can transition into a low power mode, such as sleep or doze mode, during its idle time and save energy as proposed by Telecommunication Standardisation Sector of the International Telecommunication Union (ITU-T) [23]. During doze mode, only the ONU Tx is powered down while in sleep mode, both its Tx and Rx are powered down. As an ONU in sleep mode cannot receive its synchronisation bits from the OLT, upon waking up, it spends a certain time to re-synchronise itself with the OLT. This overhead time is referred to as sleep-to-active transition time, $T_{sleep-to-active}$. Although an ONU in doze mode continues to receive its synchronisation bits from the OLT, when transitioning from doze to active mode, the Tx takes a certain time to settle. This overhead time is referred to as doze-to-active transition time $T_{doze-to-active}$. In general, $T_{sleep-to-active} \geq T_{doze-to-active}$.

As explained in Chapter 2, determining the sleep/doze duration is an important aspect of a sleep/doze DBA algorithm. The main objective of our previous algorithms, Just-In-Time (JIT) DBA with varying polling cycle times and JIT DBA with fixed polling cycle times (J-FIT), has been to improve the energy efficiency of TDM-PONs through sleep and doze mode operations. Although these algorithms successfully improved the energy savings of the 10G-EPON, the criterion used to determine the sleep/doze duration in JIT and J-FIT does not yield optimum energy savings. For an instance, the JIT DBA achieves energy savings of only 3% for normalised network loads of ≤ 0.8, which is not acceptable considering that practical networks usually operate at network loads ≤ 0.6 [134]. Meanwhile, the J-FIT DBA algorithm, which is proposed to improve the energy-savings at low network loads, may lead to increased average delay, if used with a longer polling cycle time.

The sleep-mode-aware (SMA) algorithm proposed in [22], follows a criterion similar to that of the JIT DBA in allocating sleep duration and results in low energy-

savings at low network loads. The 75% of energy-savings reported at low network loads, is attributed to the sleep overhead in the range of nanoseconds reported in [28]. The findings of this study, whose energy-savings are dependent on the type of the ONU used, emphasise the importance of maximising the energy-savings at low network loads, irrespective of the ONU architecture.

While such an effective sleep/doze criterion will enhance the energy savings, the degradation of quality of service (QoS) parameters such as average delay, is inevitable in sleep/doze mode algorithms. As explained in Chapter 3, increasing the sleep/doze duration of an ONU increases its percentage of energy savings. However, a longer sleep/doze period also increases the polling cycle time, which in turn leads to increased average delay. In order to deliver satisfactory quality of experience (QoE) to the customers, the underlying sleep/doze mode DBA algorithm should also minimise the average delay experienced by users. Allocating longer sleep/doze periods for lightly-loaded ONUs and shorter sleep/doze periods for heavily-loaded ONUs has been identified as an effective solution to achieve these objectives. The motivation behind this criterion is that when the traffic load is low, ONUs can afford to go into sleep/doze mode for a longer duration without affecting the average packet delay. To allocate sleep/doze periods based on network load, the OLT should be able to determine the traffic load of an ONU from the information received through the REPORT message. In this process, it is important that the OLT uses a statistical parameter that represents the network load as it (1) results in more reliable and stable DBA algorithms based on time-averages of the network, and (2) enables traffic prediction to minimise average delay. Since the average inter-arrival time of packets is a statistical parameter that reflects the traffic load of the ONUs, it is widely used as a key parameter in determining the sleep/doze duration [110, 139, 140, 142, 143, 187, 188]. Moreover, the average inter-arrival time of packets can also be used in traffic prediction to improve the QoS of the network. When using a statistical parameter, however, it is important to use an effective technique that estimates the parameter of interests with lower number of sampling points.

Taking all these design specifications into consideration, we propose in this

chapter, the Bayesian estimation and prediction based JIT DBA (BEP DBA) algorithm that incorporates *both* sleep and doze mode operations. For illustrative purposes, the BEP DBA is proposed for the 10G-EPON, but can be implemented in any TDM-PON. Further, similar to our JIT and J-FIT DBA algorithms, the BEP DBA is designed to exploit the 10 Gbps vertical-cavity surface-emitting laser (10G-VCSEL) ONU with a $T_{doze-to-active}$ of 330 ns and $T_{sleep-to-active}$ of 2 ms [29, 180]. Table 4.1 lists the switching and power consumption values of the 10G-VCSEL ONU considered in this work. The BEP DBA also complies with the Multi-Point Control Protocol (MPCP) messages to allocate bandwidth and also to transition the ONUs between sleep/doze and active modes [189, 190].

In the proposed BEP DBA algorithm, the ONUs estimate the average inter-arrival time of packets using Bayesian estimation. A Bayesian framework incorporates the prior knowledge of the variable to be estimated, thus making it an effective mathematical model. The estimated average inter-arrival time is then used to determine the sleep *and* doze duration of the ONUs. To mitigate the average delay arising from sleep and doze mode operations, we also implement traffic prediction at the OLT. Using traffic prediction, the OLT can allocate bandwidth for accumulated traffic before they are reported by the ONUs, thereby, reducing the average delay. Under the proposed BEP DBA algorithm, the OLT predicts the amount of traffic accumulated at the ONUs during sleep or doze period. The OLT considers both predicted bandwidth and bandwidth requests sent from the ONUs through the REPORT message when allocating bandwidth for an ONU in the subsequent cycle. Before we present our proposed BEP DBA, in the following section, we will briefly discuss existing work done on determining the sleep/doze durations.

Table 4.1: Power consumption and switching values of 10G-VCSEL ONU [29]

Parameter	**Value**
Doze-to-active transition time ($T_{doze-to-active}$)	330 ns
Sleep-to-active transition time ($T_{sleep-to-active}$)	2 ms
Power consumption - active ($P_{vcsel,act}$)	3.984 W
Power consumption - doze ($P_{vcsel,doze/sleep}$)	3.85 W
Power consumption - sleep ($P_{vcsel,doze/sleep}$)	0.75 W

4.2 Related work

As explained in the introduction, the average inter-arrival time of packets is identified as the most favourable statistical parameter that represents the traffic load of a network. To date, various DBA algorithms have been proposed, where the sleep or doze duration is determined based on the average inter-arrival time of packets. One of the earliest studies on this area is the sleep and adaptive link rate control (ALR) mechanism proposed for the 10G-EPON by Kubo *et. al* [142,143]. In the presence of traffic, the ALR function varies the link rate based on the network load. In the absence of traffic, the ONUs are transitioned into sleep mode to improve the energy-efficiency. The OLT monitors the downstream arrival rate of packets, and if it is higher than a predetermined threshold of i_{th}, the ONUs are made to sleep for a predetermined time of T_s. The ONUs however, wake up periodically to inspect their low rate links for downstream traffic. This periodic waking up reduces possible energy-savings, due to the large $T_{sleep-to-active}$. Moreover, this algorithm also requires additional slow-rate components, which makes the proposed architecture more complex and costly [191]. In order to minimise the average delay resulting from fixed T_s, especially at high network loads, Kubo *et. al* proposed an alternative adaptive sleep controlled mechanisms in [139, 143]. Instead of allocating a fixed T_s, the proposed solution in [143] assigns two sleep durations across the range of network loads, while in [139], the sleep-control function takes a more linear form. In [187], the authors proposed a hybrid deep/cyclic sleep-based DBA algorithm with batch mode transmission at the OLT and the ONUs. The algorithm allows an ONU to sleep for a maximum length of time, provided that the delay requirement is satisfied. The algorithm, however, is analysed for delay constraints in the range of 100 ms, resulting in sleep times $\geq$ 50 ms. In such an instance, the OLT may perceive the ONU to be inactive and de-register it from the list of ONUs to be served. In [110], Zhang *et. al* proposed a DBA algorithm for multi-power-level ONUs, where the sleep time of the ONUs is determined by the inter-arrival time of downstream packets. In contrast to existing algorithms where the entire ONU is powered down, the proposed algorithm powers down certain components of the

ONU based on different traffic conditions. Zhang *et. al* also proposed a sleep mode DBA where the ONUs decide on the sleep time based on the bandwidth allocation pattern of the OLT [188]. If an ONU is not allocated bandwidth for x number of cycles, it goes to sleep mode for y number of cycles, where the cycle time is set as 2 ms. The authors have shown the effect of x and y on energy consumption and average delay.

With the inter-arrival time of packets being identified as the key parameter in determining the sleep/doze time, different techniques have been adapted to estimate the average inter-arrival time. Kubo *et. al* proposed a linear sleep control function where the sleep duration is determined based on the estimated average inter-arrival time of packets [142]. In this study, the average inter-arrival time of packets is estimated using an exponential smoothing technique. In [141], Fiammengo *et. al* proposed a similar sleep-control function where the average inter-arrival time of packet is estimated using an arithmetic average technique.

In a majority of the sleep-control functions discussed so far in this chapter, only sleep mode operation is used for energy-saving purposes. As we have highlighted in Chapter 3, for an ONUs that has a larger $T_{sleep-to-active}$ compared to its $T_{doze-to-active}$, doze mode operation yields significant energy savings when the idle time is less than $T_{sleep-to-active}$. Although our proposed algorithms in Chapter 3 address this issue with doze mode operation, the approach taken in determining sleep/doze time is instantaneous. Further, the estimation techniques used in existing studies do not consider the prior knowledge of the statistical details about the parameter i.e., the average inter-arrival time, to be estimated. As importantly, the proposed methods in [22,28,110,133,140,141,187–189] do not address the issue of increased queuing delays resulting from sleep and doze mode operations. To address these shortcomings in existing literature and as an improvement to our previously proposed JIT and J-FIT algorithms [189], in this chapter, we propose a Bayesian estimation and prediction-based JIT DBA (BEP DBA) algorithm that incorporates *both* sleep and doze mode operations. The following sections discuss how the novel BEP DBA algorithm achieves these objectives, in detail.

4.3 Bayesian estimation and prediction based JIT DBA algorithm

The main objectives of the proposed BEP DBA algorithm are to: (1) effectively estimate the average inter-arrival time of packets at the ONUs using Bayesian estimation; (2) transition the ONUs between sleep/doze and active modes just-in-time to receive packets from the OLT using the Multi-Point Control Protocol (MPCP); and (3) minimise the queuing delays introduced by the sleep and doze operations using traffic prediction. In this section, we describe how our BEP DBA algorithm achieves these objectives, in detail.

4.3.1 Bayesian estimation of average inter-arrival time

Bayesian estimation is a probabilistic framework where the unknown parameters to be estimated are modelled as random variables. One of the advantages of Bayesian philosophy is that we can incorporate our knowledge of the unknown parameters in the form of prior belief [192]. In our network model, the inter-arrival times of packets arriving at the ONUs is modelled by an exponential distribution with parameter λ and we are interested in estimating the average inter-arrival time, $1/\lambda$, of packets.

Following a Bayesian framework, we model λ as a random variable. If the error criterion to assess the performance of the estimator is the Bayesian mean squared error (BMSE), then it could be shown that the optimal estimate is given by the mean of the posterior distribution [192]. After each measurement is received, the estimate of λ is updated. First, let us consider the estimation procedure when the 1^{st} measurement y_1 is received.

According to the Baye's theorem, the posterior $p(\lambda|y_1)$ is related to the likelihood $p(y_1|\lambda)$ and the prior $p(\lambda)$ by:

$$p(\lambda|y_1) \propto p(y_1|\lambda)p(\lambda), \tag{4.1}$$

At this point, we would like to introduce the concept of a conjugate prior. A conjugate prior is a distribution, which results in the posterior of the same family of distributions as the prior itself. Assuming a conjugate prior distribution usually simplifies the required computations of the posterior parameters. For the problem considered here, the likelihood function $p(y_1|\lambda)$ follows an exponential distribution and the Gamma distribution is the conjugate prior for an exponential likelihood. This could be easily verified by substituting a Gamma distribution with parameters α_0 and β_0 into (4.1). Let $\mathcal{G}(\cdot;\alpha,\beta)$ denote a Gamma distribution with shape parameter α and rate parameter β. Then,

$$p(\lambda|y_1) \propto p(y_1|\lambda)\mathcal{G}(\lambda;\alpha_0,\beta_0), \tag{4.2}$$

$$\propto \{\lambda \exp(-\lambda y_1)\} \left\{ \frac{\beta_0^{\alpha_0}}{\Gamma(\alpha_0)} \lambda^{\alpha_0-1} \exp(-\beta_0\lambda) \right\}, \tag{4.3}$$

$$\propto \lambda^{(\alpha_0+1)-1} \exp\{-(\beta_0+y_1)\lambda)\}, \tag{4.4}$$

$$\propto \mathcal{G}(\lambda;\alpha_1,\beta_1), \tag{4.5}$$

where

$$\alpha_1 = \alpha_0 + 1, \tag{4.6}$$

$$\beta_1 = \beta_0 + y_1. \tag{4.7}$$

The estimate of λ after one measurement is given by the posterior mean, i.e. mean of $\mathcal{G}(\lambda;\alpha_1,\beta_1)$.

$$\hat{\lambda}_1 = \frac{\alpha_1}{\beta_1}, \tag{4.8}$$

$$= \frac{\alpha_0+1}{\beta_0+y_1}. \tag{4.9}$$

The estimate of the average inter arrival time after one measurement is simply

given by:

$$\hat{T}_1 = 1/\hat{\lambda}_1, \tag{4.10}$$

$$= \frac{\beta_0 + y_1}{\alpha_0 + 1}. \tag{4.11}$$

When the second measurement y_2 arrives, the exact procedure is carried out with the exception that the $\mathcal{G}(\lambda; \alpha_1, \beta_1)$ now becomes the prior distribution. It is easy to see that the estimation procedure could be generalised to obtain the n^{th} estimate after observing measurements $y_1, y_2, \ldots, y_n$. The conjugate property of the Gamma distribution to the exponential likelihood ensures that after each estimation step, the posterior is always a Gamma distribution.

In general, the estimates of λ and T after observing packets $y_1, y_2, \ldots, y_n$ is given by;

$$\hat{\lambda}_n = \frac{\alpha + n}{\beta + \bar{y}}, \tag{4.12}$$

$$\hat{T}_n = \frac{\beta + \bar{y}}{\alpha + n}, \tag{4.13}$$

where $\bar{y}$ is the sum of n number of measurements. Each time an ONU receives a packet in its subscriber network interface (SNI), the ONU updates n and $\bar{y}$. If the average packet arrival rate to be estimated is λ, the α and β are chosen such that the mean value of the Gamma distribution, i.e. $\frac{\alpha}{\beta}$, is equal to λ. In a practical network, choosing α and β, such that the standard deviation of the Gamma distribution, $\frac{\alpha}{\beta^2}$, is large will ensure that the Gamma distribution can accommodate a large range of inter-arrival times under consideration. Using these values n, $\bar{y}$, α, and β, the ONU calculates the estimated average inter-arrival time of packets $\hat{T}_n$, according to eqn. 4.13.

The initial simulation to illustrate the effectiveness of the Bayesian estimation was performed using Matlab. We simulated 5000 Ethernet packets and calculated the mean squared error (MSE) in estimating the average inter-arrival time using the Bayesian estimation, arithmetic average, and exponential smoothing methods. Figure 4.1 plots the MSE in estimating the average inter-arrival time using the

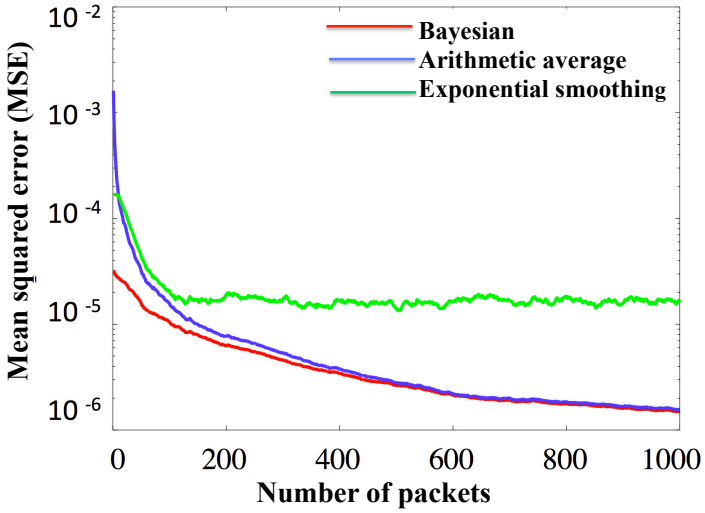

Figure 4.1: Mean squared error in estimation vs. number of packets.

Bayesian, arithmetic average, and exponential smoothing methods as a function of number of packets. Results show that Bayesian estimation yields comparatively low MSE values with a fewer number of measurements compared to the other two methods. In the next section, we discuss how this estimated average inter-arrival time of packets is used to determine the sleep/doze duration of the ONUs and how the MPCP control messages transition the ONUs between sleep/doze and active modes.

4.3.2 Multi-Point Control Protocol with sleep/doze control

As explained in Chapter 2, when multiple ONUs attempt to access the upstream bandwidth, collisions may occur. MPCP is a MAC protocol that is used to avoid such collisions in the EPON. The MPCP uses control messages such as REPORT (sent from the ONUs to the OLT) and GATE (sent from the OLT to the ONUs) to receive bandwidth requests from the ONUs and to assign bandwidth to the ONUs, respectively. In this section, we explain how the proposed BEP DBA utilises these control messages to allocate bandwidth, to assign sleep/doze durations, and to transition the ONUs between sleep/doze and active modes.

In a conventional DBA algorithm, the OLT receives REPORT messages from all

ONUs in the PON. The OLT then allocates transmission time slots to each ONU and includes this bandwidth allocation information in its GATE message to an ONU. Upon receiving this GATE message, an ONU transmits for a duration specified by the OLT and after completing its upstream transmission, sends its REPORT message to the OLT. The ONU then remains active until it receives the next GATE from the OLT. In comparison, the proposed BEP DBA incorporates sleep/doze mode operations and traffic prediction to improve the energy efficiency and the average delay, respectively.

Figure 4.2 illustrates the overall traffic flow of the proposed BEP DBA for an illustrative 10G-EPON with two ONUs. The parameters $T_{poll\ cycle}$, $T_{sleep/doze}$, T_{idle}, and T_{wakeup} represent the polling cycle time, ONU sleep/doze duration, ONU idle duration, and ONU wake up time, respectively. When an ONU receives an Ethernet frame from the OLT, the ONU analyses the GATE message and determines the data transmission start time, data transmission duration, the sleep/doze start time, and the sleep/doze duration. Note that the transmission duration is calculated considering the bandwidth request from an ONU and also using the prediction mechanism at the OLT, which will be explained in detail below. After analysing the GATE message, the ONU immediately starts upstream data transmission. After the ONU completes its upstream data transmission, the ONU generates its REPORT message, which contains the bandwidth request and also the estimated average inter-arrival time of packets, to the OLT. The ONU then enters

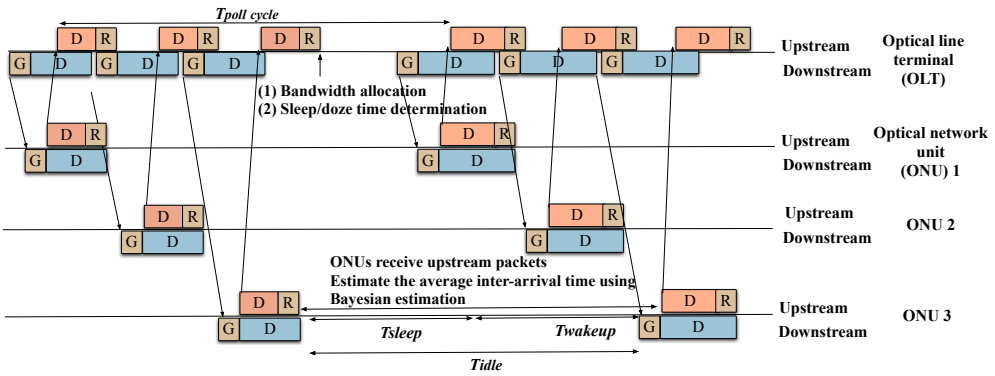

Figure 4.2: Traffic flow of the BEP DBA. D-Data, R-REPORT and G-GATE.

into sleep or doze mode for a duration specified by the GATE message. During this time, the back-end digital circuitry of the ONU is kept active [24] and continues to estimate the average inter-arrival time of upstream packets using Bayesian estimation. When the sleep or doze time elapses, the ONU wakes up just-in-time to receive the next Ethernet frame from the OLT in the subsequent cycle.

Figure 4.3 illustrates the flow chart of the BEP DBA executed at the OLT. When an ONU receives packets through its subscriber interface, it estimates the average

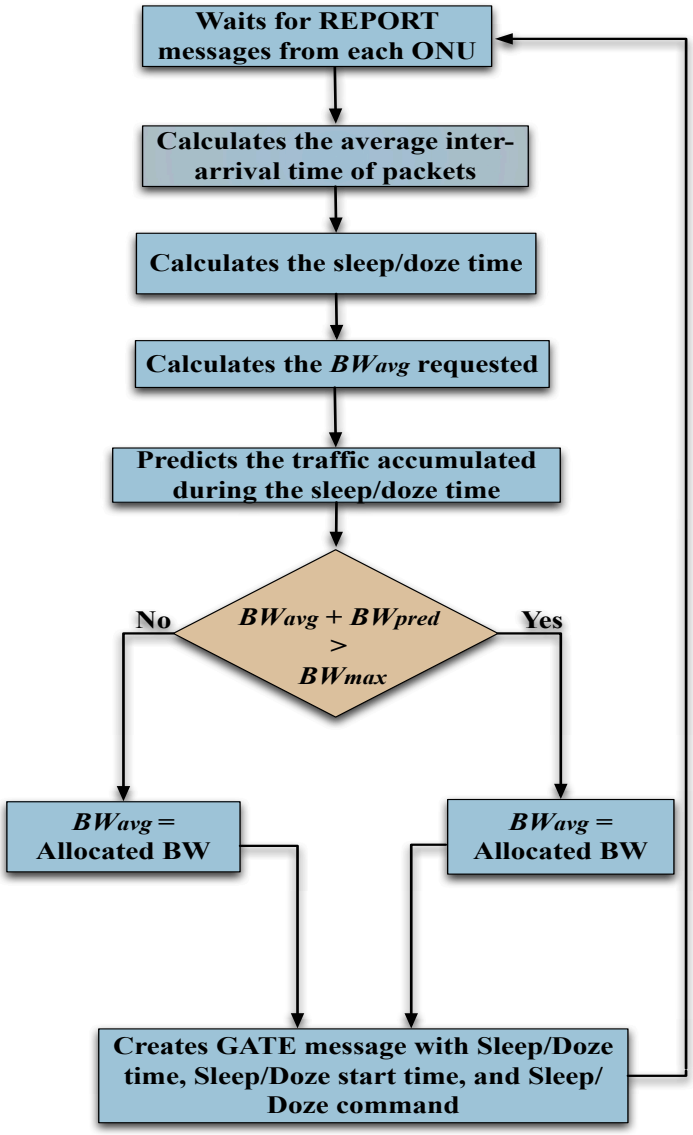

Figure 4.3: Flow chart of the BEP DBA executed at the OLT.

inter-arrival time of packets using Bayesian estimation. Additionally, the ONU inspects its incoming queue to determine its bandwidth requirement in the next cycle. The ONU then includes the estimated inter-arrival time and the bandwidth requirement in its REPORT message to the OLT. Upon receiving REPORT messages from all ONUs in the PON, the OLT calculates the average requested bandwidth, BW_{avg} and the average inter-arrival time of packets for each ONU. It is important to note that in any given instance, we assume all ONUs to operate under the same network load [181]. As a result, the ONUs have similar bandwidth requests and estimated inter-arrival times. Under this assumption, it is reasonable to take the average values of bandwidth requests and inter-arrival times. To calculate the average bandwidth requested (and average inter-arrival time), the OLT sums up the bandwidth requests (inter-arrival times) reported by all ONUs in a given cycle and divides it by the number of ONUs in the PON. Similar to the JIT and J-FIT DBA algorithms, we have also assumed the upstream and downstream traffic to be symmetrical [24, 181]. As a result, only the upstream traffic is considered when allocating upstream and downstream bandwidth and sleep/doze periods.

Using the illustrative sleep/doze control function shown in Fig. 4.4 and the

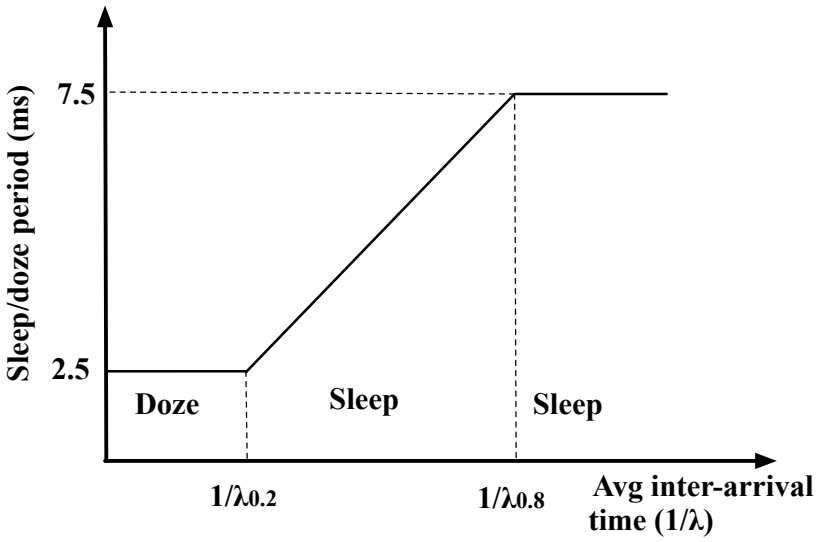

Figure 4.4: Sleep/doze duration vs. average inter-arrival time.

estimated average inter-arrival time of packets, the OLT determines the sleep or doze duration for all ONUs in the subsequent cycle. Note that the values, $1/\lambda_{0.2}$ and $1/\lambda_{0.8}$ represent the average inter-arrival times corresponding to the network loads of 0.2 and 0.8, respectively. For example, ONUs with inter-arrival times more than $1/\lambda_{0.8}$ will be transitioned into sleep mode in the next polling cycle with sleep times ranging from 2.5 ms to 7.5 ms. The network loads and doze/sleep durations that correspond to the sleep and doze regions were chosen based on the traffic profile given in [29] and an arbitrary delay constraint of 10 ms.

At this point, the OLT is aware of the sleep/doze duration and the estimated inter-arrival time of packets of an ONU. The OLT is, therefore, able to predict the packets accumulated, BW_{pred}, during the sleep or doze period of an ONU. The OLT calculates the sum of weighted predicted bandwidth, $BW_{w\ pred}$ (explained in detail in the following section) and average requested bandwidth, B_{avg}, and compares this value against the maximum allowable bandwidth, BW_{max}, that satisfies a given maximum polling cycle time. The OLT includes the sleep or doze times and the transmission time slot information in the GATE message for each ONU.

Figure 4.5 illustrates the flow chart of the proposed BEP DBA algorithm executed at the ONU. Apart from estimating the inter-arrival time of packets using Bayesian framework, the BEP DBA executed at the ONU is similar to that of the JIT and J-FIT reported in [189]. An ONU transitions from sleep or doze mode to active mode just-in-time to receive the GATE message and downstream data from the OLT. After processing the GATE message, an ONU transmits its upstream data for a period of time as specified in the GATE message. The ONU then generates and sends its REPORT message to the OLT. The REPORT message contains the bandwidth requirement and the estimated average inter-arrival time of packets of the ONU. The ONU then enters into sleep or doze mode as specified by the GATE and continues to estimate the inter-arrival time of incoming packets.

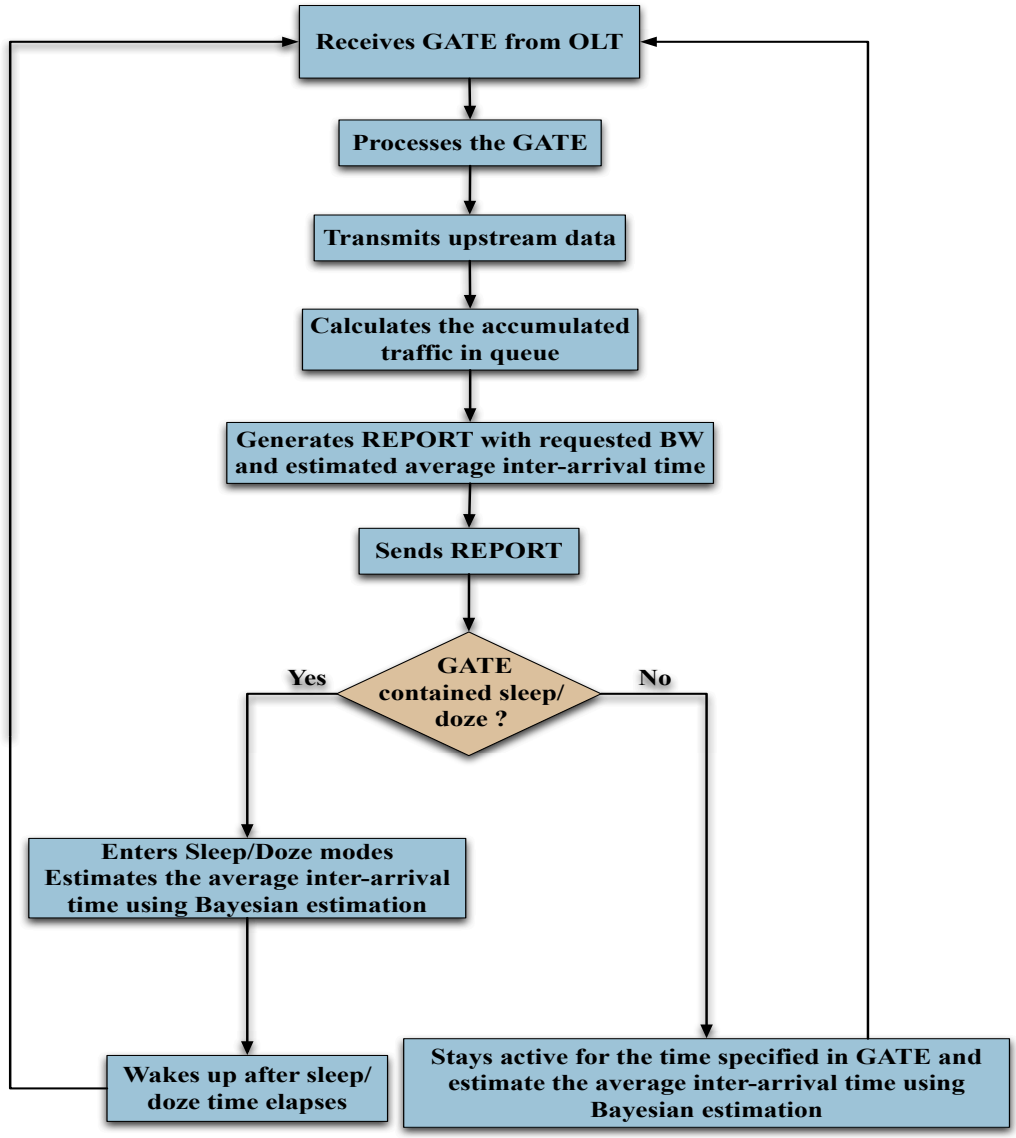

Figure 4.5: Flow chart of the BEP DBA executed at the ONU.

4.3.3 Traffic prediction mechanism

The downside of introducing sleep and doze mode operations into the normal operation of a PON is that it increases the queuing delay experienced by the packets. To address this issue, we propose traffic prediction at the OLT. The additional queuing delay can potentially be minimised if the OLT can predict the amount of traffic that is accumulated during the sleep or doze period of each ONU. This allows the OLT to allocate bandwidth for the packets accumulated during the cur-

rent cycle in the subsequent cycle, thus preventing packets from waiting in the queue for an extra cycle before any bandwidth is allocated for their transmission.

As explained in the previous section, the estimated average inter-arrival time of packets at the ONU is $1/\lambda$. Each ONU delivers this value to the OLT through its REPORT message. The OLT then determines the sleep or doze duration, $T_{sleep/doze}$, according to the sleep/doze control function shown in Fig. 4.4. Using the parameters λ, $T_{sleep/doze}$, and the average Ethernet packet size of 791 bytes, the predicted traffic, BW_{pred} in bytes, accumulated during the sleep or doze period, can be calculated as follows:

$$BW_{pred} = \lambda \, T_{sleep/doze} \, x \, 791 \, x \, W \, bytes \tag{4.14}$$

Based on our preliminary simulations, using the sum of BW_{pred} and B_{req} can in fact, lead to longer polling cycle times and, therefore, increased queuing delays. To avoid unnecessary delays, a certain proportion of the BW_{pred}, i.e., W, is considered in allocating the bandwidth. Using C++, we simulated a 10G-EPON with 32 ONUs and calculated the optimal value of W that results in the minimum average delay for each network load. Figure 4.6 illustrates the optimised W as a function of normalised network load. Using this value, the weighted predicted bandwidth, $BW_{w\ pred}$, is calculated as follows:

$$BW_{w\ pred} = BW_{pred} \, . \, W \, bytes \tag{4.15}$$

where parameter W is the weight by which the BW_{pred} is multiplied and it lies between 0 and 1. When allocating transmission time slots, the OLT considers the sum of B_{avg} and $BW_{w\ pred}$.

In the following section, we analyse the performance of the proposed BEP DBA algorithm for its energy-efficiency and average delay.

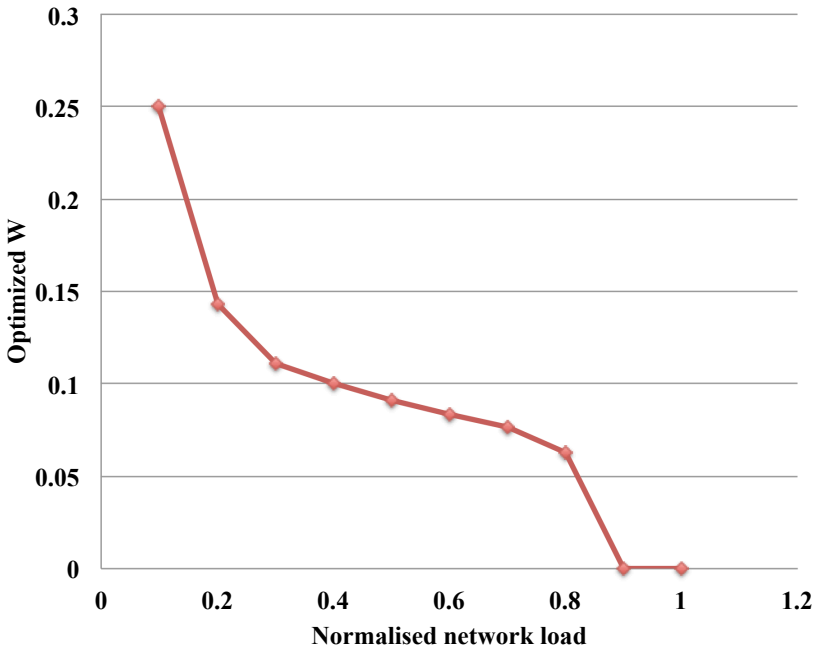

Figure 4.6: Optimised W as a function of normalised network load.

4.4 Performance evaluation

The performance of the BEP DBA algorithm is evaluated in two stages. First, we consider only Bayesian estimation and sleep/doze control to evaluate the average delay and energy savings of the network. Our findings on this analysis is presented in Section 4.4.1. Next, we quantify the percentage improvement in average delay and the percentage increase in energy consumption due to the prediction mechanism. The results of this analysis is presented in Section 4.4.2.

The simulations for the proposed BEP DBA were performed using C++. Packet arrivals at the ONUs follow a Poisson distribution. Table 4.2 lists the network and protocol parameters of the 10G-EPON considered in this work. Note that in our simulations, a normalised network load of 1 is equal to a 10 Gbps network load. Further, we have used the switching and power consumption values listed in Table 4.1 when analysing the energy efficiency of the BEP DBA algorithm. The initial simulations were performed for maximum polling cycle times ranging from 10 ms to 20 ms. Based on our findings, the BEP-DBA has a minimal dependency on max-

imum polling cycle times within this range. The results presented in this section, therefore, illustrate the performance of the proposed BEP-DBA for a maximum polling cycle time of 10 ms only.

Table 4.2: Network and protocol parameters

Parameter	Value
Downstream and upstream line rate	10 Gbps
Number of ONUs	32
Normalised network load	0.1 - 1
Propagation delay	100 μs
Inter-frame gap in upstream	1μs
Average Ethernet packet size	791 bytes

4.4.1 Performance of Bayesian estimation

Figure 4.7 illustrates the average power consumption per ONU as a function of normalised network load for the BEP DBA algorithm. As highlighted in Fig. 4.4, the ONUs enter into sleep mode for network loads ≤ 0.8. For network loads between 0.2 and 0.8, when the network load increases, the sleep time of the ONUs decreases linearly, thereby increasing the power consumption linearly as illustrated

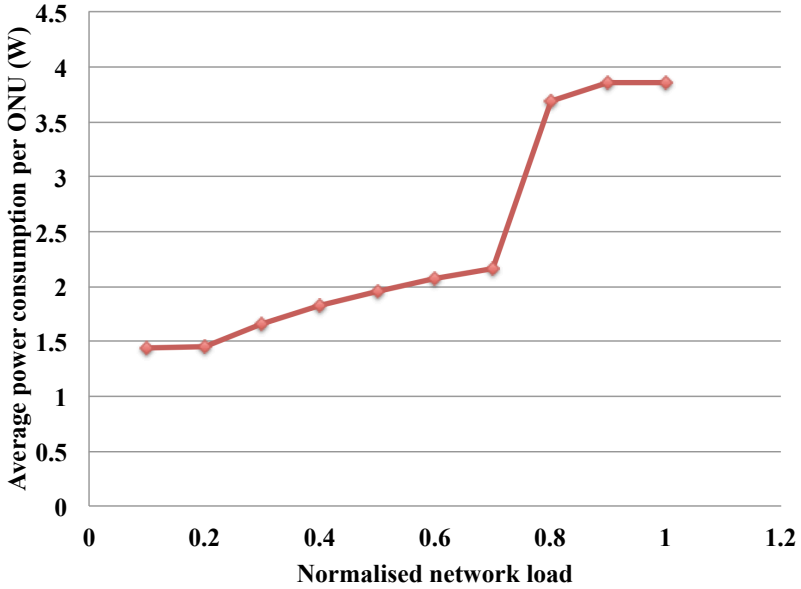

Figure 4.7: Average power consumed as a function of normalised network load.

in Fig. 4.7. For network loads ≥ 0.8, the ONUs enter into doze mode for 2.5 ms, resulting in an average power consumption of 3.85 W per ONU, which corresponds to the doze mode power consumption of the 10G-VCSEL ONU (Table 4.1).

Figure 4.8 illustrates the percentage of energy-savings per ONU as a function of normalised network load for the BEP DBA. The percentage of energy savings, μ, is calculated as follows:

$$\mu = \left(1 - \frac{P_{vcsel,act}T_{act} + P_{vcsel,doze/sleep}T_{doze/sleep}}{P_{vcsel,act}(T_{act} + T_{sleep/doze})}\right)\% \tag{4.16}$$

where parameters $P_{vcsel,act}$ and $P_{vcsel,doze/sleep}$ represent the power consumption of the 10G-VCSEL ONU in active mode and in sleep/doze modes, respectively. The parameters T_{act} and $T_{doze/sleep}$ represent the time an ONU spends in active and sleep or doze modes, respectively. It is important to note that T_{act} includes the $T_{sleep-to-active}$ or $T_{doze-to-active}$, of 2 ms and 330 ns, respectively. As explained in Fig. 4.7, for network loads ≤ 0.8, the ONUs enter sleep mode. Due to the large difference in power consumption (3.234 W) between the sleep and active modes of the 10G-VCSEL ONU, a μ as high as 63% is achieved for network loads ≤ 0.2 with

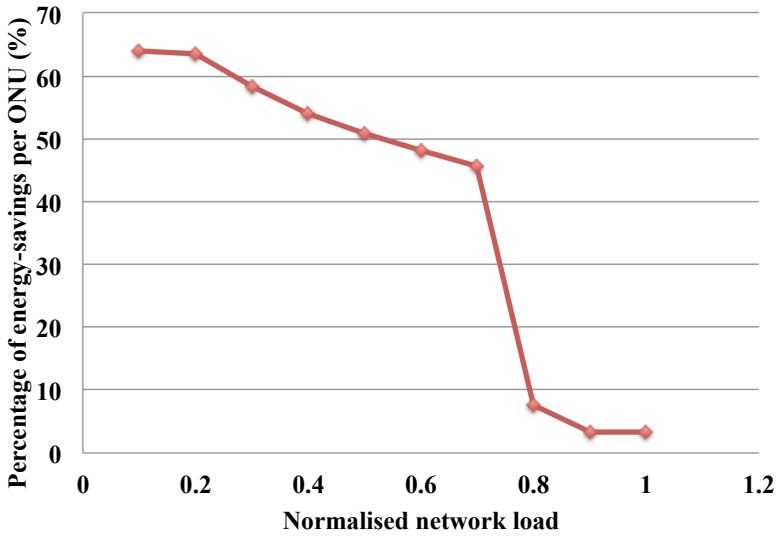

Figure 4.8: Percentage of power savings as a function of normalised network load.

the proposed algorithm. For network loads between 0.2 and 0.8, the sleep time decreases linearly with the increase in network load. Consequently, μ decreases linearly. For network loads $\geq$ 0.8, the ONUs enter into doze mode and due to the small difference in power consumption (0.134 W) between the doze and active modes of the 10G-VCSEL ONU, a μ of only 3% is achieved. However, compared to the algorithms proposed in [141,142], where no energy savings is possible for high network loads, our novel BEP DBA algorithm achieves tangible energy savings at high network loads as we have incorporated the doze capability of the ONU into the algorithm.

Figure 4.9 illustrates the average delay per ONU as a function of normalised network. For network loads $\leq$ 0.8, when the network loads increases, the average delay decreases. As shown in Fig. 4.4, when the network load increases, the sleep time decreases. This results in a decrease in average delay. For network loads $\geq$ 0.8, the network approaches its capacity limit and more packets are accumulated at the ONUs. This leads to increased queuing delays. However, it is important to note that for network loads $\leq$ 0.9, the largest value of the reported average delay remains below the specified 10 ms and thus satisfies the QoS requirements.

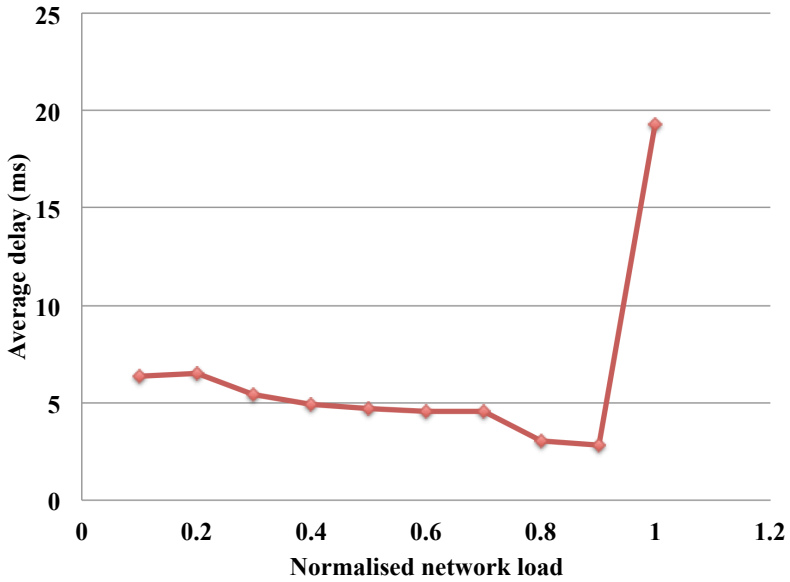

Figure 4.9: Average delay as a function of normalised network load.

4.4.2 Performance of Bayesian estimation with prediction

In this section, we present results from our impact study of the prediction mechanism on average delay and power consumption. First, we investigate the improvement in average delay presented in Fig. 4.9, due to traffic prediction. Figure 4.10 illustrates the percentage of decrease in average delay, η, due to the proposed prediction mechanism as a function of normalised network load. The value η decreases with the increase in normalised network load. According to Fig. 4.6, when the normalised network load increases, W decreases, thus decreasing the term $W * BW_{pred}$. The effectiveness of the prediction mechanism depends on the predicted bandwidth considered at the OLT. As $W * BW_{pred}$ decreases, the possible improvement due to the prediction mechanism decreases as well. Results show that with the prediction mechanism, the average delay is reduced by as much as 13%. For network loads ≥ 0.8, the network approaches capacity limit and therefore the polling cycle reaches the maximum polling cycle limit. Consequently, no improvement in average delay could be observed with the prediction mechanism.

As explained earlier, the implication of traffic prediction is the increase in ONU

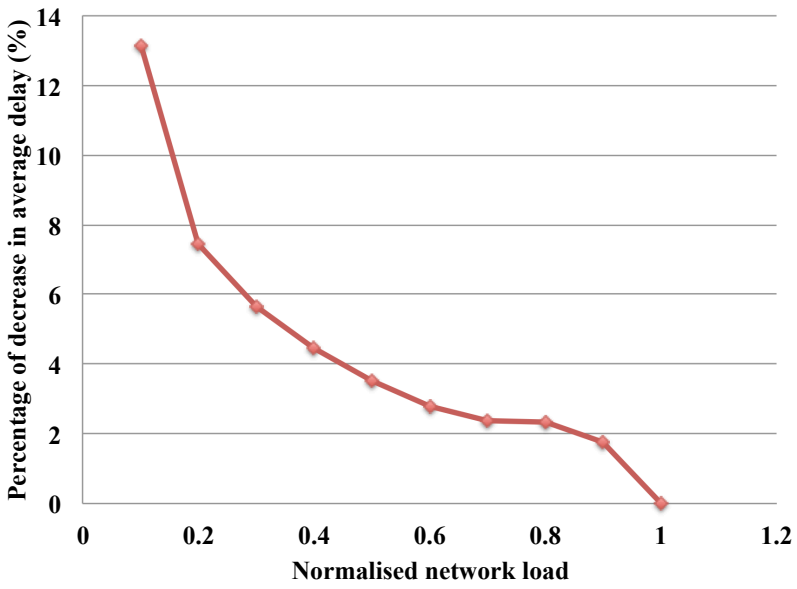

Figure 4.10: Percentage decrease in average delay as a function of normalised network load.

energy consumption. Figure 4.11 plots the percentage in power consumption increment, κ, due to the prediction mechanism as a function of normalised network load. According to our results, the value κ decreases with the increase in network load. When the network load increases, the proportion of predicted network load, W, decreases. Consequently, the allocated time slot and thus, the power consumption decreases. As shown in Fig. 4.11, the maximum increase in power consumption is negligible at 0.01%.

From a customer's perspective, the average delay should be minimised to ensure better QoE. From an energy perspective, the overall energy consumption should be minimised to minimise operational expenditure and greenhouse gas emissions. Considering the improvement of average delay and the negligible increase in energy consumption resulting from our novel BEP DBA algorithm, we can see that the BEP DBA is able to satisfy both requirements.

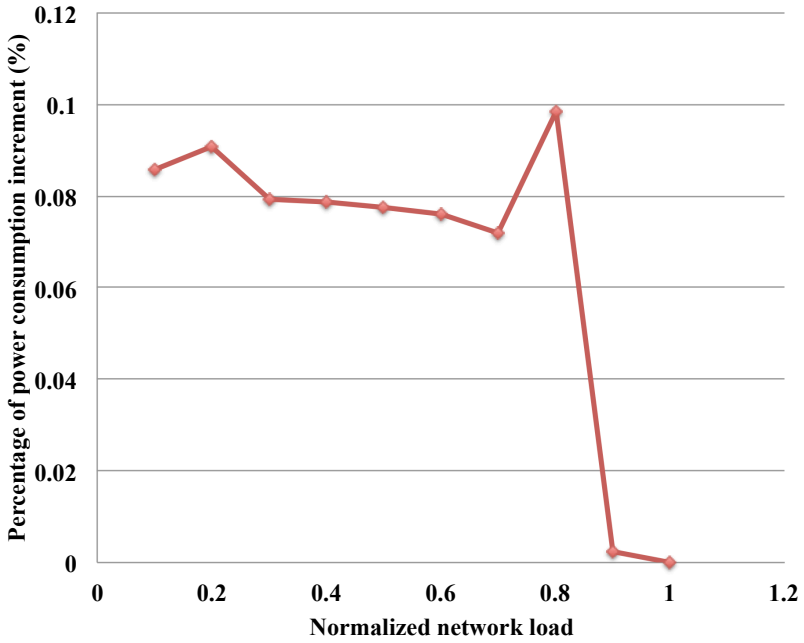

Figure 4.11: Percentage in power consumption increment as a function of normalised network load.

4.5 Conclusions

We have proposed a novel Bayesian estimation and prediction based JIT DBA algorithm (BEP DBA) exploiting the sleep and doze capabilities of the 10G-VCSEL ONU. The algorithm addresses an important aspect of a sleep/doze DBA algorithm, i.e., determining the sleep/doze duration of the ONUs. For this purpose, the ONUs estimate the average inter-arrival time of the packets using Bayesian estimation. This information, transmitted to the OLT through GATE messages, is used in determining the sleep and doze time of each ONU. The algorithm achieves 63% of energy-savings at low network loads and results in tangible energy-savings even at high network loads due to doze mode operation. The maximum average delay values of our proposed algorithm remain below the specified maximum of 10 ms for practical network loads of 0.6 and below and, therefore, satisfy QoS specifications of the network. The proposed traffic prediction mechanism of the BEP DBA reduces the average delay up to a 13%, but only at a maximum of 0.01% increase in average power consumption per ONU.

Up to this point in this thesis, the DBA algorithms namely, JIT, J-FIT, and BEP, have been proposed for TDM-PONs. However, recent statistics on user behaviour implies that the existing PONs may require to upgrade their capacity and network span to satisfy future customer demand. After evaluating potential network architectures that may fulfil these requirement, the time and wavelength division multiplexed PON (TWDM-PON) has been selected by FSAN as the most effective configuration to meet this future demand. In the next Chapter, we consider a delay-constrained TWDM-PON and examine the potential energy saving strategies to be implemented in both the OLT and ONUs.

CHAPTER 5

Energy-Efficient Framework for Time and Wavelength Division Multiplexed Passive Optical Networks

5.1 Introduction

The exponential growth of the Internet and the limitations in copper wire-line networks to meet this increasing bandwidth demand have led to the deployment of fibre-based passive optical networks (PONs) in the access networks. Next-generation PONs are evolving in two main stages, namely, next generation PON stage 1 (NG-PON1) and NG-PON2. Under the NG-PON1, two main time division multiplexed PON (TDM-PON) architectures, the Gigabit PON (GPON) and Ethernet PON (EPON), have been standardised by Full Service Access Network (FSAN)/Telecommunication Standardisation Sector of the International Telecommunication Union (ITU-T) and the IEEE 802.3 working group, respectively [193]. These TDM-PONs host an optical line terminal (OLT) at the central office (CO) and optical network units (ONUs) at the customer premises. A detailed description of a generic TDM-PON is given in Chapter 2.

In Chapters 3 and 4, we proposed energy-efficient dynamic bandwidth allocation (DBA) algorithms for such TDM-PONs, exploiting the sleep and doze capabilities of a 10 Gbps vertical-cavity surface-emitting laser (10G-VCSEL) ONU. Due to

slotted bandwidth allocation in upstream and downstream directions, an ONU in a TDM-PON remains in idle state for a significant period of time. As explained in previous chapters, an ONU is in idle state when its transceiver (TRX) is not transmitting or receiving any packets. However, an idle ONU continues to operate at its active power level. Due to a large number of ONUs present in current PONs and these ONUs continuously operating at their active power, ONUs have become the main contributor towards the energy consumption in the access segment. To minimise the ONU energy consumption, our proposed algorithms in Chapters 3 and 4 transition the ONUs into sleep or doze mode during this idle time [189, 190]. Under sleep mode operation, both transmitter (Tx) and receiver (Rx) of an ONU are powered down, while in doze mode operation, only the ONU Tx is powered down. The overhead times associated with transitioning an ONU from sleep or doze to active mode account for the time spent in re-synchronising with the OLT and settling time of the Tx circuit, respectively [29].

As the number of users in the network and the required bandwidth continue to grow, specifications set by FSAN require future PONs to support a minimum data rate of 40 Gbps, 256-1024 ONUs, 20 - 40 km network reach, low energy consumption, low capital expenditure, and coexistence with GPON [48, 194]. After considering potential network architectures, such as 40 Gbps TDM-PON, time and wavelength division multiplexed PON (TWDM-PON), wavelength division multiplexed PON (WDM-PON), and orthogonal frequency division multiplexed PON (OFDM-PON), FSAN has selected TWDM-PON as the most favourable network configuration to cater to these requirements [11, 54, 66, 195].

Let us first recap the general architecture of a TWDM-PON described in Chapter 2. Figure 5.1 illustrates the TWDM-PON architecture considered in this thesis. As explained before, a TWDM-PON consists of multiple wavelengths, fixed-tuned or tunable TRXs at the OLT, and tunable TRXs at the ONUs. A TWDM-PON stacks multiple XG-PONs using these multiple wavelengths to provide the high network capacity of a WDM-PON and resource sharing of a TDM-PON. In addition to stacking multiple XG-PONs, a TWDM-PON supports 10G/10G upstream/downstream transmission, a feature not supported in XG-PON. Unlike in

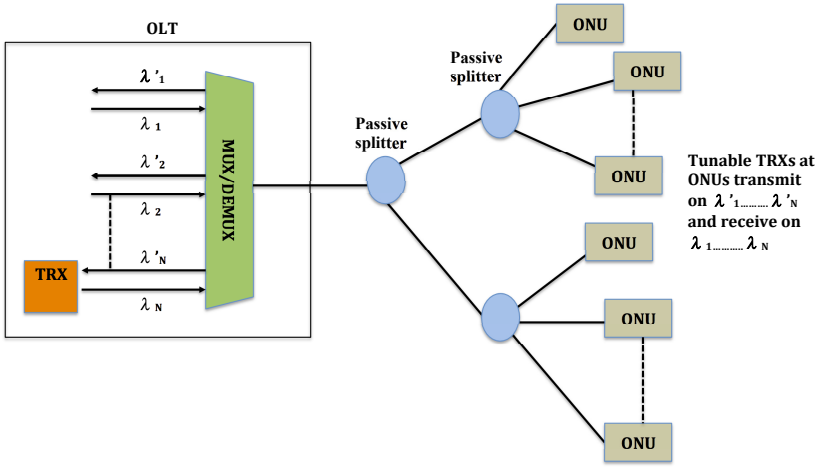

Figure 5.1: General architecture of a TWDM-PON.

seeded/reflective WDM-PONs, a TWDM-PON does not have a centralised colourless light source deployed at the OLT. As a result, the TRXs at the ONUs should be able to tune to multiple wavelengths supported by the TWDM-PON. These tunable TRXs at ONUs transmit on wavelengths λ'_1.....λ'_4 and receive on wavelengths λ_1.....λ_4 as shown in Fig. 5.1. Even though the deployment of tunable TRXs increases the cost of the access network, tunable TRXs facilitate wavelength optimisation at varying network loads for improved energy efficiency.

The prospect of deploying TWDM-PONs in the access network has motivated both academics and the industry to analyse the energy consumption of TWDM-PONs [3, 151, 152]. These studies have led to energy-efficient solutions proposed specifically for TWDM-PONs, many of which exploit the tunability of TRXs at the ONUs [163, 165, 166, 196, 197]. As explained in Chapter 2, wavelength tunability can be explored either as hardware-based or as algorithm-based solutions. As we focus on algorithm-based approaches in this thesis, our objective is to exploit the tunability in the underlying dynamic wavelength and bandwidth allocation (DWBA) algorithm of the TWDM-PON. In a TWDM-PON, energy savings can be achieved both at the OLT and at the ONUs. As discussed in Chapter 2, although a TWDM-PON consists of multiple wavelength channels, the network may not require all these channels to serve the ONUs at a given network load. In such an instance, some of the wavelengths can be switched off and the ONUs supported

by these wavelengths can tune to remaining active wavelengths [25]. This process, known as wavelength reallocation, reduces the energy consumption at the OLT. Implementing conventional sleep and doze mode operations at the ONUs can further facilitate energy savings in the network [22, 110, 133].

In existing research on the energy efficiency of TWDM-PONs, the main objective is to minimise the energy consumption of the network. In any given network, the quality of service (QoS) is an important aspect to consider when delivering improved quality of experience (QoE) to the customers. Due to service level agreements (SLAs), failure to deliver QoS can result in unsatisfied customers and penalties to network operators. As such, QoS is important from both the customer and network operator perspective. Any energy-savings without guaranteed QoS will not be beneficial to the customer or the network operator. Even though existing studies have reported acceptable network delays, these studies have not considered a general delay-constrained TWDM-PON environment. Internet-based applications, such as online gaming and IP telephony, have strict delay restrictions to ensure better user experience [198]. In such networks, the average delay experienced by users should always remain below the specified maximum delay. As such, designing a network from an average delay perspective is important.

To meet the delay requirements of TWDM-PONs, we proposed a DWBA algorithm for a delay-constrained TWDM-PON in [199]. Using a given sleep/doze control function, the proposed DWBA determines the minimum number of active wavelengths that maintains the average delay of the network under a given delay constraint. The proposed method also incorporates sleep mode at the ONUs and, therefore, improves the energy efficiency both at the OLT and at the ONUs. Previous methods proposed in [196] - [199] do not provide a proper framework to determine the number of active wavelengths and sleep/doze time for TWDM-PONs with varying delay constraints, number of ONUs, or wavelength tuning times. Additionally, these methods have not considered the doze mode capabilities of ONUs to achieve energy-savings when the idle time of the ONUs are less than sleep-to-active transition time [199].

To ensure a delayed-constrained TWDM-PON that incorporates all possible

power saving modes, in this chapter, we propose an energy-efficient framework for a DWBA algorithm. For a given delay constraint and a network load, our proposed framework determines (1) the sleep/doze duration, (2) the bandwidth allocation, and, (3) the number of active wavelengths for a delay-constrained TWDM-PON. Using this framework, the tunability of ONUs allows the OLT to switch off idle wavelengths and to reallocate ONUs to one of the remaining active wavelengths, thereby improving the energy-savings at the OLT. In addition to wavelength reallocation, incorporating both sleep and doze mode capabilities of the ONUs to improve the energy-efficiency of the ONUs.

To achieve these objectives, our framework first determines the optimum polling cycle time that results in improved energy-savings, and also satisfies a given delay constraint. This polling cycle time is used to determine the number of active wavelengths required at the OLT and the sleep/doze duration of the ONUs. Using the proposed general framework, we derive equations for optimum polling cycle times when the DWBA is online or offline. The term online implies that the OLT determines the number of active wavelengths, N_{active} and transmission time slot, T_{slot}, before it receives REPORT messages from all ONUs in the network. The term offline, on the other hand, implies that the OLT waits until it receives REPORT messages from all ONUs in the network, before determining N_{active} and T_{slot}. We then analyse the proposed framework using these offline and online Just-In-Time (JIT) DWBA algorithms, namely, OFF-DWBA and ON-DWBA. These DWBA algorithms use a 10 Gbps vertical-cavity surface-emitting laser ONU (10G-VCSEL ONU) that has a sleep-to-active transition time, $T_{sleep-to-active}$, of 2 ms and a doze-to-active transition time, $T_{doze-to-active}$, of 330 ns [29]. Most importantly, the 10G-VCSEL ONU is tunable across the range of wavelengths specified for the upstream transmission in the TWDM-PON [48]. Further, similar to the DBA algorithms proposed for TDM-PONs in the previous chapters, the OFF-DWBA and ON-DWBA utilise Multi-Point Control Protocol (MPCP) messages, such as GATE and REPORT, to transition the ONUs between sleep, doze, and active modes. The GATE message, sent from the OLT to the ONUs, carries information, such as bandwidth allocation, sleep/doze control information, and wavelength reallocation,

while the REPORT, sent from the ONUs to the OLT, contains the bandwidth requirement and estimated average inter-arrival time of packets. Before we present our technical contributions on energy-efficient TWDM-PONs, in the following section, we discuss some of the existing work done in this area.

5.2 Related work

As explained earlier, a majority of existing energy-saving solutions for TWDM-PONs exploit the tunability of TRXs at the ONUs. At low network loads, the OLT can switch off certain wavelengths and migrate the ONUs supported by these wavelengths to the remaining active wavelengths for improved energy-efficiency. Initial studies reported on TWDM-PONs presented an overview of energy consumption in potential NG-PON2 technologies [3, 151, 152]. In [3], the energy consumption of different NG-PON2 technologies has been analysed with and without energy-saving techniques, such as sleep mode, bit interleaving, energy-efficient aggregation switching, and band filtering. The authors in [151] - [152] numerically analysed the energy consumption of NG-PON2 technologies under different traffic conditions and split ratios. These initial studies led to energy-saving solutions proposed for TWDM-PONs.

As explained in Section 5.1, in a TWDM-PON, the energy-efficiency can be improved both at the OLT and at the ONUs [99, 133]. In [196], Yang *et al.* proposed a user migration scheme to minimise the number of active wavelengths. The authors in [163] proposed a resource sharing mechanism between different TWDM-PONs. Different TWDM-PONs catering to office and residential networks have different traffic patterns at different times of the day. For example, during the day, office networks are heavily loaded while domestic networks are lightly loaded and *vice versa* during night. Considering these two networks as two separate networks and provisioning resources to accommodate peak traffic in each network will result in a waste of equipment and power. To address this shortcoming, the OLT contains a pool of TRXs and wavelengths that are shared amongst multiple TWDM-PONs based on network loading. In a similar attempt, Cheng *et al.* proposed and ex-

perimentally evaluated a TWDM-PON in which, the lightly-loaded wavelengths are powered off at the OLT for improved energy-efficiency [197]. In [166], the authors proposed to use sleep mode operation in conjunction with wavelength reallocation, to improve the energy efficiency of both OLT and ONUs. In the proposed scheme, the network load is observed for a duration of T, and the number of wavelengths is determined accordingly. The authors evaluated the effect of different T values under different wavelength tuning times. The authors also analysed the energy-efficiency of a TWDM-PON with wavelength selective switches (WSS) [165]. The proposed solution involves optimising the grouping of users among wavelengths, based on data rate and the distance to the ONUs, to keep a minimal number of wavelengths active, thereby minimising the energy consumption at the OLT.

In existing solutions for energy-efficient TWDM-PONs, the primary objective has been to minimise the energy consumption of access networks. However, current Internet-based services impose various delay restrictions on networks, and it is important that our solutions can cater to these varying delay requirements. Although hardware solutions proposed in [173] for the TDM-PON, such as using optical and optomechanical switches can be applied to mitigate the QoS degradation, it may incur additional cost to the network and also does not cover varying QoS requirements of the networks. As such it is important to investigate possible algorithm-based frameworks and solutions to satisfy the QoS of the network. A possible approach to this problem would be to minimise the energy consumption of a delay-constrained TWDM-PON. In the following section, we present our proposed framework that considers a delay-constrained TWDM-PON to determine the N_{active}, T_{slot}, and ONU sleep/doze period, $T_{onu\ sleep/doze}$.

5.3 Proposed energy-efficient wavelength and bandwidth allocation framework for TWDM-PON

As discussed in Section 5.1, we wish to improve the energy-savings at both the OLT and ONUs, whilst maintaining the average delay under a given maximum.

The energy-savings at the OLT and the ONUs is improved through wavelength reallocation and sleep/doze mode operations, respectively. The main objectives of our proposed framework are (1) determining the number of active wavelengths, (2) determining the sleep duration of the ONUs, and (3) transitioning the ONUs between sleep and active modes. In the following sections, we will discuss how each of these objectives are addressed in our framework.

5.3.1 Determining the number of active wavelengths

The primary objectives of minimising the energy consumption of the TWDM-PON subjected to a delay constrain can be represented as follows:

$$\begin{aligned} &\text{minimise} && E_{cycle} \\ &\text{subject to} && D_{avg} \leq D_{cons}, \\ & && N_{active\ wl} \leq N_{total\ wl} \end{aligned} \tag{5.1}$$

where parameters E_{cycle}, D_{avg}, D_{cons}, and $N_{total\ wl}$ represent the energy consumption of the network per cycle, the average delay of upstream packets, the upstream delay constraint, and the total number of wavelengths in the network, respectively. The parameter E_{cycle} of a TWDM-PON with N_{onu} number of ONUs can be written as a function of polling cycle time, $T_{poll\ cycle}$, as follows:

$$\begin{aligned} E_{cycle} = P_{olt\ active} T_{poll\ cycle} N_{active\ wl} + P_{olt\ base} T_{poll\ cycle} \\ N_{onu}[P_{onu\ active} T_{onu\ active} + P_{onu\ sleep/doze} T_{onu\ sleep/doze}], \end{aligned} \tag{5.2}$$

where parameters $P_{olt\ active}$, $P_{olt\ base}$, $P_{onu\ active}$, and $P_{onu\ sleep/doze}$ represent the power consumption values of an OLT TRX in active state, base power of an OLT, an ONU in active state, and an ONU in sleep or doze state, respectively. It is important to note that components, such as the erbium doped fibre amplifier (EDFA), booster, and the L2 switch are shared among all wavelengths at the OLT. The collective power consumption of these shared equipment is referred to as the OLT base power, $P_{olt\ base}$. Parameters $T_{onu\ active}$ and $T_{onu\ sleep/doze}$ represent the duration an ONU spends in active and in sleep/doze state, respectively. $T_{poll\ cycle}$ is

the time between two consecutive GATE messages received at a given ONU. It is important to note that $T_{onu\ active}$ includes the upstream transmission period, T_{slot}, and also the sleep/doze-to-active transition $T_{sleep/doze-to-active}$ time of an ONU. As highlighted in the previous chapters, when using sleep and doze mode operations, the energy consumption can be reduced by increasing the time an ONU spends in sleep or doze mode, $T_{onu\ sleep/doze}$. For a given $T_{sleep/doze-to-active}$, the $T_{onu\ sleep/doze}$ is achieved through increasing $T_{poll\ cycle}$.

Meanwhile, following the general equation for average delay reported in [2], the D_{avg} of a TWDM-PON can be approximated as follows:

$$D_{\text{avg}} \approx \frac{T_{poll\ cycle}}{2} + NT_{poll\ cycle} + RTT \tag{5.3}$$

where N is the number of cycles the upstream packets have to wait in the ONU queue after they are reported to the OLT, before any bandwidth is allocated for their transmission and RTT is the round trip time. In a delay-constrained environment, if the packets have to wait multiple cycles before they are being transmitted, $T_{poll\ cycle}$ has to be reduced accordingly to ensure $D_{avg} \leq D_{cons}$. Minimising $T_{poll\ cycle}$ on the other hand, will also minimise $T_{onu\ sleep/doze}$ and thus possible energy-savings. The energy-savings at the ONUs can be maximised if the network operates at the maximum polling cycle time, $T_{poll\ max}$, that satisfies a given D_{cons}. Using eqn. 5.3 and the inequality in eqn. 5.1, we can mathematically formulate the relationship between $T_{poll\ cycle}$ and D_{cons} as follows:

$$\begin{aligned} \frac{T_{poll\ cycle}}{2} + N\ T_{poll\ cycle} + RTT &\leq D_{cons} \\ T_{poll\ cycle} &\leq \frac{D_{cons} - RTT}{N + \frac{1}{2}}, \end{aligned} \tag{5.4}$$

According to eqn. (5.4), the maximum value of $T_{poll\ cycle}$, $T_{poll\ max}$, is achieved at the minimum value of N and in our proposed framework, the TWDM-PON operates under this $T_{poll\ max}$. Algorithm 5.1 illustrates the wavelength allocation process in a TWDM-PON operating at $T_{poll\ max}$. Following either the offline or the online DBA algorithm, which will be explained in detail in the next section, the

Algorithm 5.1: Pseudocode of the wavelength allocation in the proposed framework

$N_{onu} = 64$

Phase 1: Average bandwidth calculation - OLT calculates the bandwidth requirement of each ONU

BW_{avg} = *Total BW requested* / N_{onu}

Phase 2: Number of wavelength determination - OLT determines the optimum number of active wavelengths required for a given D_{cons}

$N_{active\ wl} = 1$

Calculate BW_{max} `//Calculates the maximum bandwidth allowable for an ONU when all ONUs are tuned into one wavelength`

$BW_{max} = (T_{poll\ max} - T_{process})$ / $(N_{onu}$ / $N_{active\ wl})$ `//`$T_{process}$ `is the processing time of all ONUs supported by a given wavelength`

while $(BW_{avg} > BW_{max}$ *and* $N_{active\ wl} \leq N_{total})$ **do**

  `//Check if the requested bandwidth is higher than the current maximum allowable bandwidth`

  $N_{active\ wl} = N_{active\ wl} + 1$ `//Introduce another active wavelength to the network`

  $N_{per\ wl} = N_{onu}$ / $N_{active\ wl}$ `//The OLT distributes the number of ONUS uniformly across the wavelengths.` N_{perwl} `is the number of ONUs per wavelength.`

  Calculate BW_{max} `//Calculate the new maximum allowable bandwidth, after a wavelength is introduced`

  $BW_{max} = (T_{poll\ max} - T_{process})$ / $(N_{onu}$ / $N_{active\ wl})$

OLT first calculates the average bandwidth requested, BW_{avg}, by an ONU. It is important to note that in our proposed framework, we have assumed all ONUs in the network to operate under the same network load [189, 199]. As a result, it is reasonable to calculate the average bandwidth requested by an ONU, as shown in Phase 1 of Algorithm 5.1. The OLT then initiates the wavelength allocation process with one active wavelength. The OLT calculates the maximum allowable bandwidth, BW_{max}, of a TWDM-PON with one active wavelength as shown in Phase 2 of Algorithm 5.1. If the current BW_{avg} is greater than this BW_{max}, a new wavelength is introduced to the network. The OLT then calculates BW_{max} for a TWDM-PON with two active wavelengths, which is again compared with BW_{avg}. This process continues until $BW_{avg} \leq BW_{max}$ and the number of wavelengths at this point is taken as the number of active wavelengths, $N_{active\ wl}$.

5.3.2 Determining the sleep or doze duration

Once $N_{active\ wl}$ is calculated, the OLT initiates the sleep/doze time calculation process. Algorithm 5.2 illustrates the process of assigning sleep or doze periods to each ONU in a TWDM-PON operating at $T_{poll\ max}$. The OLT first calculates the idle time, T_{idle}, of each ONU using $T_{poll\ max}$ and T_{slot}. The parameter $T_{poll\ max}$ is calculated using eqn. 5.4 for a specified D_{cons}. Next, the OLT decides on whether an ONU is transitioned into doze, sleep, or active state as follows. If $T_{idle} \geq T_{sleep-to-active}$, the ONUs are transitioned into sleep mode and if $T_{sleep-to-active} \geq T_{idle} \geq T_{doze-to-active}$, the ONUs are transitioned into doze mode. If neither of these two conditions are satisfied, the ONUs are instructed to remain active.

Algorithm 5.2: Pseudocode of the sleep/doze period determination in the proposed framework

```
Phase 3: Sleep/doze allocation process - OLT determines the sleep/doze
  time assigned for each ONU
T_idle = T_poll max - T_slot
if (T_idle ≥ T_sleep−to−active) then
    ONU enters sleep mode
    T_sleep = T_idle - T_sleep−to−active
if ( T_sleep−to−active ≥ T_idle ≥ T_doze−to−active) then
    ONU enters doze mode
    T_doze = T_idle - T_doze−to−active
else
    ONU stays active
```

It is important to note that in our proposed framework, we have only considered upstream traffic and delay constraint when determining the $N_{active\ wl}$ and the $T_{sleep/doze}$. However, in a scenario where downstream traffic is also considered, downstream transmission can be scheduled to be synchronised with upstream transmission as proposed in [189]. In that case, for guaranteed QoS in both upstream and downstream direction, D_{cons} will be set to the minimum of the upstream and downstream delay constraint.

5.3.3 ONU reallocation and transitioning the ONUs between different modes

Once $N_{active\ wl}$ and $T_{sleep/doze}$ are determined, the OLT has to ensure that these control information is delivered to the ONUs for them to tune to a different wavelength or to enter sleep or doze mode. The proposed framework can be implemented in either as an OFF-DWBA algorithm or an ON-DWBA algorithm. In both OFF-DWBA and ON-DWBA algorithms, the OLT utilises MPCP control messages, such as GATE and REPORT to deliver the control information between the OLT and the ONUs. The next sections analyse the $T_{poll\ max}$ of the two algorithms and the control message flow in detail.

5.3.3.1 Offline DWBA algorithm

The traffic flow of the OFF-DWBA is similar to the offline DBA algorithms proposed in Chapters 3 and 4 [189, 190]. In the OFF-DWBA algorithm, the ONUs inform the OLT of their bandwidth requirement using REPORT message. The OLT waits until it receives REPORT messages from all ONUs and then calculates the BW_{avg} allocated to each ONU. Under the OFF-DWBA algorithm, upstream traffic has to wait a complete polling cycle after the REPORT message is sent to the OLT, before any bandwidth is allocated to them. As a result, the minimum value of N in this case is 1. The $T_{poll\ max}$ of the OFF-DWBA algorithm can be approximated as follows:

$$T_{\text{poll max}} \approx \frac{2\,(D_{cons} - RTT)}{3}, \tag{5.5}$$

Figure 5.2 illustrates the traffic flow of the OFF-DWBA algorithm. After the OLT receives REPORT messages from all ONUs in the network, following Algorithm 5.1 and 5.2, the OLT calculates the T_{slot}, N_{active}, and $T_{sleep/doze}$ of each ONU. This information is transmitted to the ONUs via GATE message. Upon receiving this GATE message, an ONU sends its upstream data and REPORT, and enters into sleep, doze, or active mode as specified by the OLT. The ONU then wakes up just-in-time to receive the next GATE from the OLT.

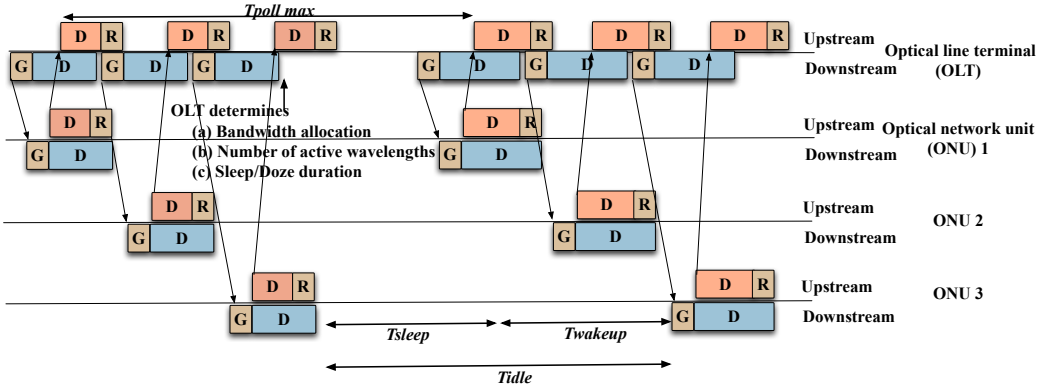

Figure 5.2: Traffic flow of the OFF-DWBA algorithm. D-Data, R-REPORT and G-GATE.

5.3.3.2 Online DWBA algorithm

The traffic flow, wavelength allocation, and sleep/doze allocation of the ON-DWBA algorithm is similar to that of the OFF-DWBA algorithm. The main differences between the two algorithms are the $T_{poll\ max}$ and at which point in time of the polling cycle are the T_{slot}, $N_{active\ wl}$, and $T_{sleep/doze}$ determined. In the OFF-DWBA algorithm, incoming traffic has to wait an extra polling cycle as the OLT has to process REPORT messages from all ONUs in the network. To overcome this problem, we use traffic prediction in our ON-DWBA algorithm. Under ON-DWBA, each ONU estimates the average inter-arrival time, λ, of its packets using the Bayesian estimation proposed in Chapter 4 [190]. This λ is reported back to the OLT via the REPORT message. The OLT uses this value to predict the traffic accumulated, BW_{pred}. Using the parameters λ, T_{poll}, and an average Ethernet packet size of 791 bytes, BW_{pred} in bytes, accumulated during a polling cycle is calculated as follows:

$$BW_{pred} = \frac{791.T_{poll\ cycle}}{\lambda}, \tag{5.6}$$

For example, the OLT uses the λ value reported in cycle $n-2$ to predict the traffic accumulated in cycle $n-1$ and the bandwidth for the traffic accumulated in cycle $n-1$ is immediately provided in cycle n. As a result, unlike in the OFF-DWBA algorithm, the upstream traffic does not have to wait an extra cycle, before any bandwidth is allocated for their upstream transmission. As a result, $N = 0$ under

the ON-DWBA algorithm. Using eqn. 5.4, the $T_{poll\ max}$ of the ON-DWBA algorithm can be approximated as follows:

$$T_{\text{poll max}} \approx 2\ (D_{cons} - RTT), \tag{5.7}$$

Based on eqns. 5.5 and 5.7, for a given D_{cons}, we can deduce that the $T_{poll\ max}$ of the ON-DWBA algorithm is longer than that of the OFF-DWBA algorithm.

5.4 Performance evaluation

This section presents the analytical and simulation results of the OFF-DWBA and ON-DWBA algorithms under our proposed energy-efficient framework. We first verify the theoretical eqns. 5.5 and 5.7 using simulations, as the validity of our proposed framework heavily depends on these two equations. For this purpose, we have considered a 40 km PON with 64 ONUs operating at a fixed polling cycle time of 10 ms. Traffic generated at each ONU is Poisson distributed and is varied between the normalised network loads of 0.1-1. For this initial simulation, we have considered the tuning time of the ONUs and all processing delays to be negligible. Figure 5.3 illustrates the theoretical and simulated average delay of the OFF-DWBA and ON-DWBA algorithms for a polling cycle time of 10 ms, as a function of normalised network load. As shown in Fig. 5.3, the average delay of the OFF-DWBA algorithm is approximately 1.5 times the polling cycle time, and that of the ON-DWBA algorithm is 0.5 times the polling cycle time. The minor difference between the theoretical and simulated values is due to the fact that in our equations, we have not considered the time, which is in nano second range, it takes a packet to reach the beginning of the ONU queue. These results, therefore, justify our $T_{poll\ max}$ calculations for OFF-DWBA and the ON-DWBA algorithms, in a delay-constrained network.

With the eqns. 5.5 and 5.7 being verified, the analytical and simulation results of the OFF-DWBA and the ON-DWBA algorithms under the proposed framework are presented next. Table 5.1 lists the network and control parameters used in our

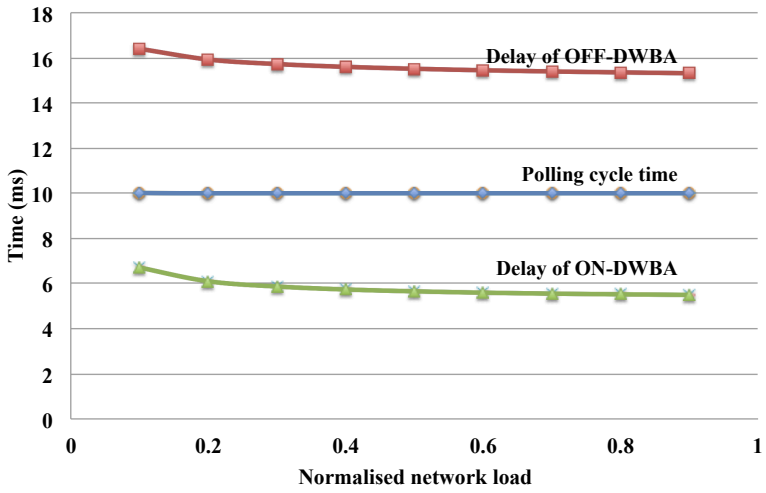

Figure 5.3: Polling cycle time and average delay of OFF-DWBA and ON-DWBA algorithms as a function of normalised network load.

Table 5.1: Network and protocol parameters

Parameter	**Value**
Network reach	40 km
Number of ONUs	64
Delay constraints	7.5, 10, and 15 ms
Propagation delay	200 μs
Inter-frame gap in upstream	1μs
Average Ethernet packet size	791 bytes
Wavelength tuning and GATE processing	50μs

Table 5.2: Power consumption and switching values of 10G-VCSEL ONUs and OLT

Parameter	**Value**
Doze-to-active transition time - VCSEL ($T_{doze-to-active}$) [29]	330 ns
Sleep-to-active transition time - VCSEL ($T_{sleep-to-active}$) [29]	2 ms
Power consumption VCSEL - active ($P_{vcsel,act}$) [29]	3.984 W
Power consumption VCSEL - doze ($P_{vcsel,doze/sleep}$) [29]	3.85 W
Power consumption VCSEL - sleep ($P_{vcsel,doze/sleep}$) [29]	0.75 W
OLT TRX - active $P_{olt\ active}$ [182]	11 W
OLT base power - EDFA Preamp + Booster + L2 switching capacity ($P_{olt\ base}$) [182]	64 W

numerical analysis and simulations. Table 5.2 lists the power consumption values of the 10G-VCSEL ONU and the OLT considered in this analysis.

5.4.1 Numerical analysis

This section presents the numerically analysed results of the proposed framework under OFF-DWBA and ON-DWBA algorithms. In our analysis, for a given D_{cons} and a network load with corresponding λ, we first calculated the corresponding $T_{poll\ max}$ using eqns. 5.5 and 5.7. We then predicted the amount of traffic accumulated during this $T_{poll\ max}$ using eqn. 5.6. Taking this predicted traffic as BW_{avg}, we have numerically analysed the number of active wavelengths and the percentage of energy-savings at the OLT and at the ONUs.

Figures 5.4 (a) and (b) plot the number of active wavelengths as a function of normalised network load, for OFF-DWBA and ON-DWBA, respectively. When the network load increases, the number of active wavelengths required to keep the average delay below a specified maximum increases. As the network load increases, BW_{avg} increases. As explained in Section 5.3.3, when BW_{avg} exceeds BW_{max}, a new wavelength is introduced to the network. Due to this reason, the number of active wavelengths increases with the increase in network load. In both OFF-DWBA and ON-DWBA algorithms, the network load at which a new wavelength is introduced, increases with the increase in D_{cons}. For example, in the OFF-DWBA algorithms, a new wavelength is introduced at the network loads of 0.2, 0.3, and 0.4 for D_{cons} of 7.5, 10, and 15 ms, respectively. In other words, when D_{cons} increases, it is possible to transmit the same amount of traffic with higher delay, i.e., with lower number of active wavelengths.

Based on Figs. 5.4 (a) and (b), for a given D_{cons} and a network load, a majority of the time, the ON-DWBA algorithm requires a lower number of active wavelengths compared to the OFF-DWBA. For example, for a D_{cons} of 7.5 ms and network load of 0.4, the OFF-DWBA requires two active wavelengths while the ON-DWBA requires only one wavelength. For a given D_{cons}, $T_{poll\ max}$ of the ON-DWBA method is higher than that of the OFF-DWBA and as explained before, this allows the ON-DWBA to operate with lower number of active wavelengths, compared to the OFF-DWBA algorithm, for a given network load. It is important to note that at certain network loads, both OFF-DWBA and ON-DWBA require the

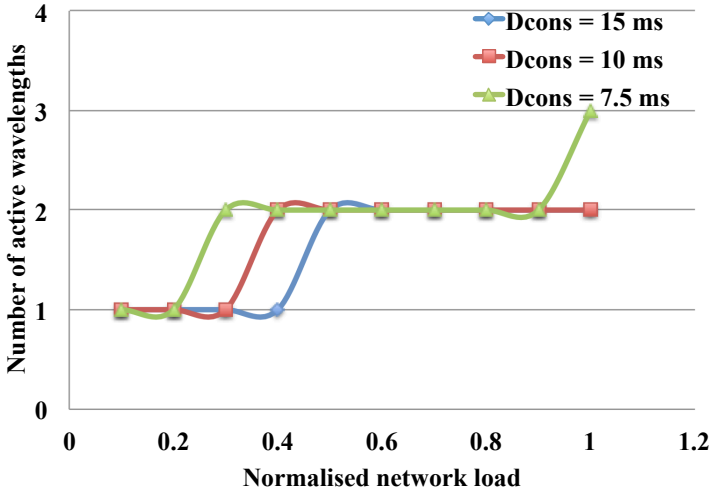

(a) OFF-DWBA

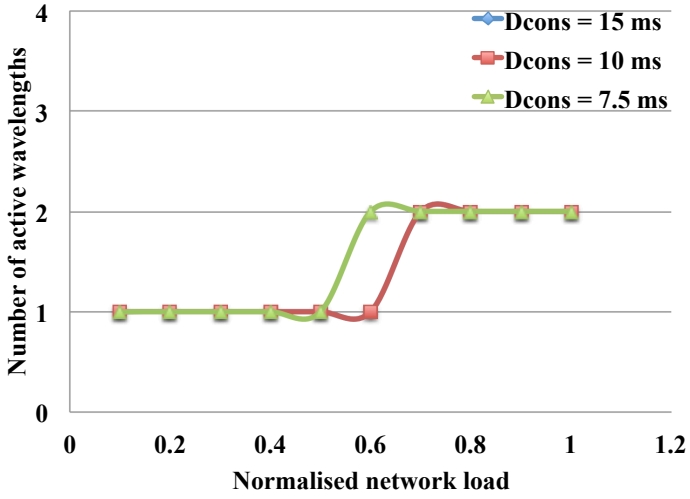

(b) ON-DWBA

Figure 5.4: The number of active wavelengths required in (a) OFF-DWBA and (b) ON-DWBA as a function of normalised network load.

same number of active wavelengths. For example at D_{cons} of 7.5 ms and network load of 0.6, both OFF-DWBA and ON-DWBA require 2 active wavelengths. However, in general, the ON-DWBA requires lower number of wavelengths compared to OFF-DWBA.

Figures 5.5 (a) and (b) illustrate the percentage of energy-savings achieved per cycle at an ONU in OFF-DWBA and ON-DWBA algorithms, respectively. The

percentage of energy-savings η is calculated as follows:

$$\eta = \left(1 - \frac{P_{vcsel,act}T_{act} + P_{vcsel,doze/sleep}T_{doze/sleep}}{P_{vcsel,act}(T_{act} + T_{sleep/doze})}\right)\% \tag{5.8}$$

where parameters $P_{vcsel,act}$, $P_{vcsel,doze/sleep}$, T_{act} and $T_{doze/sleep}$ represent the power consumption of a 10G-VCSEL in active state, in sleep/doze state and the dura-

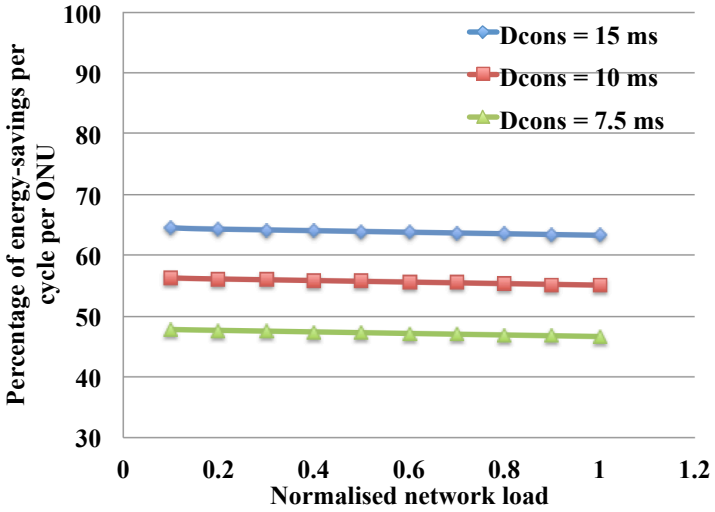

(a) OFF-DWBA

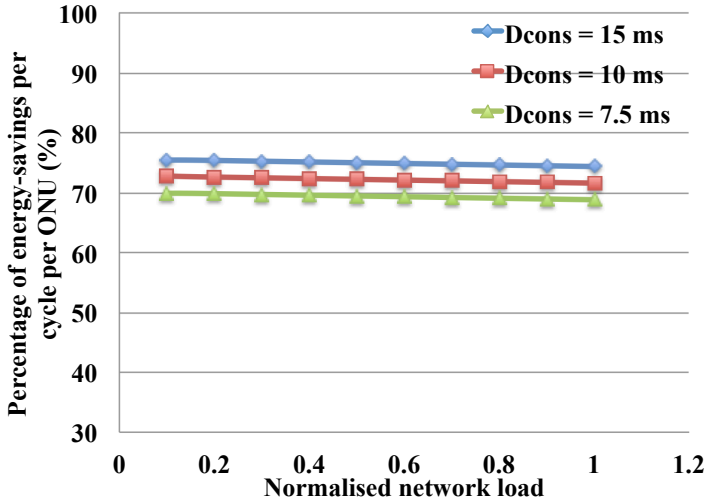

(b) ON-DWBA

Figure 5.5: Percentage of energy-savings per cycle per ONU in (a) OFF-DWBA and (b) ON-DWBA as a function of normalised network load.

tion an ONU spends in active state and sleep/doze state, respectively. In both OFF-DWBA and ON-DWBA algorithms, for every D_{cons}, the percentage of energy-savings at the ONUs decreases with the increase in network load. When the network load increases, BW_{avg} increases and as a result, the data transmission period increases. An increase in data transmission period increases T_{act}, thereby increasing the energy consumption and reducing the possible energy-savings. In both OFF-DWBA and ON-DWBA algorithms, with the increase in D_{cons}, η increases. When D_{cons} increases, $T_{poll\ max}$ increases. As per Algorithm 5.2, a longer $T_{poll\ max}$ results in a longer T_{idle}, thus allowing the ONUs to sleep/doze longer and achieve more energy-savings. Compared to the OFF-DWBA algorithm, the ON-DWBA algorithm results in a longer $T_{poll\ max}$ for a given D_{cons} and therefore, saves more energy. It is important to note that due to the range of D_{cons} considered in this work, the $T_{idle} \geq T_{sleep-to-active}$ and the ONUs enter into sleep mode. Due to the large difference in power consumption, 3.234 W, between sleep mode and active modes of an 10G-VCSEL ONU, the percentage of savings of as high as 65% and 75% is reported for OFF-DWBA and ON-DWBA algorithms, respectively. For shorter D_{cons}, when the ONU idle time is less than sleep-to-active transition time, the ONUs will transit to doze mode for energy-efficiency.

Figures 5.6 (a) and (b) plot the percentage of energy-savings achieved at the OLT as a function of normalised network load, for OFF-DWBA and ON-DWBA algorithms, respectively. The percentage of energy savings, α, is calculated as follows:

$$\alpha = \left(1 - \frac{P_{olt\ active} T_{poll\ cycle} N_{active\ wl}}{P_{olt\ active} T_{poll\ cycle} N_{totalwl} + T_{poll\ cycle} P_{olt\ base}}\right) \% \tag{5.9}$$

As explained in Fig. 5.4, for both OFF-DWBA and ON-DWBA algorithms, the number of active wavelengths increases with the increase in network load. As a result, for a given D_{cons}, the percentage of energy-savings at the OLT decreases with the increase in network load. When D_{cons} increases, for a given network load, the network requires a lower number of active wavelengths. Consequently, higher values of D_{cons} achieves more energy-savings at the OLT. Compared to the OFF-

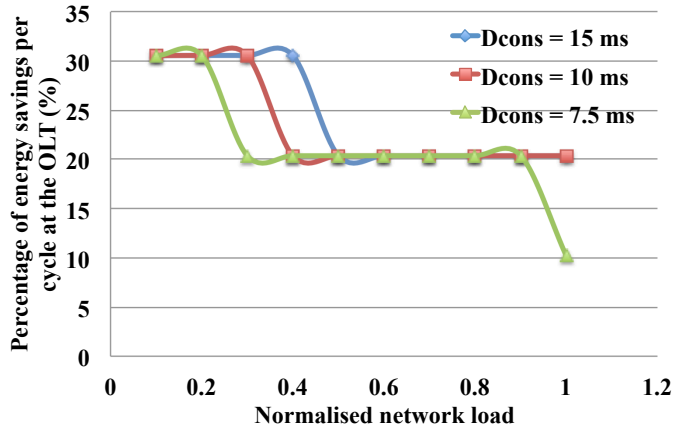

(a) OFF-DWBA

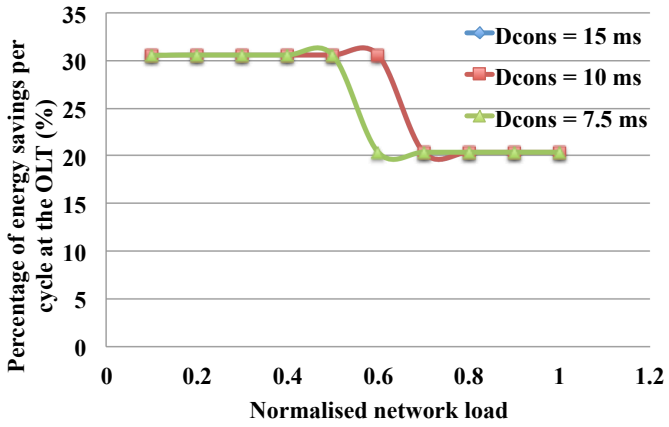

(b) ON-DWBA

Figure 5.6: Percentage of energy-savings at the OLT in (a) OFF-DWBA and (b) ON-DWBA as a function of normalised network load.

DWBA algorithm, the ON-DWBA algorithm requires a lower number of active wavelengths for a given network load and D_{cons} and therefore saves more energy at the OLT. It is important to note that even when the network operates with a single active wavelength, the percentage of energy-savings at the OLT is 30%. As explained in the previous section, the equipment, such as the EDFA, booster, and the L2 switch, are shared among multiple wavelengths and are kept active, even when a single wavelength is in operation. Collectively, these components consume

64 W of power and is significant, compared to the TRX power of 11 W. As a result, maximum energy savings of only 30% is achieved at the OLT.

5.4.2 Simulation Results

Figures 5.7, 5.8, and 5.9 illustrate the simulation results of the OFF-DWBA and ON-DWBA algorithms with respect to the number of active wavelengths, the per-

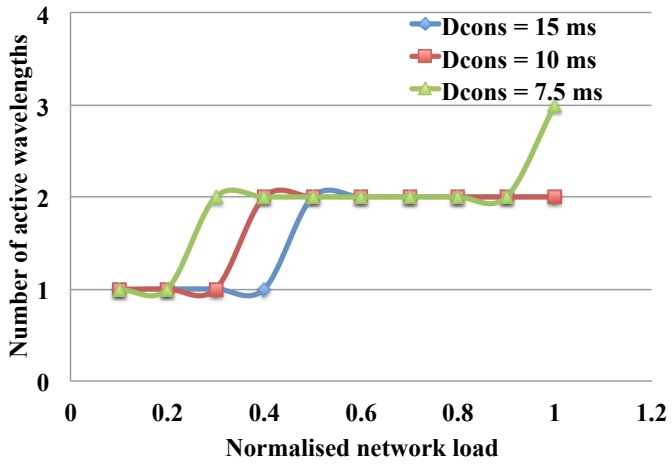

(a) OFF-DWBA

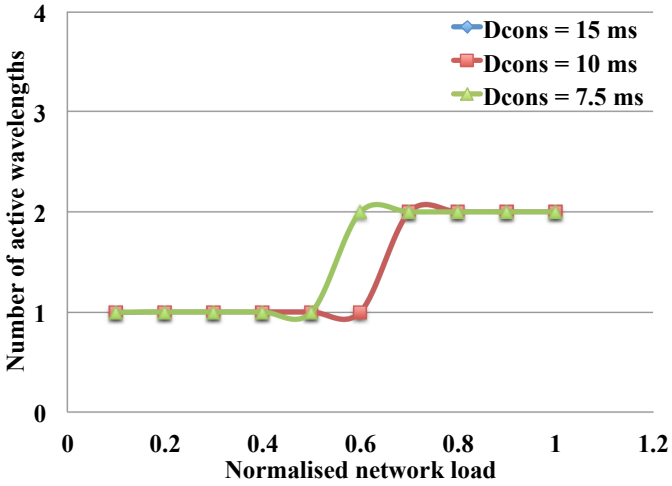

(b) ON-DWBA

Figure 5.7: Number of active wavelengths for (a) OFF-DWBA and (b) ON-DWBA as a function of normalised network load.

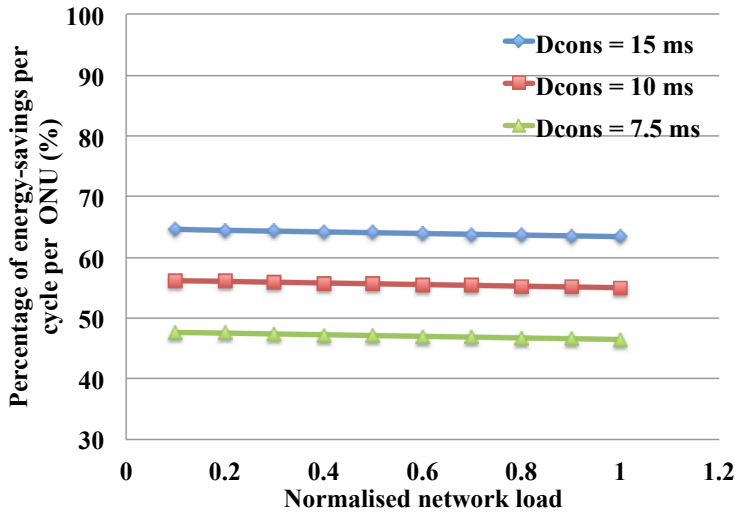

(a) OFF-DWBA

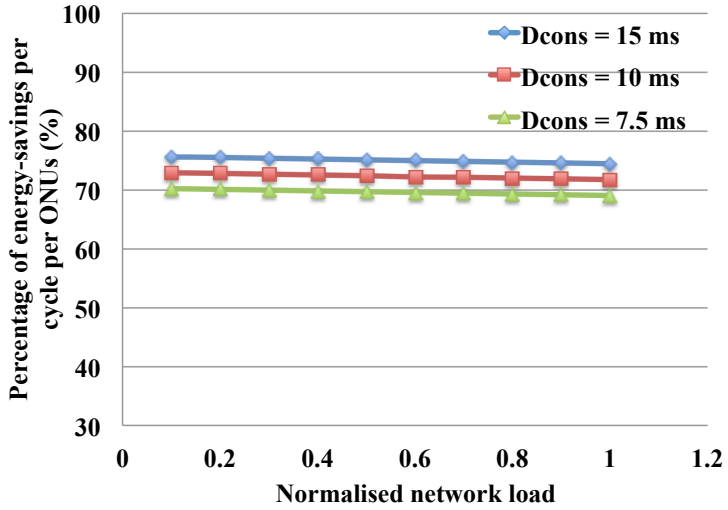

(b) ON-DWBA

Figure 5.8: Percentage of energy-savings per cycle per ONU in (a) OFF-DWBA and (b) ON-DWBA as a function of normalised network load.

centage of energy-savings at the ONUs, and the percentage of energy-savings at the OLT, as a function of normalised network load, respectively. These simulation results verify our analytical results presented in the previous section.

Figures 5.10 (a) and (b) plot the average delay of OFF-DWBA and ON-DBWA algorithms as a function of normalised network load, respectively. The simulated average delay values are very close to the given delay constraints. It is important

to note that for all cases of D_{cons}, the average delay is slightly higher than D_{cons} value. As explained in Fig. 5.3, we have not considered the time a packet takes to reach the beginning of the ONU queue. As a result, the factor by which the term $(D_{cons} - RTT)$ is divided in eqns. 5.7 and 5.5, is not exactly 0.5 and 1.5 for ON-DWBA and OFF-DBWA algorithms, respectively. This has resulted in the minor increase in D_{avg} compared to D_{cons}. Had we taken the simulated values of

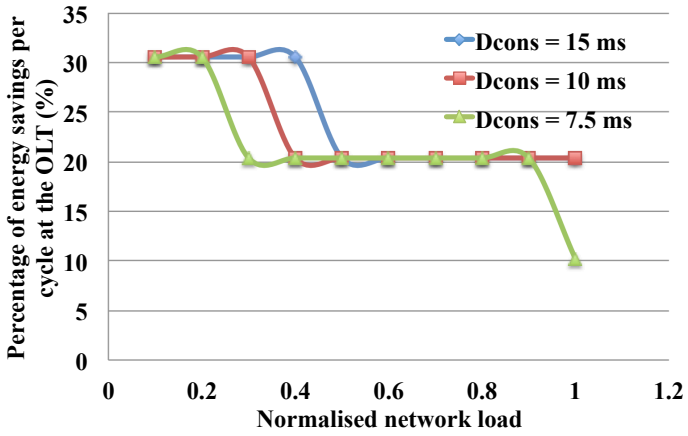

(a) OFF-DWBA

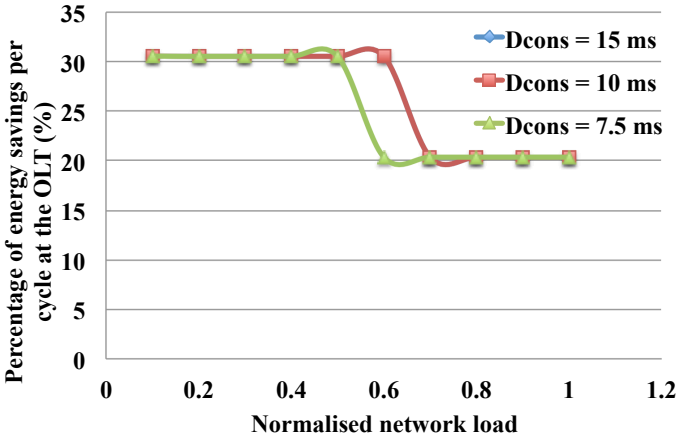

(b) ON-DWBA

Figure 5.9: Percentage of energy-savings at the OLT in (a) OFF-DWBA and (b) ON-DWBA as a function of normalised network load.

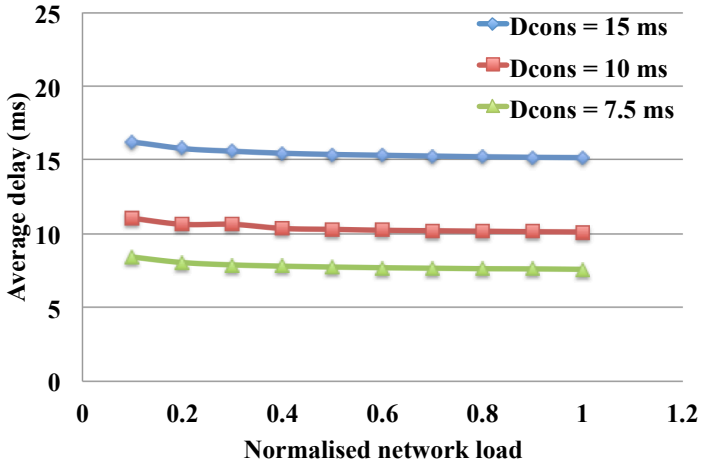

(a) OFF-DWBA

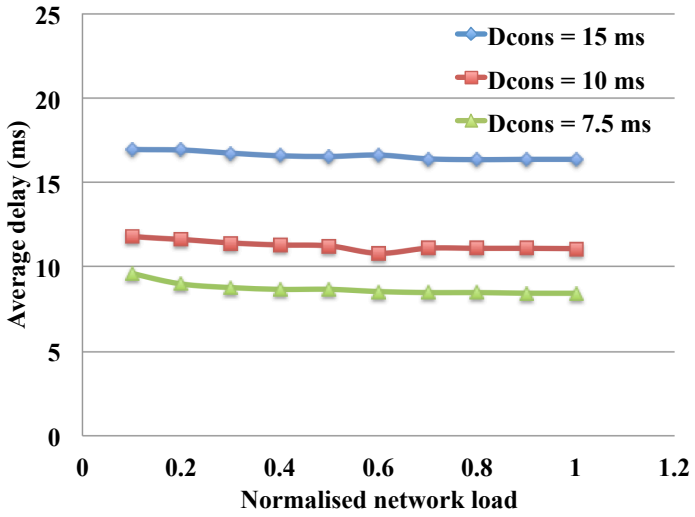

(b) ON-DWBA

Figure 5.10: Average delay in (a) OFF-DWBA and (b) ON-DWBA as a function of normalised network load

0.6 and 1.6, $T_{poll\ max}$ for each D_{cons} will decrease and D_{avg} will be reduced accordingly. However, as an initial step in introducing an energy-efficient bandwidth and wavelength allocation framework, the simulation results on average delay shows that the proposed framework maintains the average delay under a given D_{cons}.

5.5 Conclusions

We have proposed an energy-efficient framework for a delay-constrained TWDM-PON. For a given delay constraint and network load, the framework determines (a) the number of active wavelengths required to maintain this delay and (b) the sleep or doze time of the ONUs. The framework achieves energy-savings at the OLT by switching off idle wavelengths and at the ONUs, by transitioning the ONUs to sleep or doze mode during their idle time. The general framework proposed in this chapter can be applied to any network topology, to either online or offline DWBA algorithm, and to a network with any given delay constraint.

We evaluated the performance of the proposed framework using the OFF-DWBA and ON-DWBA algorithms for the number of active wavelengths, energy-savings at the ONUs and the OLT, and the average delay. The analytical and simulation results indicate that using the proposed framework, a TWDM-PON can maintain the average delay of the network under a given delay constraint whilst achieving significant energy-savings both at the OLT and the ONUs.

Our proposed algorithms discussed in Chapters 3, 4, and 5 are analysed using Poisson distributed traffic. However, over the years, the Internet traffic has become bursty in nature due to the nature of Internet-based user applications. In the next Chapter, we analyse the performance of our OFF-DWBA algorithm using bursty traffic and investigate the efficacy of our algorithm in saving energy under bursty traffic.

CHAPTER 6

Energy-Efficient Dynamic Wavelength and Bandwidth Allocation Algorithms Under Bursty Traffic

6.1 Introduction

In Chapters 3 and 4, we proposed energy-efficient dynamic bandwidth allocation (DBA) algorithms for 10 Gbps Ethernet passive optical networks (10G-EPONs) [189, 190]. As the optical line terminal (OLT) broadcast the downstream packets to all the optical network units (ONUs) placed at the customer premises, the ONUs waste a significant portion of its energy in analysing these packets. The proposed algorithms were designed to incorporate sleep and doze mode operations to minimise the energy consumption during the idle time of the ONUs. Sleep mode operation powers down both the transmitter (Tx) and the receiver (Rx) of the ONU, while in doze mode, only the Tx is powered-down.

Later, in Chapter 5, we also proposed an energy-efficient framework for the emerging time and wavelength division multiplexed PON (TWDM-PON) [200–203]. As explained in Chapter 5, a TWDM-PON consists of multiple wavelengths, fixed-tuned/tunable transceivers (TRXs) at the optical line terminal (OLT) and tunable TRXs at the ONUs. The multiple TRXs and the tunability of the ONUs facilitate energy-savings at the OLT, whereby the idling wavelengths are switched

Table 6.1: Power consumption and switching values of 10G-VCSEL ONUs and OLT

Parameter	**Value**
Doze-to-active transition time - VCSEL ($T_{doze-to-active}$) [29]	330 ns
Sleep-to-active transition time - VCSEL ($T_{sleep-to-active}$) [29]	2 ms
Power consumption VCSEL - active ($P_{vcsel,act}$) [29]	3.984 W
Power consumption VCSEL - doze ($P_{vcsel,doze/sleep}$) [29]	3.85 W
Power consumption VCSEL - sleep ($P_{vcsel,doze/sleep}$) [29]	0.75 W
OLT TRX - active $P_{olt\ active}$ [182]	11 W
OLT base power - EDFA Preamp + Booster + L2 switching capacity ($P_{olt\ base}$) [182]	64 W

off after reallocating their ONUs among the active wavelengths. In addition, the conventional sleep/doze mode operations, discussed in Chapters 3 and 4, can also be implemented at the ONUs for improved energy-efficiency at the ONUs [22, 110, 133]. The proposed framework, therefore, considers a delay-constrained TWDM-PON and determines the number of active wavelengths and sleep/doze duration.

All our proposed DBA and DWBA algorithms exploit sleep and doze capabilities and the wavelength tunability of the 10 Gbps vertical-cavity surface-emitting laser (10G-VCSEL) ONU. Table 6.1 lists the power consumption and switching values of the 10G-VCSEL ONU used in these algorithms. Also, both DBA and DWBA algorithms utilise the Multi-Point Control Protocol (MPCP) messages, such as GATE and REPORT, to control the packet flow between the ONUs and the OLT. For example, the GATE message, sent from the OLT to ONU, carries information, such as bandwidth allocation, sleep/doze control information, and wavelength reallocation. The REPORT message is sent from the ONUs to the OLT and contains the bandwidth requirement and the estimated average inter-arrival time of packets. Most importantly, when evaluating the performance of these algorithms, we generated Poisson distributed traffic at the subscriber network interface (SNI) of the ONUs.

Following a Poisson process, when generating incoming traffic, has many advantages due to the mathematical properties of the Poisson distribution [204]. First and foremost, the aggregated traffic flow of several Poisson traffic streams is also

Poisson distributed and its rate is the sum of the component rates. This feature simplifies the mathematical analysis of such traffic streams and also facilitates easy implementation of algorithms in simulation platforms. Second, in a Poisson process, the number of arrivals in disjoint intervals is statistically independent. This property, known as independent increments, simplifies the queuing of incoming traffic in a network. Finally, the Poisson processes are quite common in networks that aggregate several independent streams of network traffic. Based on Palm's Theorem [205], under suitable but mild regularity conditions, when any general traffic streams are multiplexed, the aggregated traffic flow is Poisson distributed. a Poisson process with the increase in the number of traffic streams. As a result, traffic streams on main communications links are commonly believed to follow a Poisson process. Based on the first and third properties, it is reasonable to assume Poisson distributed traffic at the customer SNI as well.

However, studies on behaviour of Internet traffic highlight that for some current Internet applications, the Poisson distribution does not accurately model the nature of incoming traffic at the ONUs [206–209]. These studies show that when modelled as a Poisson process, the burst length tends to get averaged over time. Meanwhile, statistical analysis of real Ethernet traffic indicates that there is in fact significant burstines, in network traffic [206,210,211]. The studies show that bursty Internet traffic can actually be characterised by self-similarity and long range dependency (LRD). Consequently, using a self-similar process has been identified as the best approach to generate LRD traffic. Traffic generated under a self-similar process generate traffic exhibits same patterns when viewed at different scales and are usually modelled using long-tailed distributions.

To obtain an accurate and realistic performance analysis, it is important to simulate the proposed dynamic bandwidth allocation (DBA) algorithms and dynamic wavelength and bandwidth allocation (DWBA) algorithms using appropriate traffic. In this chapter, using such LRD traffic, which preserve burstiness, we evaluate the performance of our offline DWBA (OFF-DBA) proposed in Chapter 5 [190]. The reason for considering the OFF-DWBA is because it performs both wavelength reallocation and sleep/doze mode operation. Before we present the energy and

delay performance of the OFF-DWBA under bursty traffic, we will briefly discuss some of the theoretical aspects of bursty traffic.

6.2 Self-similarity and long range dependence (LRD) (adapted from [2])

Self-similarity is a phenomena where an object is similar to a part of itself. To analyse this concept mathematically, let us consider a cumulative process $Y(t)$ with stationary increments, and let X_t be its incremental process. Then,

$$X_t = Y(t) - Y(t-1) \tag{6.1}$$

For example, $Y(t)$ can represent the number of bytes arriving up to time t, and X_t can represent the number of bytes arriving in 1 unit of time. The process $Xs(m)$ is an aggregated process of X_t if,

$$X_s^{(m)} = \frac{1}{m}(X_{sm-m+1} + X_{sm-m+2} + ... + X_{sm}) \tag{6.2}$$

The process X_t is said to be self-similar, if X_t is indistinguishable from $X_s^{(m)}$. For the purpose of aggregating multiple traffic streams into a single stream, the traffic is said to be self-similar, if the auto-covariance function of the original and the aggregated streams is the same [2]. Suppose the auto covariance function of the original traffic stream and the aggregate stream are $y(k)$ and $y^{(m)}(k)$, then the traffic streams are said to be self-similar if,

$$y(k) = y^{(m)}(k) \tag{6.3}$$

With further mathematical analysis, we can show that a self-similar traffic stream is characterised by the following equation.

$$X_s^{(m)} = m^{H-1} X_t \tag{6.4}$$

Please note that deriving eqn. 6.4 is beyond the scope of this thesis. A detailed

description of its mathematical derivation can be found in [2]. As per equation 6.4, when aggregating original traffic streams over a large time scale, the burstiness reduces very slowly. As a result, a self-similar process preserves the bursty nature of Internet traffic. Technically, the term LRD implies that in the time domain, the rate of statistical dependency decays more slowly than the exponential decay. Eqn 6.4, therefore, implies that the self-similar Internet traffic exhibits LRD. With respect to the Internet traffic, this means that traffic bursts do exists in many or all time scales.

Figure 6.1 illustrates the behaviour of LRD and SRD traffic over the time scales of 1 ms - 10 s. As shown in the figure, the time average of Poisson traffic, which has SRD characteristics, is smoothed with the increase in time scale. In contrary, the LRD traffic still shows significant number of bursts even at a scale of 10 seconds.

Based on these mathematical derivations, using a self-similar process to gen-

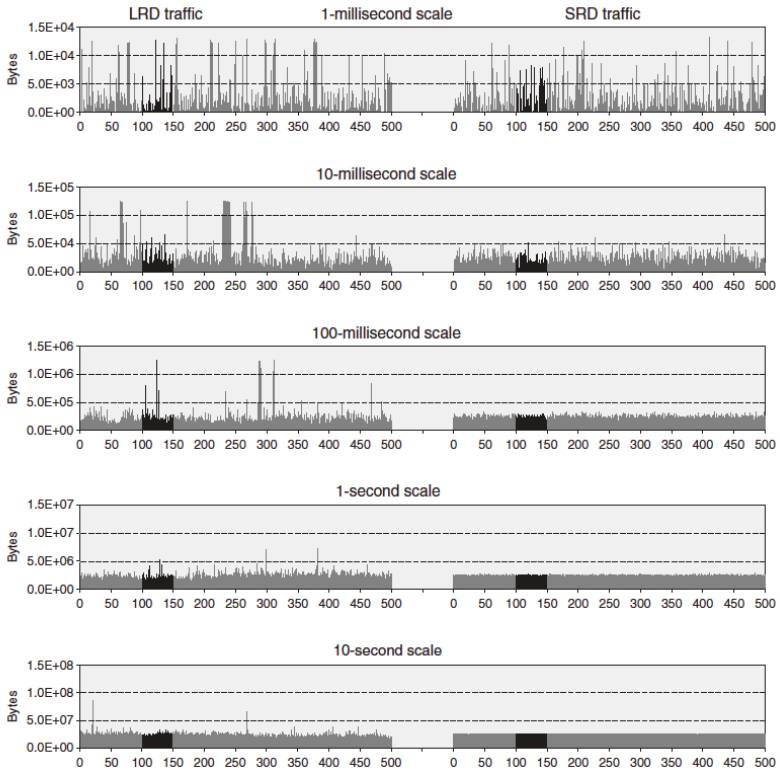

Figure 6.1: Long range dependent (LRD) and short range dependent (SRD) traffic [2]

erate Internet traffic is considered to be an effective method. As self-similar processes are usually described by long-tail distributions, in this analysis, we generate upstream traffic using a long-tail Pareto distribution, as proposed in [2,212].

6.3 Generating long-range dependent (LRD) traffic

As discussed in the previous section, to generate bursty Internet traffic, we follow a Pareto distribution. The generated traffic actually consists of alternating Pareto-distributed on/off periods. The probability density function of a general Pareto distribution can be represented as follows:

$$f(x) = \frac{\alpha b^{\alpha}}{x^{\alpha+1}} \tag{6.5}$$

where α is a shape parameter ($1 < \alpha < 2$) and b is a location parameter. Let the α and b of the Pareto distributions that generate ON and OFF periods be α_{on}, b_{on} and α_{off}, b_{off}, respectively. Based on the actual Ethernet traffic considered in [210], the α_{on} is set at 1.4. Similarly, the α_{off} is set at 1.2. With rigorous mathematical derivations and b_{on} of 1, the b_{off} can be derived as follows:

$$b_{off} = 0.597(\frac{1}{l} - 1) \tag{6.6}$$

where the parameter l represents the normalised network load. These two probability density functions are used to generate incoming traffic at the ONUs that operate under the OFF-DWBA. In the next section, we will briefly revisit the OFF-DWBA algorithm. A detailed explanation of the OFF-DWBA algorithm was presented in Chapter 5.

6.4 Offline dynamic wavelength and bandwidth allocation (OFF-DWBA) algorithm

The OFF-DWBA algorithm was derived from the energy-efficient framework proposed for a delay-constrained TWDM-PON. As explained in Chapter 5, a TWDM-

PON consists of multiple wavelengths, fixed-tuned/tunable transceivers (TRXs) at the optical line terminal (OLT) and tunable TRXs at the ONUs. The multiple TRXs and the tunability of the ONUs facilitate energy-savings at the OLT, whereby the idling wavelengths are switched off after reallocating their ONUs among the active wavelengths. In addition, the conventional sleep/doze mode operations, discussed in Chapter 3 and 4, can be implemented at the ONUs for improved energy-efficiency at the ONUs [22, 110, 133]. Considering these two energy-saving opportunities, in the proposed framework, we calculate the number of active wavelengths, N_{active}, that would satisfy a given delay constraint, D_{cons}. The main objectives of the proposed OFF-DWBA are (a) determining the sleep/doze duration of the ONUs, (b) determining the number of active wavelengths, and (c) transitioning the ONUs between different modes and wavelengths.

Based on the mathematical derivation reported in Chapter 5, the maximum polling cycle time, $T_{poll\ max}$, of an ONU operating under the OFF-DWBA algorithm is as follows:

$$T_{poll\ max} \approx \frac{2\,(D_{cons} - RTT)}{3}, \tag{6.7}$$

where RTT is the round trip time. In any given bandwidth allocation algorithm that incorporates sleep/doze mode operations, increasing the time an ONU spends in sleep or doze mode, $T_{sleep/doze}$, increases the energy-savings. Although a longer polling cycle time, T_{poll}, will result in increased $T_{sleep/doze}$, it will also result in increased average delay. The $T_{poll\ max}$ given in eqn. 6.7, however, is the maximum polling cycle time that an ONU can operate on, without compromising a given delay constraint. As such, under the proposed OFF-DWBA, the ONUs operate at the $T_{poll\ max}$ given in eqn. 6.7.

As OFF-DWBA is an offline DWBA algorithm, in any given cycle, the OLT waits until it receives the REPORT messages from all ONUs in the network. Once the REPORT messages are received, the OLT determines the average bandwidth requested, BW_{avg}, by an ONU. The rational behind considering BW_{avg} is that in our design, we have assumed all ONUs to operate under the same network load

Algorithm 6.1: Pseudocode of the wavelength allocation in the proposed framework

N_{onu} = 64
Phase 1: Average bandwidth calculation - OLT calculates the bandwidth requirement of each ONU
BW_{avg} = *Total BW requested* / N_{onu}
Phase 2: Wavelength optimization process - OLT determines the optimum number of active wavelengths required for a given D_{cons}
$N_{active\ wl}$ = 1
Calculate BW_{max} `//Calculates the maximum bandwidth allowable for an ONU when all ONUs are tuned to one wavelength`
BW_{max} = ($T_{poll\ max}$ - $T_{process}$) / (N_{onu} / $N_{active\ wl}$) `//`$T_{process}$ `is the processing time of all ONUs supported by a given wavelength`
while ($BW_{avg} > BW_{max}$ *and* $N_{active\ wl} \leq N_{total}$) **do**
    `//Check if the requested bandwidth is higher than the current maximum allowable bandwidth`
    $N_{active\ wl} = N_{active\ wl} + 1$ `//Introduce another active wavelength to the network`
    $N_{\text{per wl}} = N_{onu}$ / $N_{active\ wl}$ `//The OLT distributes the number of ONUS uniformly across the wavelengths.` $N_{per\ wl}$ `is the number of ONUs per wavelength.`
    Calculate BW_{max} `//Calculate the new maximum allowable bandwidth, after a wavelength is introduced`
    BW_{max} = ($T_{poll\ max}$ - $T_{process}$) / (N_{onu} / $N_{active\ wl}$)

[189, 190]. After determining BW_{avg}, the OLT determines $N_{active\ wl}$ and $T_{sleep/doze}$, as to be discussed in the following sections.

6.4.1 Determining the number of active wavelengths

For a given $T_{poll\ max}$, there exists a corresponding maximum bandwidth, BW_{max}. If the BW_{avg} exceeds the BW_{max}, packets will have to wait extra cycles before being transmitted to the OLT. In the OFF-DWBA algorithm, if $BW_{max} \leq BW_{avg}$, a new wavelength is introduced to the network. A detailed explanation of this process is presented in Algorithm 6.1.

6.4.2 Determining the sleep/doze duration

In a given polling cycle, the OLT is aware of the transmission time slot, T_{slot} of each ONU. The OLT then determines the $T_{sleep/doze}$ of an ONU as discussed in Algorithm 6.2.

Algorithm 6.2: Pseudocode of the sleep/doze period determination in the proposed framework

```
Phase 3: Sleep/doze allocation process - OLT determines the sleep/doze
  time assigned for each ONU
T_idle = T_poll max - T_slot
if (T_idle ≥ T_sleep−to−active) then
    ONU enters sleep mode
    T_sleep = T_idle - T_sleep−to−active
if ( T_sleep−to−active ≥ T_idle ≥ T_doze−to−active) then
    ONU enters doze mode
    T_doze = T_idle - T_doze−to−active
else
    ONU stays active
```

6.4.3 Transitioning the ONUs between different modes and wavelengths

As explained earlier, the OFF-DWBA algorithm utilises MPCP control messages, GATE and REPORT, to control the traffic flow between the OLT and the ONUs. Figure 6.2 presents the traffic flow between the OLT and the ONUs, for an illustrative TWDM-PON with an OLT and three ONUs. The MPCP REPORT message is sent from the ONUs to the OLT and contains the bandwidth requirement of each ONU. Upon receiving the REPORT messages from all the ONUs in the network, the OLT determines the T_{slot}, number of active wavelengths, $N_{active\ wl}$, and the $T_{sleep/doze}$ of each ONU, as discussed in Section 6.4.1 and 6.4.2, respectively. This information is included in the GATE message to each ONU in the PON.

Upon receiving this GATE message, an ONU analyses it and tunes to the appropriate wavelength as specified by the OLT. The ONU then transmits upstream data and the next REPORT message within T_{slot} and then enters into sleep or doze mode for $T_{sleep/doze}$. In the next cycle, the ONU wakes up just-in-time to receive

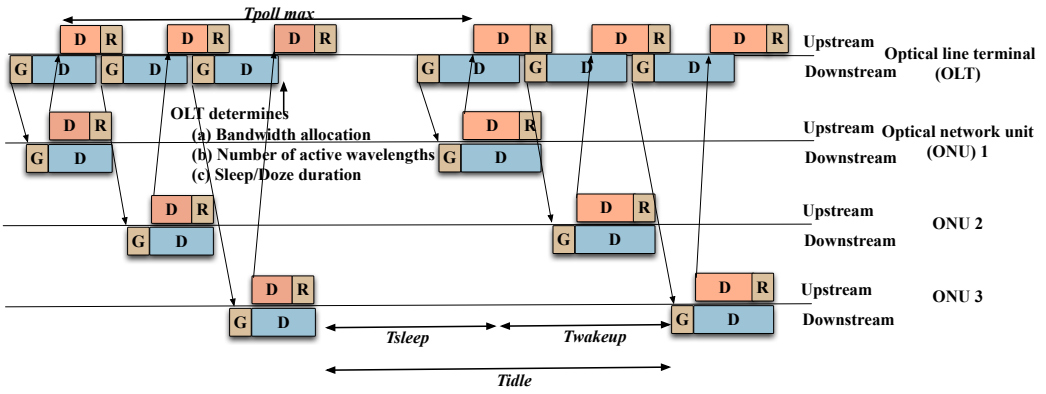

Figure 6.2: Traffic flow of the OFF-DWBA algorithm. D-Data, R-REPORT and G-GATE.

the next GATE message from the OLT.

6.5 Performance evaluation

This section presents a comparative analysis of the performance of the OFF-DWBA under bursty traffic and Poisson-distributed traffic. The performance is measured in terms of the number of active wavelengths, percentage of energy-savings, and average delay. Using C++, we have simulated a TWDM-PON with the network and protocol parameters listed in Table 6.2. Table 6.1 lists the power consumption and switching values of the 10G-VCSEL ONU considered in this work.

Figures 6.3 (a) and (b) plot the number of active wavelengths as a function of normalised network load under bursty and Poisson traffic, respectively. Under both bursty and Poisson traffic, when the network load increases, for any given

Table 6.2: Network and protocol parameters

Parameter	Value
Network reach	40 km
Number of ONUs	64
Delay constraints	7.5, 10, and 15 ms
Propagation delay	200 μs
Inter-frame gap in upstream	1μs
Ethernet packet size	791 bytes
Wavelength tuning and GATE processing	50μs

D_{cons}, the number of active wavelengths increases. As explained in Algorithm 1, a new wavelength is introduced, when $BW_{max} \leq BW_{avg}$. When the network load increases, BW_{avg} increases, thereby increasing the number of active wavelengths.

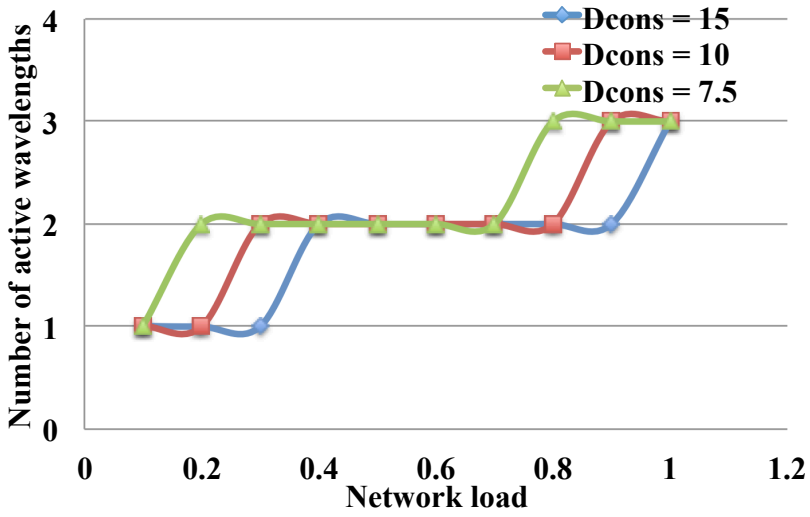

(a) Bursty traffic

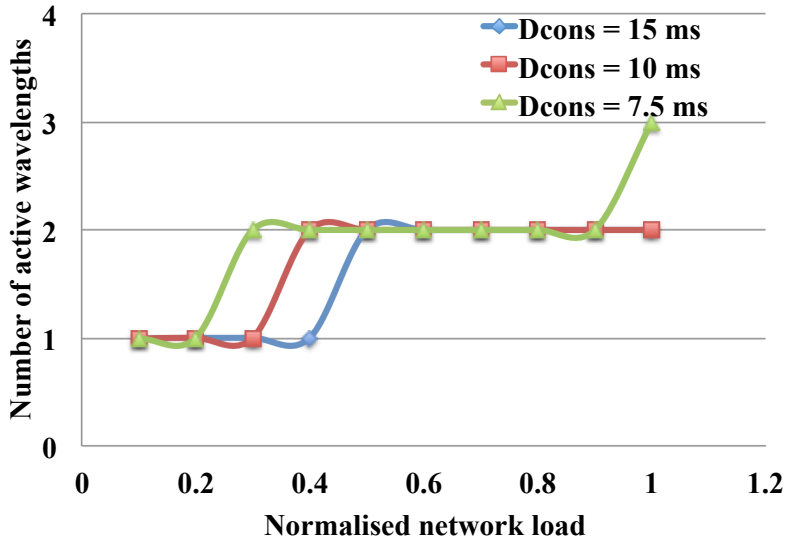

(b) Possion traffic

Figure 6.3: Number of active wavelengths under (a) bursty traffic and (b) Poisson traffic as a function of normalised network load.

When D_{cons} increases, the network load at which a new wavelength is introduced, increases as well. For example, under bursty traffic, the second active wavelength is introduced at the network loads of 0.2, 0.3, and 0.4 for D_{cons} of 7.5, 10, and 15 ms, respectively. In other words, when D_{cons} increases, it is possible to transmit the same amount of traffic with a higher delay, i.e., with a lower number of active wavelengths. When the D_{cons} increases, it increases the corresponding $T_{poll\ max}$ and BW_{max}. As a result, the condition $BW_{max} \leq BW_{avg}$, occurs at higher network loads.

Based on results depicted in Figs. 6.3 (a) and (b), under both bursty traffic and Poisson-distributed traffic, the variation in number of active wavelengths follows the same pattern. However, under bursty traffic, for a D_{cons} of 7.5 ms, a third wavelength is introduced at the network load of 0.8, whereas under Poisson-distributed traffic, this value is 1. Moreover, our OFF-DWBA under bursty traffic requires three wavelengths beyond the network loads of 0.9 and 1 for D_{cons} of 10 ms and 15 ms, respectively. Under Poisson-distributed traffic however, the maximum number of wavelengths required at these delay constraints is two. This variation in number of active wavelengths is attributed to the packet distributions used in our simulations. When generating Poisson-distributed traffic, we considered an uniform packet length distribution, with minimum and maximum values of 512 bits and 1712 bits, respectively. However, when generating bursty traffic, we considered a fixed packet length of 719 bytes for simplicity.

Figures 6.4 (a) and (b) plot the percentage of energy-savings, α, achieved at the OLT as a function of normalised network load under bursty and Poisson traffic, respectively. As explained in Chapter 5, the energy-savings at the OLT, resulting from switching off idle wavelengths, can be quantified as follows:

$$\alpha = \left(1 - \frac{P_{olt\ active} T_{poll\ cycle} N_{active\ wl}}{P_{olt\ active} T_{poll\ cycle} N_{totalwl} + T_{poll\ cycle} P_{olt\ base}}\right) \% \tag{6.8}$$

where parameter $P_{olt\ active}$ represents the power consumption of the OLT in active state. Under bursty traffic, for a given D_{cons}, when network load increases, α decreases. As explained in Fig. 6.3, when network load increases, $N_{active\ wl}$ increases and therefore, α decreases. Meanwhile, for a given network load, an increase in

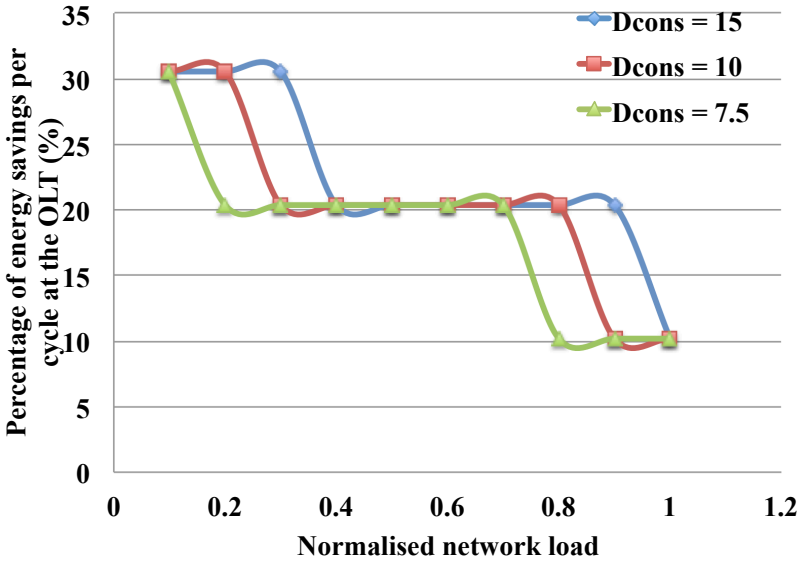

(a) Bursty traffic

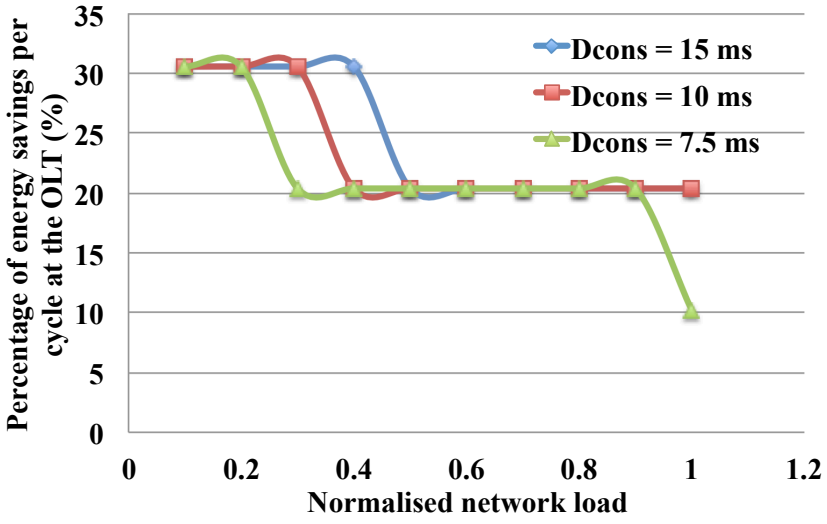

(b) Poisson traffic

Figure 6.4: Percentage of energy-savings per cycle at the OLT under (a) bursty traffic and (b) Poisson traffic as a function of normalised network load.

D_{cons}, increases α. When D_{cons} increases, it is possible to transmit the same amount of traffic with a higher delay, i.e., with a lower number of active wavelengths. A

lower number of active wavelengths results in improved energy-savings at the OLT. As shown in Fig. 6.4, the maximum possible energy-savings at the OLT is 30 %. Based on the power consumption values listed in Table 6.1, the base power of the OLT consists of the power consumption of its Erbium doped fibre amplifier (EDFA), booster, and layer 2 switching capacity. As these components are shared by all wavelengths in the network, they have to be kept ON all the time. Compared to the 11 W of power consumed by a wavelength, the base power of the OLT is significant at 64 W. As a result, even when the network is operating at one wavelength, only 30% of savings is possible.

It is important to note that under both Poisson and bursty traffic, α achieved under OFF-DWBA follows the same pattern, i.e., decrease in α when the network load increases for a given D_{cons} and increase in α when D_{cons} increases for a given network load. However, as explained in Fig. 6.3, for network loads over 0.8, $N_{active\ wl}$ required under each D_{cons} is different. As a result, α, which depends on $N_{active\ wl}$, is different as well.

Figure 6.5 plots the percentage of energy-savings per cycle per ONU, η, as a function of normalised network load. The value η represent the energy-savings achieved through a sleep/doze-capable 10G-VCSEL ONU, compared to an always-ON VCSEL ONU and is calculated as follows:

$$\eta = \left(1 - \frac{P_{vcsel,act}T_{act} + P_{vcsel,doze/sleep}T_{doze/sleep}}{P_{vcsel,act}(T_{act} + T_{sleep/doze})}\right)\% \tag{6.9}$$

where parameters $P_{vcsel,act}$, $P_{vcsel,doze/sleep}$, T_{act} and $T_{doze/sleep}$ represent the power consumption of a 10G-VCSEL in active state, in sleep/doze state and the duration an ONU spends in active state and sleep/doze state, respectively. For a given network load, when the D_{cons} increases, the corresponding $T_{poll\ max}$ increases as well. A longer $T_{poll\ max}$ allows an ONU to sleep or doze for a longer duration, achieving more energy-savings. Meanwhile, for a given D_{cons}, when the network load increases, the T_{slot} increases. An increase in T_{slot} increases the T_{act}, thereby reducing the value of η. It is important to note that due to the D_{cons} values selected for the simulations, the ONUs always enter into sleep mode. As the difference in

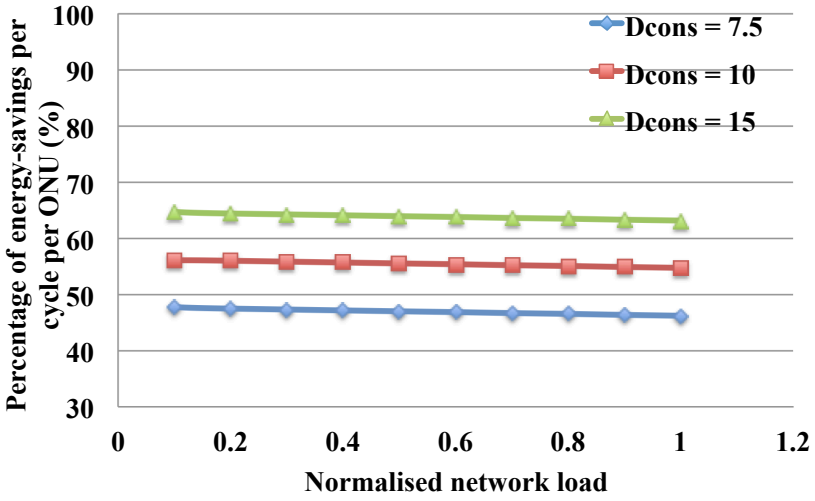

(a) Bursty traffic

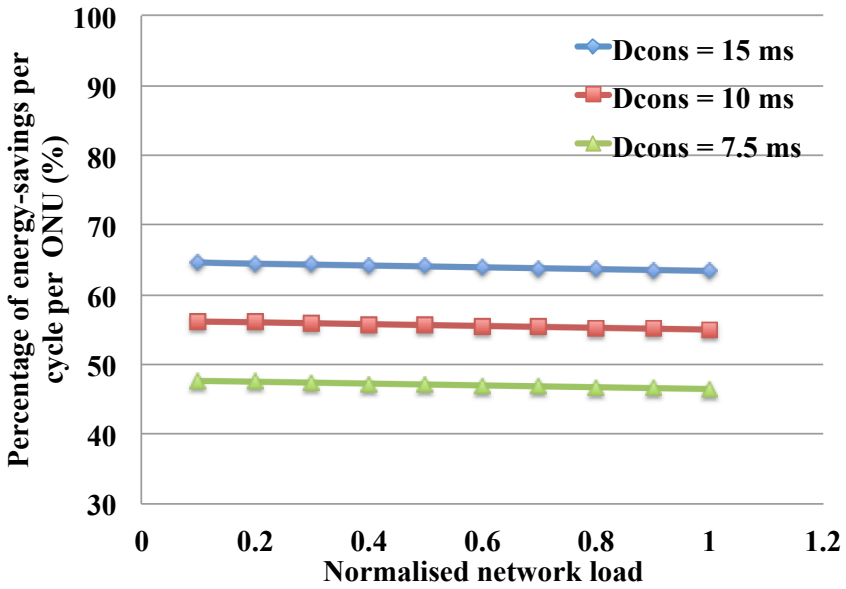

(b) Possion traffic

Figure 6.5: Percentage of energy-savings per cycle per ONU under (a) bursty traffic and (b) Poisson traffic as a function of normalised network load.

power consumption between sleep and active modes is quite significant at 3.234 W, the percentage of energy-saving as high as 65% is achieved in these simulations. Similar to $N_{active\ wl}$ and α, the percentage of energy-savings at the ONUs follows

similar patterns under both bursty and Poisson-distributed traffic.

Figure 6.6 presents the average delay of the OFF-DWAB as a function of normalised network load. The average delay values of our simulations closely repre-

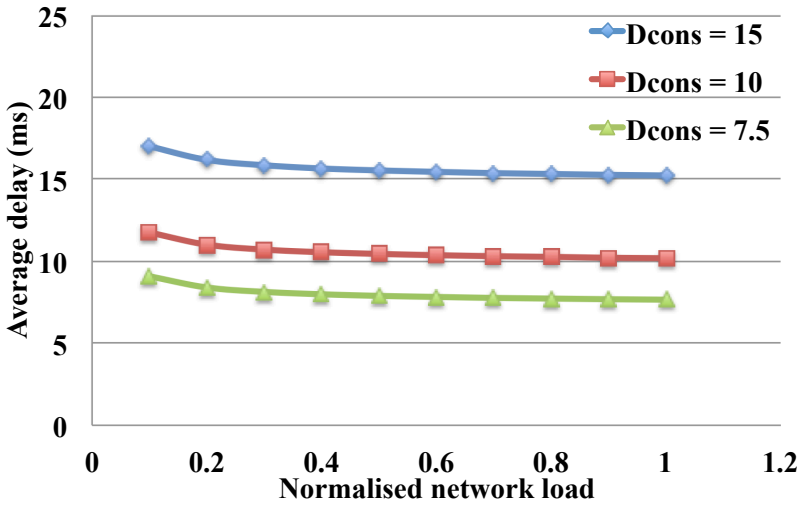

(a) Bursty traffic

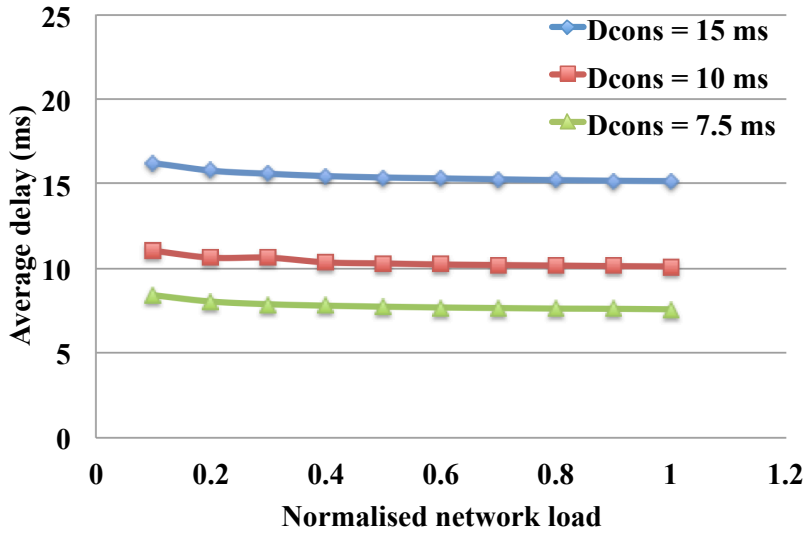

(b) Possion traffic

Figure 6.6: Average delay under (a) bursty traffic and (b) Poisson traffic as a function of normalised network load.

sent the given D_{cons} values. As discussed in Chapter 5, for all cases of D_{cons}, the average delay is slightly higher than D_{cons} value, as we have not considered the time a packet takes to reach the beginning of the ONU queue, in our mathematical analysis. Except for minor differences in average delay, the OFF-DWBA algorithm yields similar results under bursty and Poisson-distributed traffic.

6.6 Conclusions

In this chapter we have analysed the OFF-DWBA algorithm, proposed previously in Chapter 5, under bursty traffic. The OFF-DWBA algorithm, which is designed for a delay-constrained TWDM-PON, incorporates wavelength reallocation and sleep/doze mode operations to improve the energy-efficiency of the OLT and the ONUs, respectively. Based on our findings, the OFF-DBA algorithm achieves 30% of energy-savings at the OLT, and energy savings as high as 65% at the ONUs. The simulated results further proves that the network operates under the given delay constraints.

Comparing these results against our findings in Chapter 5, which corresponds to the Poisson-distributed traffic, we observe that in both scenarios, the OFF-DWBA algorithm yields similar results. As such, we can conclude that our proposed framework for a delay-constrained TWDM-PON can be effectively implemented in a TWDM-PON with either continuous or bursty traffic.

CHAPTER 7

Conclusions and Future Directions

7.1 Introduction

Passive optical networks (PONs) have been deployed in the access segment to deliver fibre to the home/cabinet/curb/office (FTTx) services to customers [6]. The use of optical fibre in the access segment helps overcome the capacity limitations of conventional copper wire-line infrastructure and to cater to high-bandwidth demands of fixed [1] and mobile [7] users. A PON consists of an optical line terminal (OLT) at the central office (CO) and optical network units (ONUs) at the customer premises [213]. The components in between, such as optical splitters and splicers are all passive, meaning they do not consume any power. Due to passive nature of components, low transmission losses, and high capacity, PONs are characterised by low energy-per-bit [3–5]. However, with wider deployment of PONs, the increase in the number of customers and high-speed components have led to increased energy consumption in communication networks. The complications of increased energy consumption, such as greenhouse gas emissions and increased operational expenditure, have motivated energy saving solutions for PON.

The main focus of this thesis has been to improve the energy efficiency of PONs; specifically, the time division multiplexed PON (TDM-PON) and time and wavelength division multiplexed PON (TWDM-PON), using algorithm-based solutions. To propose energy saving solutions for the TDM-PON and TWDM-PON, we first analysed their operational and physical attributes to identify potential energy saving methods. In both TDM-PON and TWDM-PON, due to slotted nature of upstream and downstream bandwidth access, an ONU transceiver (TRX) spends a majority of its time in the idle state, i.e., it does not transmit/receive

any packets. Despite being idle, ONUs continue to operate at their active power level. As a result, the high energy consumption of PONs has been attributed to the ONUs [1].

To minimise the energy consumption of ONUs, ITU-T has proposed to transition them into sleep or doze mode during their idle time [23]. In sleep mode, both ONU transmitter (Tx) and receiver (Rx) are powered down. In doze mode, only ONU Tx is powered down. Further, as discussed in Chapters 2 and 5, a TWDM-PON consists of multiple wavelengths and tunable ONUs that can tune to any of these wavelengths [11, 54]. The wavelength tunability of ONUs presents further energy-saving opportunities at the OLT. At a given network load, a TWDM-PON may not require all available wavelengths to serve ONUs in the network. As such, lightly loaded wavelengths can be switched off and the ONUs can be reallocated among remaining active wavelengths. This technique, referred to as wavelength reallocation, reduces the energy consumption of the OLT. In this thesis, we incorporate sleep/doze mode operations and wavelength reallocation into our dynamic bandwidth allocation (DBA) algorithms and dynamic wavelength and bandwidth allocation (DWBA) algorithms to improve the energy efficiency of the TDM-PON and TWDM-PON, respectively.

Our proposed algorithms exploit the sleep/doze capabilities and wavelength tunability of the 10 Gbps vertical-cavity surface-emitting laser (10G-VCSEL) ONUs. Compared to a conventional distributed feedback (DFB) ONU, the 10G-VCSEL ONU consumes less power in active mode and has a shorter doze-to-active transition time, making it an excellent candidate for energy-efficient communication networks. Consequently, the 10G-VCSEL ONU is used as the Tx of our ONU, while the Rx and digital back-end circuitry are kept the same as that of a DFB ONU. The following sections summarise the key contributions of this thesis and discuss the future directions of our research.

7.2 Key contributions

In Chapter 1, we briefly discussed the current bandwidth trends in communication networks and the deployment of PONs to cater to this demand. We highlighted the importance of reducing the energy consumption of next-generation PONs to minimise greenhouse gas emissions and operational expenditure. The chapter then summarised our objectives in reducing energy consumption by exploiting the sleep/doze capabilities and wavelength tunability of the ONUs. These objectives are associated with different methods of fine-tuning the DBA and DWBA algorithms, such as incorporating sleep/doze mode operations into the underlying DBA/DWBA algorithms, determining the sleep/doze durations, minimising the average delay resulting from sleep/doze operations, and determining the number of active wavelengths. The chapter then outlined how these objectives are achieved through our technical contribution, followed by research work published.

The motivation behind our technical contributions lies in existing studies that incorporate sleep/doze mode operations and wavelength reallocation for energy-efficient PONs. As such, in Chapter 2, we critically analysed existing solutions proposed for TDM-PONs and TWDM-PONs. The chapter presented a detailed account of these particular network architectures, such as their physical deployment, operational attributes, and evolution. Based on this analysis: (1) the slotted nature of upstream/downstream bandwidth access; and (2) multiple wavelengths in conjunction with tunable ONUs are identified as the basis for energy saving sleep/doze mode operations and wavelength reallocation in TDM-PON and TWDM-PON, respectively. The existing solutions that exploit these two techniques are categorised into hardware and algorithm-based solutions. The hardware-based solutions involve minimising the power consumption of an ONU in each state, reducing the overhead time associated with transitioning an ONU between sleep/doze and active modes, and improving the tunability of the ONUs. The algorithm-based solutions, however, involve incorporating the sleep/doze mode operations and wavelength reallocation into the algorithms, determining the sleep

or doze duration or the number of active wavelengths, and preserving the quality of service (QoS) of the network.

In Chapter 3, we presented our initial technical contributions, Just-In-Time DBA (JIT DBA) with varying polling cycle times, and JIT DBA with fixed polling cycle times (J-FIT DBA) [189]. The algorithms address the challenge of incorporating low-power modes into the underlying DBA algorithm of a TDM-PON. The novelty of these algorithms lies in incorporating *both* sleep and doze capabilities of an ONU to improve energy efficiency of a TDM-PON. The proposed algorithms transition an ONU into sleep or doze mode, depending on its idle time and transition it back to active mode just-in-time to receive the next downstream packet from the OLT. Both algorithms are designed for an illustrative 10 Gbps Ethernet PON (10G-EPON), and therefore, comply with the Multi-Point Control Protocol (MPCP) messages GATE and REPORT to transition the ONUs between sleep, doze, and active modes. At low network loads, the JIT-DBA operates at shorter polling cycle times, and therefore, achieves energy savings of only 3% compared to an always-ON 10G-VCSEL ONU [189]. The JIT DBA yields significant energy savings of 61% at network loads greater than 0.8. In general, communication networks operate at moderate network loads less than 0.6 [29]. In such an environment, the JIT DBA will not achieve any noticeable energy savings. To overcome this shortfall, we extend the idle time of an ONU using fixed polling cycle times in the J-FIT DBA. At low network loads, J-FIT DBA yields a percentage of energy savings of 65%, a significant improvement compared to the JIT DBA. Further, for practical network loads of 0.6 and below, the average delay experienced by the packets under both JIT and J-FIT DBA algorithms, is less than 100 ms and supports delay-sensitive services over the TDM-PON.

Further in Chapter 3, we quantified the percentage improvement achieved by using the 10G-VCSEL ONU, in place of a conventional DFB ONU. The percentage of energy savings achieved using an always-ON DFB ONU and a sleep/doze-capable DFB ONU is compared against our sleep/doze-capable 10G-VCSEL ONU. Under both scenarios, the 10G-VCSEL ONU outperforms the DFB ONU regards to energy efficiency, on the grounds of low power consumption and shorter doze-

to-active transition time.

In Chapter 4, we proposed the JIT DBA algorithm with Bayesian estimation and prediction (BEP DBA) to address the challenges of determining the sleep/doze duration and minimising the average delay arising from sleep/doze mode operations. When the traffic load is low, an ONU can spend more time in sleep/doze mode without compromising QoS parameters, such as average delay. In Chapter 4, we identified that allocating sleep/doze duration based on network load is a favourable technique to increase the energy savings while preserving average delay requirements of the network. For this purpose, the OLT should be made aware of the traffic load of each ONU. The average inter-arrival time of packets is a statistical parameter that closely represents the traffic load of an ONU and can be easily estimated by the ONU back-end digital circuitry. As a result, in Chapter 4, the average inter-arrival time of incoming packets at the ONUs is used as the indicator of network load. Once the OLT receives the estimated inter-arrival time of incoming packets at each ONU, a pre-defined sleep/doze control function is used to map a given average inter-arrival time of packets to sleep/doze duration. The underlying sleep/doze control function depends on the QoS parameters, such as average delay of the network.

As the operation of our BEP DBA heavily depends on the estimated average inter-arrival time of packets, the techniques used in estimating this value are an important design consideration. As such, we evaluated different estimation techniques, such as arithmetic average, exponential smoothing, and Bayesian framework, in Chapter 4. We then choose the one that achieves the lowest mean squared error (MSE) with a low number of samples (packets). Based on our findings, the Bayesian framework yields comparatively low MSE values with a fewer number of measurements compared to the other two methods. The comparative advantage of the Bayesian framework lies in the use of prior knowledge of the parameter to be estimated.

Most importantly in Chapter 4, we addressed the shortcoming of increased average delay, arising from the sleep/doze mode operations, using traffic prediction. If the OLT can allocate bandwidth to traffic accumulated during the sleep/doze

duration, these packets are prevented from waiting for extra cycles. For this purpose, we used the already available average inter-arrival time of packets in conjunction with the traffic prediction technique, whereby the estimated average inter-arrival time of upstream packets is used by the OLT to determine the amount of traffic accumulated during the sleep/doze duration. When granting transmission time slots to the ONUs, OLT considers both average requested bandwidth and the predicted bandwidth. Based on our initial simulations, using the actual predicted bandwidth in conjunction with the average requested bandwidth, increases the average delay. To address this problem, we optimised the proportion of predicted bandwidth considered in the BEP DBA algorithm. To highlight the performance of the sleep/doze control and the prediction mechanisms, we first evaluated the energy and delay performance of the Bayesian estimation alone. Based on our findings, the proposed sleep/doze control function achieves energy savings as high as 65%. When the prediction mechanism is added to the algorithm, the average delay is reduced by 13% at an increase of 0.01% in average power consumption.

The DBA algorithms, JIT, J-FIT, and BEP, conclude our energy-efficient solutions for TDM-PONs. Although the proposed algorithms are designed for an illustrative 10G-EPON, they can be applied to any TDM-PON after minor modifications to the control frame structure. Overall, our proposed DBA algorithms improve the energy efficiency of TDM-PONs and satisfy the delay requirements of the network. As customer demand for bandwidth-intensive services continues to grow, the communication networks are expected to evolve as well. To be precise, the next-generation PONs are expected to deliver a 40 Gbps data rate, 40 km network reach, and 256-1024 customers. After evaluating different network architectures concerning these requirements, the TWDM-PON has been selected as the most appropriate configuration by FSAN [11]. As such, in Chapters 5 and 6 of this thesis, we proposed energy saving QoS-aware solutions for TWDM-PONs.

As discussed in Chapter 2, a TWDM-PON does not have a centralised colourless light source deployed at the OLT and as a result, tunable TRXs at the ONUs are a key requirement of the TWDM-PON. Although the tunability adds to the capital expenditure of the network, it also presents an opportunity to save energy at the

OLT. At low network loads, the network may not require all available wavelength channels to serve the ONUs. As the ONUs are tunable across all wavelengths supported by the networks, the OLT can switch off the idle wavelengths and allocate the ONUs among remaining active wavelengths. In Chapter 5, we proposed to use this wavelength reallocation technique in conjunction with the sleep/doze mode operations to minimise the overall energy consumption. In DWBA algorithms that incorporate wavelength reallocation, the most important decision to make is the number of active wavelengths. From a customer perspective, quality of experience (QoE) is more important than potential energy savings. For this purpose, network parameters, such as average delay, should be kept below a specified maximum. Meanwhile, network operators are encouraged to minimise the energy consumption to reduce the operational expenditure and carbon footprint. Taking both energy and delay considerations into account, in Chapter 5, we proposed a framework that determines the number of active wavelengths for a delay-constrained TWDM-PON.

For a given delay-constrained TWDM-PON, the framework first determines the maximum polling cycle time the network can operate on, such that the delay requirement is satisfied. The reason for selecting the maximum polling cycle time is because it leads to longer sleep/doze durations and yields more energy savings at the ONUs. Using the maximum allowable bandwidth that corresponds to this maximum polling cycle time as a threshold, the OLT determines the number of active wavelengths required to satisfy a specified delay constraint. Based on this maximum polling cycle time, the framework also calculates the sleep/doze duration of the ONUs.

The proposed framework is applied to two types of DWBA algorithms, online DWBA (ON-DWBA) and offline DWBA (OFF-DWBA). The OFF-DWBA allocates bandwidth after receiving REPORT messages from all ONUs in the network, prompting the ONUs to wait for an extra cycle before receiving its bandwidth grant. The ON-DWBA algorithm, however, allocates bandwidth in the cycle the traffic is received. Based on our results, both OFF-DWBA and ON-DWBA algorithms satisfy the delay requirements of the network. However, the ON-DWBA,

which operates on comparatively longer polling cycle times, achieves more energy savings at the ONUs. Further, as the ON-DWBA can support the delay constraints of the network with a lower number of active wavelengths, the ON-DWBA also yields more energy savings at the OLT.

The energy-efficient DBA and DWBA algorithms proposed in Chapters 3, 4, and 5 are evaluated with Poisson-distributed incoming traffic at the ONUs. As explained in Chapter 6, using Poisson-distributed traffic can be justified due to its mathematical simplicity and the fact that aggregating large number of traffic flows eventually leads to a Poisson-distributed flow. The Internet traffic, however, is becoming more bursty in nature [204] and exhibits long-range dependent behaviour, which is usually prevalent in long-tailed probability density functions. As such, analysing the performance of our proposed algorithms under bursty traffic is important. As the Pareto distribution is a long-tailed probability density function that complies with the nature of bursty traffic, we used this distribution to generate incoming bursty traffic at the ONUs. Using this bursty traffic, the performance of our OFF-DWBA algorithm is analysed for a differing number of active wavelengths, the percentage of energy savings, and average delay. The reason for selecting the OFF-DWBA algorithm is because it includes both wavelength reallocation and sleep/doze mode operations. Based on simulation results, our proposed wavelength reallocation and sleep/doze mechanisms works effectively, even under the bursty traffic.

7.3 Future Direction

As highlighted in the previous section, this thesis comprises of a comprehensive study of DBA and DWBA algorithms proposed to minimise the energy consumption of the TDM-PON and TWDM-PON. During this study, related topics on sleep and doze mode operations and wavelength reallocation were identified but could not be pursued due to time limitations. This section outlines such areas that need further investigation.

7.3.1 Key assumptions

One of the key assumptions that we used throughout this thesis is that all ONUs in the network operate under the same network load. This assumption simplified the mathematical analysis and the processes involved in determining the bandwidth allocated to each ONU, scheduling order, sleep/doze duration of each ONU, and a number of active wavelengths at the OLT. However, in certain instances, networks may experience different network loads at each ONU. In such a scenario, allocating bandwidth among ONUs require fairness assurance, as a heavily loaded ONU will use a majority of the network capacity. The scheduling order of the ONUs has to be properly optimised as different ONUs may enter into different sleep/doze durations and wake up at different times. The sleep/doze mode operation is further complicated by the fact that due to different network loads, these ONUs may enter into different modes, sleep, doze, or active, in a given cycle. This challenge is more prevalent in algorithms, such as BEP DBA, where a dedicated sleep/doze function is used to determine the sleep/doze duration. Our proposed algorithms can still be applied to such networks, given that the ONUs with similar network loads are grouped together. It will be worthwhile investigating how these groups are scheduled such that the optimum energy savings and average delay are achieved.

Further in our proposed algorithms, we have assumed that the upstream and downstream traffic load of an ONU is symmetrical. However, due to different customer behaviour within a network, traffic load in a given direction may be dominant. When allocating bandwidth, the average bandwidth requirement of an ONU in each direction is considered and the maximum out of the two is compared against a threshold. Although this bandwidth allocation scheme is straightforward, asymmetrical traffic loads facilitate additional energy savings at the ONUs. For example, consider a scenario where the upstream bandwidth requirement is higher that of the downstream. As explained before, the bandwidth will be allocated based on the upstream bandwidth requirement, resulting in an over-provisioning of bandwidth in the downstream. As a result, the ONU Rx remains idle within the allocated transmission time slot. The ONU Rx can be transitioned

into sleep/doze mode, depending on the idle time of the Rx and the sleep/doze overhead time of the ONU. In such a scenario, it would be interesting to investigate how this idle duration within a transmission time slot can be maximised for improved energy savings.

7.3.2 Bursty traffic and estimation

In Chapter 6, we evaluated the performance of our OFF-DWBA algorithm under bursty traffic. However, the ON-DWBA algorithm, under bursty traffic, is yet to be investigated. The ON-DWBA requires the inter-arrival time of packets to be estimated at the ONUs. As such, evaluating the performance of the ON-DWBA will require the analysis of different estimation techniques that will effectively determine the average inter-arrival time of packets. This study will also require re-evaluating the effectiveness of our previously proposed Bayesian framework and investigating relevant conjugate prior distributions. This analysis will also affect the BEP DBA proposed in Chapter 4.

7.3.3 Micro base stations

Based on the Cisco Visual Networking Index (VNI) report published in 2015, the mobile data traffic is expected to grow by 57% by 2019. To cater this demand, more dense base station deployment will be required in the future. In regards to the energy consumption of the mobile networks, a majority of it is attributed to the base stations, whereas the energy consumption attributed to mobile devices and servers are significantly smaller by a factor of about four or five. If the coverage of the network is increased with such conventional macro base stations, the energy consumption of the mobile networks will increase significantly. As a result, micro base stations are deployed in such dense areas. The micro base stations are more energy-efficient than the conventional macro base stations as they consume comparatively less power in active mode. In any mobile network, energy can be saved through sleep mode operation at the base station. The implication of sleep mode operation is the degradation of QoS of the network. However, due to the

deployment of micro base stations, some of the high-power macro base stations can be powered down after handing over their traffic to the low-power micro base stations. The DBA and DWBA algorithms we proposed in our thesis can be extended to these micro base station environments. Specifically, it will be interesting to apply our delay-constrained framework proposed for the TWDM-PON to the mobile network and investigate the number of macro base stations that could be powered down and the number of micro base stations that is required to replace these macro base stations. Further, the delay constraint can also be replaced with blocking probability, spectral efficiency, and coverage performance to analyse the network for different QoS.

7.4 Conclusions

The exponential growth of the Internet and the evolution of broadband technologies have led to the deployment of PONs in the access networks. The wide deployment of PONs, however, has raised concerns about greenhouse emissions and operational expenditure associated with the increased energy consumption of the PON. This chapter summarises our motivation and technical contribution to improving the energy efficiency of the PON. As TDM-PONs and TWDM-PONs are popular choices for current and future access networks, respectively, in this thesis, energy saving solutions are designed primarily for these two configurations. Motivated by the operational characteristics, traffic patterns, and the physical layout of these configurations, we propose the sleep/doze mode operations and wavelength reallocation as means of saving energy in the PONs. Using these power saving techniques, algorithm-based solutions, DBA and DWBA algorithms, are proposed for the TDM-PON and TWDM-PON, respectively. The proposed algorithms for the TDM PON address different aspects of energy-efficient DBA algorithms, such as incorporating sleep/doze mode operations, determining the sleep/doze duration, and minimising the average delay arising from the sleep/doze mode operations. Our algorithms proposed for TWDM-PONs are more focused on minimising the energy consumption of a delay-constrained TWDM-PON. In the proposed

DWBA algorithms, the number of active wavelengths is determined based on the delay requirements of the network. The proposed DBA and DWBA algorithms improve the energy saving capability of the PON while also keeping the average delay at levels suitable for delay-sensitive applications. Finally, in this chapter, we discussed the potential areas of research that can extend our technical contribution further.

Bibliography

[1] J. Baliga, R. Ayre, K. Hinton, W. V. Sorin, and R. S. Tucker, "Energy consumption in access networks," *IEEE/OSA Journal of Lightwave Technology*, vol. 27, pp. 2391–2401, 2009. (Cited on pages 1, 33, 62, 90, 157 and 158.)

[2] G. Kramer, *Ethernet passive optical networks*. New York N.Y.: McGraw-Hill, 2005. (Cited on pages 1, 21, 121, 142, 143 and 144.)

[3] P. Vetter, D. Suvakovic, H. Chow, P. Anthapadamanabhm, K. Kanonakis, K. Lee, F. Saliou, X. Yin, and B. Lannoo, "Energy-efficiency improvements for optical access," *IEEE Communication Magazine*, vol. 52, pp. 136–144, 2014. (Cited on pages 1, 3, 31, 50, 115, 118 and 157.)

[4] A. Gladisch, C. Lange, and R. Leppla, "Power efficiency of optical versus electronic access networks," *Proc. of 34thEuropean Conference and Exhibition on Optical Communication (ECOC)*, 2008. (Cited on pages 1, 3, 31 and 157.)

[5] J. Baliga, R. Ayre, K. Hinton, W. V. Sorin, and R. S. Tucker, "Energy consumption in optical IP networks," *Proc. of Optical Fibre Communication Conference and Exhibition/National Fibre Optic Engineers Conference (OFC/NFOEC)*, 2008. (Cited on pages 1, 3, 31 and 157.)

[6] J. Kani, F. Bourgart, A. Cui, A. Rafel, and S. Rodrigues, "Next-generation PON-Part 1: Technology roadmap and general requirements," *IEEE Communications Magazine*, vol. 47, pp. 43–49, 2009. (Cited on pages 1, 20 and 157.)

[7] S. Gangxiang, R. S. Tucker, and C. Chang-Joon, "Fixed mobile convergence architectures for broadband access," *IEEE Communication Magazine*, vol. 45, pp. 44–50, 2007. (Cited on pages 1, 23 and 157.)

[8] M. M. N. Ghazisaidi and A. Assi, "Fibre-wireless (fiwi) access networks: A survey," *IEEE Communication Magazine*, vol. 47, pp. 160–167, 2009. (Cited on pages 1 and 23.)

[9] S. Sarkar, S. Dixit, and B. Mukherjee, "Hybrid wireless-optical broadband-access networks (WOBAN): A review of relevant challenges," *IEEE/OSA Journal of Lightwave Technology*, vol. 25, pp. 3329–3340, 2007. (Cited on pages 1 and 23.)

[10] C. Lam, *Passive Optical Networks: Principles and Practice*. San Diego: Academic Press Inc, 2007. (Cited on pages 2 and 21.)

[11] Y. Luo, X. Zhou, F. Effenberger, X. Yan, G. Peng, Y. Qian, and Y. Ma, "Time- and wavelength-division multiplexed passive optical network (TWDM-PON) for next-generation PON stage 2 (NG-PON2)," *IEEE/OSA Journal of Lightwave Technology*, vol. 31, pp. 587–593, 2013. (Cited on pages 2, 114, 158 and 162.)

[12] E. Harstead, "Future bandwidth demand favours TDM PON not WDM PON," *Proc. of Optical Fibre Communication Conference and Exhibition/National Fibre Optic Engineers Conference (OFC/NFOEC)*, 2011. (Cited on pages 2 and 22.)

[13] ITU-T G.984.x-series recommendations, "Gigabit-capable passive optical networks (G-PON): General characteristics (G.984.1)," 2008. (Cited on pages 2 and 22.)

[14] IEEE:802.3ah, "Ethernet in the first mile task force," (Cited on pages 2, 22, 25, 27, 59 and 66.)

[15] Cisco VNI, "Forecast and methodology, 2014-2019," (Cited on pages 2 and 3.)

[16] K. Grobe, "Next-generation access/backhaul based on ITU G.989, NG-PON2," *Proc. of Photonic Networks ITG Symposium*, 2012. (Cited on pages 2 and 23.)

[17] ITU-T G.p89.2:, *40-Gigabit-capable passive optical networks 2 (NG-PON2): Physical media dependent (PMD) layer specification*. (Cited on pages 2 and 23.)

[18] ITU-T G.989.1, *40-Gigabit-capable passive optical networks (NG-PON2): General requirements*. (Cited on pages 2 and 23.)

[19] M. Gupta and S. Singh, "Greening of Internet," *Proc. of ACM SIGCOMM*, pp. 19–26, 2003. (Cited on pages 3, 4, 31, 60 and 64.)

[20] M. Gupta, S. Grover, and S.Singh, "A feasibility study for power management in LAN switches," *Proc. of the 12th IEEE International Conference on Network Protocols*, 2004. (Cited on pages 3, 4, 31, 33 and 60.)

[21] C. Lange, D. Kosiankowski, R. Weidmann, and A. Gladisch, "Energy consumption of telecommunication networks and related improvement options," *IEEE Journal of Selected Topics in Quantum Electron*, vol. 17, pp. 285–295, 2011. (Cited on pages 3, 4 and 31.)

[22] A. Dixit, B. Lannoo, D. Colle, M. Pickavet, and P. Demeester, "ONU power saving modes in next generation optical access networks: progress, efficiency, and challenges," *Optics Express*, vol. 20, pp. B52–B63, 2012. (Cited on pages 4, 33, 48, 51, 90, 94, 116, 140 and 145.)

[23] ITU-T G. Supp 45, "Means and impact of GPON power saving," (Cited on pages 4, 33, 34, 42, 59, 62, 90 and 158.)

[24] S. W. Wong, L. Valcarenghi, S. H. Yen, D. R. Campelo, S. Yamashita, and L. Kazovsky, "Sleep mode for energy saving PONs: Advantages and drawbacks," *Proc. of IEEE Global Telecommunications Conference (GLOBCOM) Workshops*, 2007. (Cited on pages 4, 6, 34, 37, 45, 64, 68, 100 and 101.)

[25] L. Valcarenghi, Y. Yoshida, A. Maruta, P. Castodi, and K. Kitayama, "Energy savings in TWDM(A) PONs: challenges and opportunities," *Proc. of 15th IEEE Transparent Optical Networks (ICTON)*, p. We.A4.4, 2014. (Cited on pages 5, 51 and 116.)

[26] T. Smith, R. S. Tucker, K. Hinton, and A. V. Tran, "Implications of sleep mode on activation and ranging protocols in PONs," *Proc. of 21st Annual meeting of the IEEE Lasers and Electro-Optics Society*, 2008. (Cited on pages 6, 42, 64 and 65.)

[27] J. Mandin, "EPON power saving via sleep mode," *IEEE 802.3az Meeting*. (Cited on pages 6, 42, 62, 64 and 66.)

[28] S. W. Wong, S.-H. Yen, P. Afshar, S. Yamasitha, and L. G. Kazovsky, "Demonstration of energy conserving TDM-PON with sleep mode ONU using fast clock recovery circuit," *Proc. of IEEE/OSA Optical Fibre Communication Conference (OFC)*, p. OThW7, 2010. (Cited on pages 6, 37, 42, 64, 66, 73, 91 and 94.)

[29] E. Wong, M. Muller, P. I. Dias, C. A. Chan, and M. C. Amann, "Energy-efficiency of optical network units with vertical-cavity surface-emitting lasers," *Optics Express*, vol. 20, pp. 14960–14970, 2012. (Cited on pages 8, 19, 39, 40, 64, 65, 82, 92, 102, 114, 117, 127, 140 and 160.)

[30] B. Mukherjee, "WDM optical communication networks: Progress and challenges," *IEEE Journal of Selected Areas of Communication*, vol. 18, pp. 1810 – 1824, 2000. (Cited on page 19.)

[31] N. Ghani, S. Dixit, and T. S. Wang, "On IP-over-WDM integration," *IEEE Communication Magazine*, vol. 38, pp. 72–84, 2000. (Cited on page 19.)

[32] B. Lung, "PON architecture future proofs FTTH," *IEEE/OSA Journal of Lightwave Technology*, vol. 16, pp. 104–107, 1999. (Cited on page 19.)

[33] P. E. Green, *Fibre optics networks*. Michigan: Prentice Hall, 1993. (Cited on page 19.)

[34] G. Kramer, B. Mukherjee, S. Dixit, Y. Ye, and R. Hirth, "Supporting differentiated classes of service in the Ethernet passive optical networks," *Journal of Optical Networking*, vol. 1, pp. 280–298, 2002. (Cited on pages 20 and 82.)

[35] K. Minefuji, R. Kawate, and H. Mukai, "A proposal of novel power-saving scheme employing watchdog ONUs in redundant PON systems," *Proc. of 18 th OptoElectronics and Communications Conference/International Conference on Photonics in Switching (OECC/PS)*, 2013. (Cited on page 20.)

[36] A. R. Dhaini, P. Ho, G. Shen, and B. Shihada, "Energy efficiency in TDMA-based next-generation passive optical access networks," *IEEE/ACM Transactions on Networking*, vol. 22, pp. 850–863, 2014. (Cited on page 20.)

[37] C. Lee, W. V. Sorin, and B. Y. Kim, "Fiber to the home using a PON infrastructure," *IEEE/OSA Journal of Lightwave Technology*, vol. 24, pp. 4568–4583, 2006. (Cited on page 20.)

[38] N. Ansari and J. Zhang, *"Media access control and resource allocation for next generation passive optical networks"*. Springer, 2013. (Cited on pages 20 and 26.)

[39] C. H. Lee, W. V. Sorin, and B. Y. Kim, "Fibre to the home using a PON infrastructure," *IEEE/OSA Journal of Lightwave Technology*, vol. 24, pp. 4568–4583, 2006. (Cited on page 22.)

[40] ITU-T G.984.x-series recommendations, *Gigabit-capable passive optical networks (G-PON): Physical media dependent (PMD) layer specification (G.984.2)*, 2003. (Cited on page 22.)

[41] ITU-T G.984.x-series recommendations, *Gigabit-capable passive optical networks (G-PON): Transmission convergence layer specification (G.984.3)*, 2008. (Cited on page 22.)

[42] ITU-T G.984.x-series recommendations, *Gigabit-capable passive optical networks (G-PON): ONT management and control interface specification (G.984.4)*, 2008. (Cited on page 22.)

[43] ITU-T G.987.x-series recommendations, *10-Gigabit-capable passive optical networks XG-PON (G.987.3)*, 2010. (Cited on page 22.)

[44] IEEE802.3-2012, "IEEE standard for Ethernet - Section 5, (revision to IEEE std 802.3-2008)," 2012. (Cited on pages 22 and 59.)

[45] E. Wong, "Next-generation broadband access networks and technologies," *IEEE/OSA Journal of Lightwave Technology*, vol. 30, pp. 597–608, 2012. (Cited on page 23.)

[46] Cisco VNI, *Forecast and methodology, 2013-2018*, 2014. (Cited on pages 23 and 31.)

[47] Cisco VNI, *Forecast and methodology, 2008-2013*, 2009. (Cited on page 23.)

[48] E. Wong, M. Muller, and M. Amann, "Characterization of energy-efficient and colorless ONUs for future TWDM-PONs," *Optics Express*, vol. 21, pp. 20747–20761, 2013. (Cited on pages 23, 52, 114 and 117.)

[49] . W. Chow, L. Xu, C. H. Yeh, H. K. Tsang, W. Hofmann, and M. C. Amann, "40 Gb/s upstream transmitters using directly-modulated 1.55 μm VCSEL array for high-split-ratio PONs," *IEEE Photonics Technology Letters*, vol. 22, pp. 347–349, 2010. (Cited on page 23.)

[50] C. H. Yeh, C. W. Chow, and C. H. Hsu, "40 Gb/s time division multiplexed passive optical networks using downstream OOK and upstream OFDM modulations," *IEEE Photonics Technology Letters*, vol. 22, pp. 118–120, 2010. (Cited on page 23.)

[51] C. H. Yeh, C. W. Chow, C. H. Wang, Y. F. Wu, F. Y. Shih, and S. Chi, "Using OOK modulation for symmetric 40 Gb/s long reach time-sharing passive optical networks," *IEEE Photonics Technology Letters*, vol. 22, pp. 619–621, 2010. (Cited on page 23.)

[52] C. W. Chow, C. H. Yeh, Y. F. Wu, Y. H. Lin, F. Y. Shih, and S. Chi, "Rayleigh backscattering circumvention in ring-based access network using RSOA-ONU," *IEEE Photonics Technology Letters*, vol. 23, pp. 1121– 1123, 2011. (Cited on page 23.)

[53] C. H. Yeh, C. W. Chow, S. B. Huang, Y. L. Liu, H. Y. Chen, and C. L. Pan, "Ring-based WDM access network providing both rayleigh backscattering noise mitigation and fiber-fault protection," *IEEE/OSA Journal of Lightwave Technology*, vol. 30, pp. 3211–3218, 2012. (Cited on page 23.)

[54] Y. Luo, M. Sui, and F. Effenberger, "Wavelength management in time and wavelength division multiplexed passive optical networks (TWDM-PONs)," *Proc. of IEEE Global Communications Conference (GLOBECOM)*, 2012. (Cited on pages 24, 114 and 158.)

[55] Y. Luo, M. Sui, and F. Effenberger, "Wavelength management in time and wavelength division multiplexed passive optical networks (TWDM-PONs)," *Proc. of IEEE Global Telecommunications Conference (GLOBECOM)*, 2012. (Cited on pages 24 and 54.)

[56] "EPON-GPON comparison," *CommScope Solutions Marketing*, 2013. (Cited on pages 26, 27 and 28.)

[57] A. Nikoukar, I. Hwang, A. T. Liem, C. Wang, Y. Lin, and V. Golderzehi, "A new QoS-aware green dynamic bandwidth allocation in Ethernet passive optical network," *Proc. of International Conference on Intelligent Green Building and Smart Grid (IGBSG)*, 2014. (Cited on page 26.)

[58] F. Effenberger, "The XG-PON system: cost effective 10Gb/s access,," *IEEE/OSA Journal of Lightwave Technology*, vol. 29, pp. 403–409, 2011. (Cited on page 29.)

[59] A. Dixit, M. V. Wee, B. Lannoo, D. Colle, S. Verbrugge, M. Pickavet, and P. Demeester, "Fiber and wavelength open access in WDM and TWDM passive optical networks," *IEEE Journal on Network*, vol. 28, pp. 74–82, 2014. (Cited on pages 29 and 30.)

[60] N. Cheng, J. Gao, C. Xu, B. Gao, X. Wu, D. Liu, L. Wang, X. Zhou, H. Lin, and F. Effenberger, "World's first demonstration of pluggable optical transceiver modules for flexible TWDM-PONs," *Proc. of 39th European Conference and Exhibition on Optical Communication (ECOC)*, pp. 1269–1271, 2014. (Cited on page 30.)

[61] N. Cheng, "Flexible TWDM PONs," *Proc. of Optical Fibre Communications Conference (OSA/OFC)*, p. W1D.2, 2014. (Cited on page 30.)

[62] E. Wong, "Survivable architectures of time and wavelength division multiplexed networks: A comparison of reliability, cost, and energy efficiency," *Proc. of 17th International Conference on Transparent Optical Networks (ICTON)*, p. Mo.C3.3, 2015. (Cited on page 30.)

[63] E. Wong, "Survivable architectures for time and wavelength division multiplexed passive optical networks," *Optics Communications*, vol. 325, pp. 152–159, 2014. (Cited on page 30.)

[64] A. Dixit, B. Lannoo, D. Colle, M. Pickavet, and P. Demeester, "Dynamic bandwidth allocation with optimal wavelength switching in TWDM-PONs," *Proc. of 15th International Conference on Transparent Optical Networks (ICTON)*, p. Tu.D3.2, 2013. (Cited on pages 30 and 56.)

[65] J. Li, W. Sun, H. Yang, and W. Hu, "Adaptive registration in TWDM-PON with ONU migrations," *Journal of Optical communication and Networking*, vol. 6, pp. 943–951, 2014. (Cited on page 30.)

[66] Y. Ma, Y. Qian, G. Peng, X. Zhou, X.Wang, J. Yu, Y. Luo, X. Yan, and F. Effenberger, "Demonstration of a 40 Gb/s time and wavelength division multiplexed passive optical network prototype system," *Proc. of IEEE/OSA Optical Fibre Communication Conference (OFC)*, 2012. (Cited on pages 30 and 114.)

[67] M. Nogami, S. Ihara, S. Yoshima, E. Igawa, M. Noda, J. Nakagawa, and T. Suehiro, "Experimental demonstration of C-band burst-mode transmission for high power budget (64-split with 40km distance) TWDM-PON systems," *Proc. of 39th European Conference and Exhibition on Optical Communication (ECOC)*, pp. 158–160, 2013. (Cited on page 30.)

[68] Y. Guo, S. Zhu, G. Kuang, Y. Yin, D. Zhang, and X. Liu, "Demonstration of a symmetric 40 Gbitps TWDM-PON over 40 km passive reach using 10G burst-mode DML and EDC for upstream transmission," *Journal of Optical communication and Networking*, vol. 7, pp. 363–371, 2015. (Cited on page 30.)

[69] K. Kondepu, A. Sgambelluri, L. Valcarenghi, F. Cugini, and P. Castoldi, "An SDN-based integration of green TWDM-PONs and metro networks preserving end-to-end delay," *Proc. of Optical Fibre Communications Conference (OSA/OFC)*, p. Th2A.62, 2015. (Cited on page 30.)

[70] N. Cheng, M. Zhou, K. Litvin, and F. Effenberger, "Delay modulation for TWDM PONs," *Proc. of Optical Fibre Communications Conference (OSA/OFC)*, p. W1D.3, 2014. (Cited on page 30.)

[71] K. Kondepu, L. Valcarenghi, and P. Castoldi, "Dynamic wavelength and bandwidth allocation versus OSU-ONU cyclic sleep in TWDM-PONs: An experimental evaluation," *Proc. of International Conference on Optical Network Design and Modelling (ONDM)*, pp. 162–167, 2015. (Cited on page 30.)

[72] N. Cheng, L. Wang, D. Liu, B. Gao, J. Gao, X. Zhou, H. Lin, and F. Effenberger, "Flexible TWDM PON with load balancing and power saving," 2014. (Cited on pages 30, 32, 39 and 54.)

[73] J. Kani, "Power saving techniques and mechanisms for optical access networks systems," *IEEE/OSA Journal of Lightwave Technology*, vol. 31, pp. 563–570, 2013. (Cited on page 31.)

[74] J. Kani, S. Shimazu, N. Yoshimoto, and H. Hadama, "Energy-efficient optical access networks: issues and technologies," *IEEE Communications Magazine*, vol. 51, pp. S22–S26, 2013. (Cited on page 31.)

[75] R. Bolla, "Energy efficiency in the future Internet: A survey of existing approaches ad trend in energy-aware fixed network infrastructures," *IEEE Communications Surveys and Tutorials*, vol. 13, pp. 223–244, 2010. (Cited on page 31.)

[76] L. Valcarenghi, M. Chincoli, P. Castoldi, P. Monti, and L. Wosinska, "Improving energy efficiency in TDMA passive optical networks from theory to practice," *Photonics In Switching*, 2012. (Cited on page 31.)

[77] P. Chowdhury, M. Tornatore, S. Sarkar, and B. Mukherjee, "Building a green wireless-optical broadband access network (WOBAN)," *IEEE/OSA Journal of Lightwave Technology*, vol. 28, pp. 2219–2229, 2010. (Cited on page 31.)

[78] L. Valcarenghi, D. P. Van, and P. Castoldi, "How to save energy in passive optical networks," *Proc. of 13th International Conference on Transparent Optical Networks (ICTON)*, 2011. (Cited on page 31.)

[79] R. S. Tucker, "Green optical communications - part II: Energy limitations in networks," *IEEE Journal of Selected Topics in Quantum Electronics*, vol. 17, pp. 261–274, 2011. (Cited on page 31.)

[80] D. Kilper, G. Atkinson, S. Korotky, S. Goyal, P. Vetter, D. Suvakovic, and O. Blume, "Power trends in communication networks," *IEEE Journal of Selected Topics in Quantum Electronics*, vol. 17, pp. 275–284, 2011. (Cited on page 33.)

[81] Q. Yu and H. Zhou, "Advanced MAC protocol with adjustable sleep mode for wireless sensor networks," *Proc. of International Conference on Wireless Communications, Networking and Mobile Computing (WiCOM)*, 2006. (Cited on page 33.)

[82] R. Jurdak, A. G. Ruzzelli, and G. M. P. O'Hare, "Radio sleep mode optimization in wireless sensor networks," *IEEE Transactions on Mobile Computing*, vol. 9, pp. 955–968, 2010. (Cited on page 33.)

[83] R. Jurdak, A. G. Ruzzelli, and G. M. OâĂŹHare, "Adaptive radio modes in sensor networks: How deep to sleep?," *Proc. of IEEE Communications Society Conference on Sensor, Mesh and Ad Hoc Communications and Networks (SECON)*, 2008. (Cited on page 33.)

[84] C. Gunaratne, K. Christensen, and B. Nordman, "Managing energy consumption costs in desktop PCs and LAN switches with proxying, split TCP connections, and scaling of link speed," *International Journal of Network Management*, vol. 5, pp. 297–310, 2005. (Cited on pages 33 and 47.)

[85] M. Gupta and S. Singh, "Using low-power modes for energy conservation in Ethernet LANs," *Proc. of 26th IEEE International Conference on Computer Communications (INFOCOM)*, pp. 2451–2455, 2007. (Cited on page 33.)

[86] H. Tamura, Y. Yahiro, Y. Fukuda, K. Kawahara, and Y. Oie, "Performance analysis of energy saving scheme with extra active period for LAN switches," *Proc. of IEEE Global Telecommunications Conference (GLOBCOM)*, pp. 198–203, 2007. (Cited on page 33.)

[87] IEEE, *IEEE Standard for local and metropolitan area networks - Part 16: Air Interference for Fixed Broadband Wireless Access Systems, IEEE Standard 802.16*, 2004. (Cited on page 33.)

[88] IEEE Standard 802.16e, *IEEE Standard for Local and Metropolitan Area Networks - Part 16: Air Interference for Fixed Broadband Wireless Access Systems, Amendment 2: Physical and Medium Access Control Layers for Combined Fixed and Mobile Operation in Licensed Bands and Corrigendum 1*, 2005. (Cited on page 33.)

[89] IEEE standard 802.16-2009, *IEEE Standard for Local and Metropolitan Area Networks - Part 16: Air Interference for Fixed Broadband Wireless Access Systems*, 2009. (Cited on page 33.)

[90] IEEE (P)802.16m/D4, *DRAFT Amendment to IEEE Standard for Local and Metropolitan Area Networks - Part 16: Air Interference for Fixed Broadband Wireless Access Systems âĂŞ Advanced Air Interface*, 2010. (Cited on page 33.)

[91] C. Y. Chen, C. H. HsuâĂă, and K. T. Feng, "Performance analysis and comparison of sleep mode operation for IEEE 802.16m advanced broadband

wireless networks," *Proc. of IEEE 21st International Symposium on Personal Indoor and Mobile Radio Communications (PIMRC)*, 2010. (Cited on page 33.)

[92] Y. Xiao, "Energy saving mechanism in the IEEE 802.16e wireless man," *IEEE Communication Letters*, vol. 9, pp. 595–597, 2005. (Cited on page 34.)

[93] J. Xiao, S. Zou, B. Ren, and S. Cheng, "An enhanced energy saving mechanism in IEEE 802.16e," *Proc. of IEEE Global Communications Conference (GLOBECOM)*, 2006. (Cited on page 34.)

[94] D. T. T. Nga and H. Lim, "Performance evaluation and optimisation guidelines for the type II power-saving class of mobile world interoperability for microwave access," *IET Communications*, vol. 6, pp. 2250–2257, 2012. (Cited on page 34.)

[95] D. T. T. Nga and H. Lim, "Power saving mechanism with delay bound for mobile WiMAX systems," *IET Communications*, vol. 5, pp. 1854–1859, 2011. (Cited on page 34.)

[96] D. T. T. Nga and H. Lim, "Performance analysis of sleep mode operation in IEEE 802.16e mobile broadband wireless access systems," *Proc. of IEEE 63rd Vehicular Technology Conference (VTC)*, pp. 1141–1145, 2006. (Cited on page 34.)

[97] A. P. Azad, S. Alouf, and E. Altman, "Analysis and optimization of sleeping mode in WiMAX via stochastic decomposition techniques," *IEEE Journal of Selected Areas of Communications*, vol. 29, pp. 1630–1640, 2011. (Cited on page 34.)

[98] D. A. Khotimsky, D. Zhang, L. Yuan, R. O. C. Hirafuji, and D. R. Campelo, "Unifying sleep and doze modes for energy-efficient PON systems," *IEEE Communications Letters*, vol. 18, pp. 688–691, 2014. (Cited on page 34.)

[99] L. Valcarenghi, I. Cerutti, and P. Castoldi, "Energy efficient optical access and metro networks," *Proc. of 12th International Conference on Transparent Optical Networks (ICTON)*, 2010. (Cited on pages 35, 60, 64 and 118.)

[100] A. Dixit, B. Lannoo, D. Colle, M. Pickavet, and P. Demeester, "Energy efficient DBA algorithms for TWDM-PONs," *Proc. of 17th International Conference on Transparent Optical Networks (ICTON)*, 2015. (Cited on pages 35 and 55.)

[101] E. K. Kanonakis and I. Tomkos, "Online upstream scheduling and wavelength assignment algorithms for WDM-EPON networks," *Proc. of 35th European Conference and Exhibition on Optical Communication (ECOC)*, 2009. (Cited on page 35.)

[102] E. Igawa, M. Nogami, and J. Nakagawa, "Symmetric 10G-EPON ONU BMT employing dynamic power save control circuit," *Proc. of IEEE/OSA Optical Fibre Communication Conference (OFC)*, p. NTuD5, 2011. (Cited on pages 37, 39, 64 and 65.)

[103] S. H. S. Newaz, A. Cuevas, G. Lee, N. Crespi, and J. Choi, "Improving energy saving in time-division multiplexing passive optical networks," *IEEE Internet Computing*, vol. 17, pp. 23–31, 2013. (Cited on page 38.)

[104] M. Amann, E. Wong, and M. Muller, "Energy efficient high speed short cavity VCSELs," *Proc. of Optical Fibre Communication Conference and Exhibition/National Fibre Optic Engineers Conference (OFC/NFOEC)*, p. paper OTh4F1, 2012. (Cited on page 38.)

[105] M. Muller, W. Hofmann, G. Bhm, and M. Amann, "Short-cavity long-wavelength VCSELs with modulation bandwidths in excess of 15 GHz," *IEEE Photonics Technology Letters*, vol. 21, 2009. (Cited on pages 38 and 39.)

[106] M. Muller and M. Amann, "State-of-the-art and perspectives for long-wavelength high speed VCSELs," *Proc. of International Conference on Transparent Optical Networks (ICTON)*, 2011. (Cited on pages 38, 39 and 64.)

[107] M. Muller, W. Hofmann, A. Nadtochiy, A. Mutig, G. Bhm, M. Ortsiefer, and D. Bimberg, "1.55nm high-speed VCSELs enabling error-free fibre-transmission up to 25 Gbit/s," *Proc. of International Semiconductor Laser Conference (ISLC)*, 2010. (Cited on page 38.)

[108] M. Muller, W. Hofmann, T. Grundl, M. Horn, P. Wolf, R. Nagel, E. Ronneberg, G. Bohm, D. Bimberg, and M. Amann, "1550-nm high-speed short-cavity VCSELs," *IEEE Journal of Selected Topics in Quantum Electronics*, vol. 17, 2011. (Cited on page 38.)

[109] E. Wong, M. Muller, P. I. Dias, C. A. Chan, and M. C. Amann, "Vertical cavity surface emitting laser transmitters for energy efficient broadband access networks," *Proc. of IEEE International Conference on Communications (ICC)*, pp. 3041–3045, 2012. (Cited on page 39.)

[110] J. Zhang and N. Ansari, "Toward energy-efficient 1G-EPON and 10G-EPON with sleep-aware MAC control and scheduling," *IEEE Communications Magazine*, vol. 49, pp. s33 – s38, 2011. (Cited on pages 40, 55, 91, 93, 94, 116, 140 and 145.)

[111] C. M. Assi, Y. Ye, S. Dixit, and M. A. Ali, "Dynamic bandwidth allocation for quality-of-service over Ethernet PONs," *IEEE Journal on Selected Areas in Communications*, vol. 21, pp. 1467–1477, 2003. (Cited on page 41.)

[112] H. Miyoshi, T. Inoue, and K. Yamashita, "Qos-aware dynamic bandwidth allocation scheme in Gigabit-Ethernet passive optical networks," *Proc. of IEEE International Conference on Communications (ICC)*, 2004. (Cited on page 41.)

[113] L. Zhang and G. Paa, "Delay constraint dynamic bandwidth allocation in Ethernet passive optical networks," *Proc. of 4 th International Conference on Networking*, pp. 126–130, 2004. (Cited on page 41.)

[114] J. Joo and Y. Ban, "Dynamic bandwidth allocation algorithm for next generation access network," *Proc. of Optical Fibre Communication Conference and Exhibition/National Fibre Optic Engineers Conference (OFC/NFOEC)*, p. OThK6, 2006. (Cited on page 41.)

[115] J. Zheng and S. Zheng, "Dynamic bandwidth allocation with high efficiency for EPONs," *Proc. of IEEE International Conference on Communications (ICC)*, pp. 2699–2703, 2006. (Cited on page 41.)

[116] P. Garfias, L. GutiÃl'rrez, and S. Sallent, "Enhanced dba to provide QoS to coexistent EPON and 10G-EPON networks," *IEEE/OSA Journal of Optical Communications and Networking*, vol. 4, pp. 978–988, 2012. (Cited on page 41.)

[117] S. Choi and J. Park, "Sla-aware dynamic bandwidth allocation for QoS in EPONs," *IEEE/OSA Journal of Optical Communications and Networking*, vol. 2, pp. 773–781, 2010. (Cited on page 41.)

[118] A. Dixit, G. Das, B. Lannoo, D. Colle, M. Pickavet, and P. Demeester, "Jitter performance for QoS in ethernet passive optical networks," *Proc. of 37thEuropean Conference and Exhibition on Optical Communication (ECOC)*, 2011. (Cited on page 41.)

[119] N. A. M. Radzi, N. M. Din, M. S. A. Majid, and M. H. Al-Mansoori, "The bandwidth and jitter study in EPON upstream traffic," *Proc. of IEEE Student Conference on Research and Development (SCOReD)*, 2013. (Cited on page 41.)

[120] T. D. Nguyen, T. Eido, and T. Atmaca, "An enhanced QoS-enabled dynamic bandwidth allocation mechanism for ethernet PON," *Proc. of 1st International Conference on Emerging Network Intelligence*, pp. 135–140, 2009. (Cited on page 41.)

[121] H. Ikeda and K. Kitayama, "Dynamic bandwidth allocation with adaptive polling cycle for maximized TCP throughput in 10G-EPON," *IEEE/OSA Journal of Lightwave Technology*, vol. 27, pp. 5508–5516, 2009. (Cited on page 41.)

[122] N. A. M. Radzi, N. M. Din, M. H. Al-Mansoori, I. S. Mustafa, and S. K. Sadon, "Efficient dynamic bandwidth allocation algorithm for upstream EPON," *Proc. of IEEE 9th Malaysia International Conference on communications*, vol. 27, pp. 376–380, 2009. (Cited on page 41.)

[123] D. P. Van, L. Valcarenghi, M. Chincoli, and P. Castoldi, "Experimental evaluation of an energy efficient TDMA PON," *Proc. of IEEE International Conference on Communications (ICC)*, pp. 2461–2465, 2013. (Cited on pages 42 and 43.)

[124] Z. Wang, W. Yu, and L. Wang, "Energy saving mechanism based on double-way polling DBA algorithm and ONU sleep mode for EPON," *Proc. of International Conference on Electronic and Mechanical Engineering and Information Technology (EMEIT)*, pp. 2222–2225, 2011. (Cited on page 43.)

[125] D. P. Van, L. Valcarenghi, M. Chincoli, and P. Castoldi, "Full FPGA-based implementation of an energy efficient ONU with cooperative cyclic sleep," *Proc. of Asia Communications and Photonics Conference (ACP)*, 2013. (Cited on page 43.)

[126] J. Li, K. L. Lee, N. Dinh, C. A. Chan, and P. Vetter, "A comparison of sleep mode mechanisms for PtP and TDM-PONs," *Proc. of IEEE International Conference on Communications (ICC)*, pp. 543–547, 2013. (Cited on page 43.)

[127] J. Li, K. L. Lee, N. Dinh, C. A. Chan, N. P. Anthapadmanabhan, and P. Vetter, "Dynamic power management at the access node and customer premises in point-to-point and time-division optical access," *IEEE Journal on Selected Areas in Communications*, vol. 32, pp. 1575–1584, 2014. (Cited on page 44.)

[128] D. P. Van, M. P. I. Dias, K. Kondepu, L. Valcarenghi, P. Castoldi, and E. wong, "Energy-efficient dynamic bandwidth allocation for long-reach passive optical networks," *Proc. of OECC / ACOFT*, 2014. (Cited on page 44.)

[129] K. Minefuji, R. Kawate, and H. Mukai, "A proposal of novel power-saving scheme employing watchdog ONUs in redundant PON systems," *Proc. of 18 th OptoElectronics and Communications Conference/International Conference on Photonics in Switching (OECC/PS)*, pp. ThP2–4, 2013. (Cited on pages 44 and 45.)

[130] A. F. Y. Mohammed, S. H. Newaz, and J. K. Choi, "Understanding TCP throughput performance in TDM-PONs with sleep mode," *Proc. of 12th International Conference on Optical Internet*, 2014. (Cited on page 45.)

[131] A. F. Y. Mohammed, S. H. Newaz, and J. K. Choi, "Modeling and simulation of EPON with sleep mode enabled using OPNET," *Proc. of International Conference on Information and Communication Technology Convergence (ICTC)*, 2014. (Cited on page 45.)

[132] L. Zhang, L. Guo, and Y. Liu, "Energy saving mechanism based on sleep mode and dynamic double-threshold link selection in EPON," *Proc. of IEEE Global Communications Conference (GLOBECOM)*, pp. 291–296, 2012. (Cited on page 45.)

[133] A. Dixit, B. Lannoo, D. Colle, M. Pickavet, and P. Demeester, "Energy efficient dynamic bandwidth allocation for Ethernet passive optical networks," *Proc. of IEEE International Conference on Advanced Networks and Telecommunications Systems (ANTS)*, 2012. (Cited on pages 45, 94, 116, 118, 140 and 145.)

[134] Y. Hongliang, Z. Dongdong, Y. Z. Ben, and Z. Weimin, "Understanding user behaviour in large-scale video-on-demand systems," *Proc. of 1st ACM SIGOPS/EuroSys European Conference on Computer Systems*, pp. 1–12, 2012. (Cited on pages 45 and 90.)

[135] D. Ren, H. Li, and Y. Ji, "Power saving mechanism and performance analysis for 10 Gigabit class passive optical systems," *Proc. of 2nd IEEE International Conference on Network Infrastructure and Digital Content*, pp. 920–924, 2010. (Cited on pages 46, 49, 64 and 66.)

[136] S. H. S. Newaz, A. Cuevas, G. Lee, and J. Choi, "On understanding the influence sleep mode on packet delay variation in TDM-PONs," *12th International Conference on Optical Internet*, 2014. (Cited on page 46.)

[137] S. H. S. Newaz, A. Cuevas, G. Lee, and J. Choi, "Adaptive delay-aware energy efficient TDM-PON," *Computer Networks*, vol. 57, 2013. (Cited on page 46.)

[138] X. Guo, G. Shou, Q. Xiao, Y. Hu, and Z. Guo, "Toward green PON with adaptive sleep mode," *Proc. of 3rd IEEE International Conference on Network Infrastructure and Digital Content (IC-NIDC)*, 2012. (Cited on page 46.)

[139] R. Kubo, J. Kani, H. Ujikawa, T. Sakamoto, N. Yoshimoto, and H. Hadama, "Hybrid power-saving mechanism with cyclic sleep and adaptive link rate functions for 10G-EPON systems," *IEEE Electronics Letters*, vol. 46, 2010. (Cited on pages 47, 91 and 93.)

[140] R. Kubo, J. Kani, Y. Fujimoto, N. Yoshimoto, and K. Kumozaki, "Adaptive power saving mechanism for 10 Gigabit class PON systems," *IEICE Transactions on Communications*, vol. E93-B, 2010. (Cited on pages 47, 91 and 94.)

[141] M. Fiammengo, A. Lindstrom, P. Monti, L. Wosinska, and B. Skubic, "Experimental evaluation of cyclic sleep with adaptable sleep period length for PON," *Proc. of 37th European Conference and Exhibition on Optical communication (ECOC)*, 2011. (Cited on pages 47, 64, 66, 94 and 108.)

[142] R. Kubo, J. Kani, Y. Fujimoto, N. Yoshimoto, and K. Kumozaki, "Sleep and adaptive rate control for power saving in 10G-EPON systems," *Proc. of IEEE Global Telecommunications Conference (GLOBECOM)*, 2009. (Cited on pages 47, 48, 64, 66, 91, 93, 94 and 108.)

[143] R. Kubo, J. Kani, Y. Fujimoto, N. Yoshimoto, and K. Kumozaki, "Study and demonstration of sleep and adaptive link rate control mechanisms for energy efficient 10G-EPON," *IEEE/OSA Journal of Optical Communications and Networking*, vol. 2, pp. 716–729, 2008. (Cited on pages 47, 48, 91 and 93.)

[144] N. Dinh and A. Walid, "Power saving protocol for 10G- EPON systems: A proposal and performance evaluations," *Proc. of IEEE Global Communications Conference (GLOBECOM)*, pp. 3135–3140, 2012. (Cited on page 48.)

[145] P. G. Sarigiannidis, D. Vasiliki, and M. D. Louta, "Towards an effective energy efficient passive optical network," *Proc. of IEEE Symposium on Computers and Communications (ISCC)*, pp. 391–396, 2011. (Cited on pages 48 and 49.)

[146] H. Bang, J. Kim, S. S. Lee, and C. S. Park, "Determination of sleep period for cyclic sleep mode in XG-PON power management," *IEEE Communications Letters*, vol. 16, pp. 98–100, 2012. (Cited on page 49.)

[147] H. Bang, J. Kim, S. S. Lee, and C. S. Park, "Analysis of ONT buffer and power management performances for XG-PON cyclic sleep mode," *Proc. of IEEE*

Global Communications Conference (GLOBECOM), pp. 3116–3121, 2012. (Cited on page 49.)

[148] P. Wiatr, J. Chen, P. Monti, and L. Wosinska, "Energy saving in access networks: Gain or loss from the cost perspective?," *Proc. of International Conference on Transparent Optical Networks (ICTON)*, 2013. (Cited on page 49.)

[149] L. Coffin, "A study of the effects of cyclic thermal stresses on a ductile metal," 1953. (Cited on page 50.)

[150] S. S. Manson, "Behavior of materials under conditions of thermal stress," *NACA Report 1170*, pp. 931–950, 1954. (Cited on page 50.)

[151] S. Lambert, J. Montalvo, J. A. Torrijos, B. Lannoo, D. Colle, and M. Packavet, "Energy demand of high speed connectivity services in NG-PON massive developments," *Proc. of 39th European Conference and Exhibition on Optical Communication (ECOC)*, p. P.6.5, 2013. (Cited on pages 50, 115 and 118.)

[152] S. Lambert, J. Montalvo, J. A. Torrijos, B. Lannoo, D. Colle, M. Packavet, and P. Vetter, "Power consumption evaluation of next-generation passive optical networks," *Proc. of 24th Tyrrhenian International Workshop on Digital Communications - Green ICT (TIWDC)*, 2013. (Cited on pages 50, 115 and 118.)

[153] L. Valcarenghi, Y. Yoshida, A. Maruta, P. Castodi, and K. Kitayama, "TWDM PON: How much energy can we really save?," *Proc. of 15th IEEE Transparent Optical Networks (ICTON)*, p. We.A4.4, 2015. (Cited on page 51.)

[154] H. Suzuki, M. Fujiwara, T. Suzuki, N. Yoshimoto, H. Kimura, and M. Tsubokawa, "Wavelength-tunable DWDM-SFP transceiver with a signal monitoring interface and its application to coexistence-type colorless WDM-PON," *39th European Conference and Exhibition on Optical Communication (ECOC)*, 2013. (Cited on page 52.)

[155] K. Taguchi, H. Nakamura, K. Asaka, and S. Nakano, "100-ns lambda-selective burst-mode transceiver for 40 km reach symmetric 40-Gbit/s WDM/TDM-PON," *39th European Conference and Exhibition on Optical Communication (ECOC)*, 2013. (Cited on page 52.)

[156] D. S. Millar, S. J. Savory, and B. C. Thomsen, "Fast wavelength switching 100gbps burst mode transceiver for coherent metro networks," *International Conference on Photonics in Switching (PS)*, 2012. (Cited on page 52.)

[157] E. Scholtzl, D. Korcekl, L. Ladanyil, and L. Mtilleroval, "Tunable thin film filters for the next generation," *Proc. of ELEKTRO*, pp. 98–102, 2014. (Cited on page 52.)

[158] C. J. C. Hasnain, "Tunable VCSEL," *IEEE Journal on Selected Topics in Quantum Electronics*, vol. 6, pp. 978–987, 2000. (Cited on page 52.)

[159] C. J. C. Hasnain, "Optically-injection locked tunable multimode VCSEL for WDM passive optical networks," *Proc. of International Nano-Optoelectronics Workshop (i-NOW)*, pp. 98–99, 2008. (Cited on page 52.)

[160] E. G. Lee, J. C. Lee, S. G. Mun, E. S. Jung, J. H. Lee, and S. S. Lee, "16-channel tunable VCSEL array with 50 Ghz channel spacing for TWDM-PON ONUs," *Proc. of 39th European Conference and Exhibition on Optical Communication (ECOC)*, pp. 2012–2013, 2013. (Cited on page 53.)

[161] L. Valcarenghi, "Where do we stand and where are we heading in making NG-PONs more energy efficient?," *Porc. of International Conference on Optical Network Design and Modeling (ONDM)*, 2015. (Cited on page 53.)

[162] H. Yang, W. Sun, W. Hu, and J. Li, "ONU migration in dynamic time and wavelength division multiplexed passive optical network (TWDM-PON)," *Optics Express*, vol. 21, pp. 285–295, 2011. (Cited on page 54.)

[163] H. Yang, W. Sun, J. Li, and W. Hu, "Energy efficient TWDM multi-PON system with wavelength relocation," *Journal of Optical Communication Networking*, vol. 6, pp. 571–577, 2014. (Cited on pages 54, 115 and 118.)

[164] W. Sun, H. Yang, J. Li, and W. Hu, "Dynamic wavelength sharing in time and wavelength division multiplexed PONs (TWDM-PONs)," *Proc. of 17th International Conference on Transparent Optical Networks (ICTON)*, 2015. (Cited on page 54.)

[165] A. Dixit, B. Lannoo, D. Colle, M. Pickavet, and P. Demeester, "Flexible TDMA/WDMA passive optical network: energy-efficient next-generation optical access solution," *Journal of Optical switching and networking*, vol. 10, pp. 491–506, 2013. (Cited on pages 54, 115 and 119.)

[166] A. Dixit, B. Lannoo, D. Colle, M. Pickavet, and P. Demeester, "Novel DBA algorithm for energy efficiency in TWDM-PONs," (Cited on pages 55, 115 and 119.)

[167] K. Asaka, "What will be killer devices and components for NG-PON2," *Proc. of 40th European Conference and Exhibition on Optical Communication (ECOC)*, 2014. (Cited on page 55.)

[168] K. Kondepu, L. Valcarenghi, D. P. Van, and P. Castoldi, "Trading energy savings and network performance in reconfigurable TWDM-PONs," *Journal of Optical Communication and Networking*, vol. 7, pp. 470–479, 2015. (Cited on page 55.)

[169] K. Kondepu, L. Valcarenghi, D. P. Van, and P. Castoldi, "Impact of ONU tuning time in TWDM-PON with dynamic wavelength and bandwidth allocation: An FPGA-based evaluation," *Proc. of 40th European Conference and Exhibition on Optical Communication (ECOC)*, 2014. (Cited on page 56.)

[170] A. Buttaboni, M. D. Andrade, and M. Tornatore, "Dynamic bandwidth and wavelength allocation with coexistence of transmission technologies in TWDM PONs," *Proc. of 16th International Telecommunications Network Strategy and Planning Symposium (Networks)*, 2014. (Cited on pages 56 and 57.)

[171] W. Xu, M. Fu, and Z. Le, "Energy efficiency scheme for delay aware TWDM-PON," *14th International Conference on Optical Communications and Networks (ICOCN)*, pp. 14–16, 2015. (Cited on page 56.)

[172] H. Wang, S. Su, R. Gu, and Y. Ji, "A minimum wavelength tuning scheme for dynamic wavelength assignment in TWDM-PON," *Proc. of 14th International Conference on Optical Communications and Networks (ICOCN)*, 2015. (Cited on page 57.)

[173] M. Taheri, J. Zhang, and N. Ansari, ""Design and analysis of green optical line terminal for TDM passive optical networks",," *IEEE/OSA Journal of Optical Communications and Networks*, vol. 8, pp. 221–228, 2016. (Cited on pages 57 and 119.)

[174] J. Zhang and N. Ansari, "Scheduling hybrid WDM/TDM passive optical networks with nonzero laser tuning time," *IEEE/ACM Transactions on Networking*, vol. 19, pp. 1014–1027, 2011. (Cited on page 58.)

[175] T. Yoshida, S. Kaneko, S. Kimura, and N. Yoshimoto, "An automatic load-balancing DWBA algorithm considering long-time tuning devices for lambda-tunable WDM/TDM-PON," *Proc. of 39th European Conference and Exhibition on Optical Communication (ECOC)*, 2013. (Cited on page 58.)

[176] Y. Senoo, S. Kaneko, T. Yoshida, J. Sugawa, T. Odaka, S. Kimura, N. Yoshimoto, and H. Kimura, "Dynamic load-balancing algorithm suppressing the number of wavelength reallocations for lambda-tunable WDM/TDM-PON," *Proc. of 40th European Conference and Exhibition on Optical Communication (ECOC)*, 2014. (Cited on page 58.)

[177] IEEE 802.3az, "Energy efficient ethernet task force, 2010," (Cited on page 60.)

[178] C. V. Praet, H. Chow, D. Suvakovic, D. V. Veen, A. Dupas, R. Boislaigue, R. Farah, M. F. Lau, J. Galaro, G. Qua, N. P. Anthapadmanabhan, G. Torfs, X. Yin, and P. Vetter, "Demonstration of low-power bit-interleaving TDM PON," *Optics Express*, vol. 20, pp. B7–B14, 2012. (Cited on pages 64 and 66.)

[179] Y. Yan and L. Dittman, ""Energy efficiency in Ethernet Passive Optical Networks (EPONs): Protocol design and performance evaluation"," *Journal of Communication*, vol. 6, pp. 249–261, 2011. (Cited on pages 64 and 67.)

[180] M. C. Amann, E. Wong, and M. Muller, "Energy-efficient high speed short cavity VCSELs," *Proc. of IEEE/OSA Optical Fibre Communication Conference (OFC)*, p. OTh4F1, 2012. (Cited on pages 64 and 92.)

[181] M. P. I. Dias and E. Wong, "Energy-efficient dynamic bandwidth allocation algorithm for sleep/doze mode VCSEL ONU," *Proc. of Asia Communications and Photonics conference (ACP)*, p. ATh1D.4, 2012. (Cited on pages 64 and 101.)

[182] M. P. I. Dias and E. Wong, "Performance evaluation of VCSEL ONU using energy-efficient just-in-time dynamic bandwidth allocation algorithm," *Proc. of Photonics Global Conference (PGC)*, 2012. (Cited on pages 64, 127 and 140.)

[183] C. Gunaratne, K. Christensen, B. Nordman, and S. Suen, "Reducing the energy consumption of Ethernet with adaptive link rate (ALR)," *IEEE Transactions in Computing*, vol. 57, pp. 448–461, 2008. (Cited on page 66.)

[184] J. Zhang, M. T. Hosseinabadi, and N. Ansari, ""Standards-compliant EPON sleep control for energy efficiency: Design and analysis"," *IEEE/OSA Journal of Optical Communications and Networking*, vol. 5, pp. 677–685, 2013. (Cited on page 67.)

[185] M. Taheri and N. Ansari, ""Multi-power-level energy saving management for passive optical networks"," *IEEE/OSA Journal of Optical Communications and Networks*, vol. 6, pp. 965–973, 2014. (Cited on page 67.)

[186] Cisco VNI, "Forecast and methodology, 2011-2016," *Available: www.cisco.com*. (Cited on page 68.)

[187] A. R. Dhaini, P. Ho, and G. Shen, "Toward green next-generation passive optical networks," *IEEE Communications Magazine*, vol. 49, pp. 94–101, 2011. (Cited on pages 91, 93 and 94.)

[188] J. Zhang and N. Ansari, "Standards-compliant EPON sleep control for energy efficiency: design and analysis," *Proc. of IEEE International Conference of Communications (ICC)*, pp. 2994–2998, 2012. (Cited on pages 91 and 94.)

[189] M. P. I. Dias and E. Wong, "Sleep/doze controlled dynamic bandwidth allocation algorithms for energy-efficient access networks," *Optics Express*, vol. 21, pp. 9931–9946, 2012. (Cited on pages 92, 94, 102, 114, 122, 123, 124, 139, 146 and 160.)

[190] M. P. I. Dias, B. S. Karunaratne, and E. Wong, "Bayesian estimation and prediction based dynamic bandwidth allocation algorithm for sleep/doze mode passive optical networks," *IEEE/OSA Journal of Lightwave Technology*, vol. 32, pp. 2560–2568, 2014. (Cited on pages 92, 114, 124, 125, 139, 141 and 146.)

[191] L. Shi and B. Mukherjee, "Efficient PON with sleep-mode ONU: progress, challenges, and solutions," *IEEE Network Magazine*, vol. 26, pp. 36–41, 2012. (Cited on page 93.)

[192] S. M. Kay, *Fundamentals of statistical signal processing*. Michigan: Prentice-Hall, 1993. (Cited on page 95.)

[193] S. Bindhaiq, A. S. M. Supa'at, N. Zulkifli, A. B. Mohammad, R. Q. Shaddad, and M. A. Elmagzoub, "Recent development on time and wavelength development passive optical networks (TWDM-PON) for next-generation passive optical network stage 2 (NG-PON2)," *Journal of Optical Switching and Networking*, 2014. (Cited on page 113.)

[194] FSAN, "Available: http://www.fsan.org/," (Cited on page 114.)

[195] G. Talli, "Hybrid DWDM-TDM long-reach PON for next-generation optical access," *IEEE/OSA Journal of Lightwave Technology*, vol. 24, pp. 2827–2834, 2006. (Cited on page 114.)

[196] H. Yang, W. Sun, J. Li, and W. Hu, "User migration in time and wavelength division multiplexed PON," *Proc. of IEEE Transparent Optical Networks (ICTON)*, p. We.B3.2, 2013. (Cited on pages 115, 116 and 118.)

[197] N. Cheng, L. Wang, D. Liu, B. Gao, J. Gao, and X. Zhou, "Characterization of energy-efficient and colourless onus for future TWDM-PONs," *Proc. of 39thEuropean Conference and Exhibition on Optical communication (ECOC)*, p. We.3.F.6, 2013. (Cited on pages 115 and 119.)

[198] ITU-T G 1010, "End-user multimedia categories," (Cited on page 116.)

[199] M. P. I. Dias, D. P. Van, L. Valcarenghi, and E. Wong, "Energy-efficient dynamic wavelength and bandwidth allocation algorithm for TWDM-PONs with tunable VCSEL ONUs," *Proc. of IEEE Optoelectronic and Communications conference (OECC)*, 2014. (Cited on pages 116 and 122.)

[200] M. P. I. Dias, D. P. Van, L.Valcarenghi, and E.Wong, "Anenergy-efficientframe- work for wavelength and bandwidth allocation in twdm pon," *Journal of Optical Communication and Networks (JOCN)*, vol. 7, pp. 496–504, 2015. (Cited on page 139.)

[201] M. P. I. Dias, D. P. Van, L. Valcarenghi, and E.Wong, "Energy-efficient dynamic bandwidth allocation algorithm for TWDM PON with tunable VCSEL ONUs," *Proc. of Opto Electronics and Communications Conference (OECC)*, 2014. (Cited on page 139.)

[202] M. P. I. Dias, D. P. Van, L. Valcarenghi, and E.Wong, "Energy-efficient TWDM PON with VCSEL ONUs," *Proc. of Asia Communications and Photonics conference (ACP)*, 2014. (Cited on page 139.)

[203] M. P. I. Dias, D. P. Van, L. Valcarenghi, and E.Wong, "Offline energy-efficient dynamic wavelength and bandwidth allocation algorithm for TWDM-PONs," *Proc. of International Conference on Communications (ICC)*, 2015. (Cited on page 139.)

[204] V. S. Frost and B. Melamed, "Traffic modeling for telecommunications networks," *IEEE Communications Magazine*, vol. 32, pp. 70–81, 1994. (Cited on pages 140 and 164.)

[205] H. J. Larson and B. O. Shubert, "Probabilistic models in engineering sciences," *New York, NY: John Wiley and Sons, 1979*. (Cited on page 141.)

[206] R. Gusella, "A measurement study of diskless work-station traffic on an ethernet," *IEEE Transactions on Communications*, vol. 38, pp. 1557–1568, 1990. (Cited on page 141.)

[207] R. Jain and S. Routhier, "Packet trains measurements and a new model for computer network traffic," *IEEE Journal on Selected Areas in Communications*, vol. 4, pp. 986–995, 1986. (Cited on page 141.)

[208] H. Fowler and W. Leland, "Local area network traffic characteristics, with implications for broadband network congestion management," *IEEE Journal on Selected Areas in Communications*, vol. 9, pp. 1139–1149, 1991. (Cited on page 141.)

[209] P. Danzig, S. Jamin, R. Caceres, D.Mitzel, and D. Estrin, "An empirical workload model for driving wide-area TCP/IP network simulations," *Internetworking: Research and Experience*, vol. 3, pp. 1–26, 1992. (Cited on page 141.)

[210] W. Leland, M. Taqqu, W.Willinger, and D.Wilson, "On the self-similar nature of Ethernet traffic," *IEEE/ACM Transactions on Networking*, vol. 2, pp. 1–15, 1994. (Cited on pages 141 and 144.)

[211] R. S. W. Willinger, M. S. Taqqu, and D. V.Wilson, "Wide area traffic: The failure of Poisson modelling," *IEEE/ACM Transactions on Networking*, vol. 5, 1997. (Cited on page 141.)

[212] M. S. Taqqu, W. Willinger, and R. Sherman, "Proof of a fundamental result in self-similar traffic modelling," *ACM/SIGCOMM Computer Communication Review*, vol. 27, pp. 5–23, 1997. (Cited on page 144.)

[213] M. Bokhari and P. Saengudomlert, "Integrated sleep mode for improving energy efficiency of NG-PONs," *Proc. of 11th International Conference on Optical Communications and Networks (ICOCN)*, 2012. (Cited on page 157.)

Author/s:
Dias, Maluge Pubuduni Imali

Title:
Next-generation energy-efficient broadband access networks

Date:
2016

Persistent Link:
http://hdl.handle.net/11343/113591

File Description:
Next-generation Energy-efficient Broadband Access Networks